N° d'ordre

THESE DE DOCTORAT

Présentée à l'Université Djillali Liabes de Sidi- Bel-Abbes
Faculté de Génie Electrique
Département de Télécommunications
Laboratoire Télécommunications et de Traitement Numérique du Signal

Pour l'obtention du Diplôme de Doctorat LMD
Filière : Télécommunications
Spécialité : Télécommunications

M. Mouad ADDAD

Codes de zone à corrélation nulle : Conception, analyse et applications

Soutenu le 31 / 10 / 2018

Devant le jury composé de :

M. NAOUM Rafah	Pr	Président	**UDL-SBA**
M. DJEBBARI Ali	Pr	Directeur de thèse	**UDL-SBA**
M. ELAHMAR Sid Ahmed	Pr	Examinateur	**UDL-SBA**
M. BOUZIANI Merahi	Pr	Examinateur	**UDL-SBA**
M. DJEBBAR Ahmed Bouzidi	Pr	Examinateur	**UDL-SBA**
M. BENAISSA Mohamed	MCA	Examinateur	**CU-Ain Temouchent**

Année Universitaire: 2018-2019

Acknowledgement

This thesis is the result of my research at the Laboratory of Telecommunications and Digital Signal Processing, Djillali Liabes University of Sidi Bel Abbes. I would like to thank all my Lab colleagues for creating a nice and friendly working environment.

First and foremost, I offer sincere gratitude to my advisor Prof. Ali Djebbari who has guided me through my Ph.D. pursuit with his knowledge. It has been an exceptional experience to work with Prof. Djebbari in the past years. The dissertation would have been next to impossible without his supervision and research support.

Furthermore, I am grateful for the collaboration with Prof. Iyad Dayoub of Valenciennes University, France. I heartily appreciate his contribution to my research journey.

I acknowledge my committee members Professors Naoum Rafah, Elahmar Sid Ahmed, Bouziani Merahi, and Djebbar Ahmed Bouzidi from the University of Djillali Liabes and associate prof. Benaissa Mohamed from the University Center of Ain Temouchent. I am truly thankful for the time and efforts that they spent on reviewing and commenting my research proposal.

Last but not the least, I am greatly indebted to my parents and people closest to me. They have provided me with immense understanding and support all these years. I have enjoyed every moment we spent together with care and love. This dissertation is dedicated to them.

Abstract

In order to make efficient use of the available resources, the users of communication systems, which are more and more numerous, have to cohabit. The problem posed by this cohabitation then consists in examining how to organize the access of a large number of users to a resource. Code Division Multiple Access (CDMA) is one of the techniques that allows access to a communication network, but suffers from interference between users (MUI: Multiuser Interference). The latter depends heavily on the spreading sequences that must be constructed in order to minimize cross-correlation function (CCF) between sequences and to minimize the correlation between each sequence and its shifted version (ACF: Auto-Correlation Function). The aim of the thesis is to study the spreading sequences and in particular the so-called Zero Correlation Zone (ZCZ) sequences. We have four contributions. The first concerns the construction of two sequence families for the optical CDMA system: a ZCZ family and a Zero Cross-Correlation (ZCC) family of sequences. The second is to establish a new Bit Error Rate (BER) expression for the quasi-synchronous, uplink DS-CDMA system, based on the CCF properties of the spreading sequences. We have shown that to eliminate MUI interference, sequences must have zero even and odd CCF functions. This new expression has not only made it possible to evaluate the performance of said system for the case of ternary sequences, but to show that the elimination of MUIs in the case of ZCZ sequences is only possible if the even and odd CCF functions are both zero; contrary to what is generally accepted: to have only zero even CCF. The third is dedicated to the generalization of the BER of the quasi-synchronous MC-CDMA system, uplink, to include ternary sequences, which made it possible to evaluate the performances of suitable sequences. Also, a comparative study was developed in terms of Crest Factor (CF) concerning the binary sequences; ZCZ sequences have been shown to have low CF compared to conventional sequences (Walsh-Hadamard and Orthogonal Gold). At last, the fourth is to show that the optical ZCZ sequences for the quasi-synchronous, uplink SAC-OCDMA system eliminate the MUIs, if the maximum delay between users is within the ZCZ zone, but their performance remains low compared to the ZCC codes with the same parameters (number of sequences and weight).

Résumé

Afin d'obtenir une utilisation efficace des ressources disponibles, les utilisateurs des systèmes de communications, de plus en plus nombreux, sont amenés à cohabiter. Le problème posé par cette cohabitation, consiste alors à examiner comment organiser l'accès d'un nombre important d'utilisateurs à une ressource. L'accès multiple par répartition de code (CDMA : Code Division Multiple Access) est une des techniques qui permet l'accès à un réseau de communication, mais soufre des interférences entre utilisateurs (MUI : Multiuser Interference). Ces dernières dépendent fortement des séquences d'étalement qui doivent être construites de façon à minimiser la corrélation croisée (CCF : Cross-Correlation Function) entre les séquences et à minimiser la corrélation entre chaque séquence et sa version décalée (ACF : Auto-Correlation Function). Cette thèse a pour objectifs d'étudier, donc, les séquences d'étalement et notamment les séquences dites de zone à corrélation nulle (ZCZ : Zero Correlation Zone). Nous avons présenté quatre contributions. La première concerne la construction de deux familles de séquences pour le système CDMA optiques : une famille ZCZ et une famille de séquences à corrélation croisée nulle (ZCC : Zero Cross-Correlation). Quant à la deuxième, il s'agit d'établir une nouvelle expression du taux d'erreurs binaires (BER : Bit error rate) pour le système DS-CDMA quasi synchrone, en liaison montante, en fonction des propriétés de CCF des séquences d'étalement. Nous avons montré que pour éliminer les interférences MUI, les séquences doivent posséder des fonctions de CCF paires et impaires nulle. Cette nouvelle expression a permis non seulement l'évaluation des performances dudit système pour le cas des séquences dites ternaires, mais de montrer que l'élimination des MUI dans le cas des séquences ZCZ n'est possible que si les fonctions CCF paires et impaires sont conjointement nulles ; contrairement à ce qui généralement répandu : le fait d'avoir seulement la CCF paire nulle. La troisième est dédiée à la généralisation du BER du système MC-CDMA quasi synchrone, liaison montante, dans le cas des séquences ternaires, ce qui a permis non seulement d'évaluer les performances de ces dernières mais d'en choisir les familles de séquences les plus adaptés. Aussi, nous élaborons une étude comparative en termes de facteur de crête (Crest Factor : CF) concernant les séquences binaires ; il a été montré que les séquences ZCZ ont un faible CF comparativement aux séquences conventionnelles (Walsh-Hadamard et Gold orthogonal). Enfin, la dernière consiste à montrer que les séquences ZCZ optiques pour le système SAC-OCDMA quasi synchrone, en voie montante, éliminent les MUI, si le retard maximal entre utilisateur est à l'intérieur de la zone ZCZ, mais leur performance reste faible comparativement au codes ZCC de même paramètres (nombre de séquences et poids).

ملخص

من أجل الاستخدام الفعال للموارد المتاحة، يجب على مستخدمي أنظمة الاتصالات التعايش. تتكون المشكلة في فحص كيفية تنظيم وصول هؤلاء المستخدمين إلى مورد. يوفر النفاذ المتعدد بتقسيم الشفرة
(CDMA: Code Division Multiple Access) الوصول إلى شبكة اتصالات، ولكنه يخضع لتداخل بين المستخدمين (MUI: Multiuser Interference). هذه تعتمد بشدة على الرموز التي يجب بناؤها لتقليل وظيفة الارتباط المتبادل (CCF: Cross-Correlation Function) ووظيفة الارتباط التلقائي
(ACF: Auto-Correlation Function). الهدف من الأطروحة هو دراسة الرموز وتحديدًا رموز منطقة الصفر (ZCZ: Zero Cross-Correlation). قدمنا أربع مساهمات. تتعلق الأولى ببناء عائلتين من الرموز لنظام CDMA البصري: عائلة ZCZ وعائلة رموز (ZCC: Zero Cross-Correlation). والثاني هو إنشاء تعبير جديد لخطأ البتات (BER) لنظام DS-CDMA شبه المتزامن (QS: quasi synchrone)، استناداً إلى CCFs للرموز. لقد أظهرنا أنه للتخلص من تداخل MUI، يجب أن تحتوي الرموز على CCFs زوجية وفردية منعدمة. سمح هذا التعبير الجديد ليس فقط بتقييم أداء الرموز الثلاثية، ولكن لإظهار أن القضاء على MUIs في حالة الرموز ZCZ ممكن فقط إذا كان CCFs زوجية وفردية منعدمة؛ على عكس ما هو منتشر بشكل عام: CCFs زوجية فقط. أما الثالث فهو مخصص لتعميم نظام QS-MC-CDMA الرموز الثلاثية، والذي يسمح لنا ليس فقط بتقييم أدائها ولكن لاختيار مجموعة رموز ملاءمة. أيضا، تم تطوير دراسة مقارنة من حيث (CF: Crest Factor) فيما يتعلق بالرموز الثنائية؛ وقد ثبت أن لرموز ZCZ منخفضة في CF مقارنة بالرموز التقليدية (Walsh-Hadamard and Orthogonal Gold). والرابع هو إظهار أن الرموز ZCZ البصرية لنظام QS-SAC-OCDMA ، تقضي على MUI ، إذا كان الحد الأقصى للتأخر بين المستخدمين هو داخل المنطقة ZCZ ، ولكن أدائها لا يزال منخفضاً بالمقارنة مع رموز ZCC مع نفس المعلمات (عدد الرموز والوزن).

Contents

List of Figures

List of Tables

Acronyms

ACF	Auto Correlation Function
AP	Access Point
AWGN	Additive White Gaussian Noise
BER	Bit Error Rate
BPSK	Binary Phase Shift Keying
BS	Base Station
CC	Complementary Codes
CCF	Cross Correlation Function
CDMA	Code Division Multiple Access
CF	Crest Factor
DS	Direct Sequence
DSSS	Direct Sequence Spread Spectrum
FDMA	Frequency Division Multiple Access
FH	Frequency Hopping
ICI	Inter Channel Interference
ISI	Inter-Symbol Interference
LED	Light Emitting Diode
LOS	Line of Sight
LTE	Long Term Evolution
MAI	Multiple Access Interference
MC	Multicarrier
MPI	Multipath Interference
MUI	Multiuser Interference
MT	Multi-Tone
NOMA	Non-Orthogonal Multiple Access

OFDM Orthogonal Frequency Division Multiplexing
OWC Optical Wireless Communication
PAPR Peak-to-Average Power Ratio
PCF Periodic Correlation Function
PN Pseudo-Noise
QS Quasi-Synchronous
SAC Spectral Amplitude Coding
SINR Signal to Interference Plus Noise Ratio
SNR Signal to Noise Ratio
SS Spread Spectrum
TDMA Time Division Multiple Access
TH Time Hopping
UWB Ultra wide Band
WDMA Wavelength Division Multiple Access
VLC Visible Light Communication
V2V Vehicle-To-Vehicle
WH Walsh-Hadamard
ZCC Zero Cross-Correlation
ZCZ Zero Correlation Zone

Introduction

Wireless access technologies have been continuously evolving in response to the rapid increase in the use of smartphones, tablets, and other data devices. The scarcity of radio frequency spectrum is a limiting factor in meeting this demand. Current 4^{th} generation wireless systems will not be able to cope with the growing traffic. Spread spectrum (SS) is a mature technology that being applied in various communications systems such as non-cooperative surveillance, underwater wireless communications, navigation, and Ad-hoc network. In direct sequence (DS) SS, sequences are used to provide channel access; each user is assigned a unique spreading sequence. DSSS is being considered as a potential candidate for future 5^{th} networks such as coded non-orthogonal multiple access (NOMA) systems. Multi-carrier (MC) transmission is the predominant transmission technique in today's communication systems. Orthogonal frequency division multiplexing (OFDM) technique is already been used in current standards such as Long Term Evolution (LTE) and Wi-Fi and is believed to be adopted in future 5^{th} communication systems. MC-CDMA is a MC technique that combines the merits of both OFDM and CDMA techniques. The main advantages of the combined system are variable data rate, high spectral efficiency, and robustness against frequency selective fading. In applications where high bandwidth is required, visible light communication (VLC) can be used as a complementary technology to radio frequency systems. A key advantage of VLC is its potential to simultaneously provide energy sufficient lighting and high speed communication using light emitting diodes (LEDs). VLC is being adopted in, to name a few, vehicle to vehicle communication, indoor positioning, and underwater communications.

When CDMA system is synchronous, orthogonal sequences are employed. When system users are transmitting asynchronously, such as the uplink channel of cellular mobile systems, pseudo-noise sequences are used. When system users are transmitting asynchronously i.e., there is a timing misalignments among users, the multiuser

interference (MUI) occurs. A major drawback of MC-CDMA technology is the large peak-to-average power ratio (PAPR) or CF. In fact, high CF reduces power efficiency and causes implementation issues. Therefore, achieving very low CF values is of major importance. To mitigate MUI and CF, several techniques were proposed recently. However, these techniques only add to the complexity of the CDMA system.

Sequences with good correlation properties are extensively applied in communication CDMA-based systems. However, the problem with CDMA systems based on traditional sequences is that their design ignores real application scenario such as MUI and multipath interference (MPI). Sequences with impulsive autocorrelation function (ACF) and zero cross-correlation function (CCF) could be employed to eliminate MUI and MPI. However, these ideal sequences are theoretically impossible to obtain. Therefore, a new class of sequences called zero-correlation zone (ZCZ) have been extensively studied. Binary, ternary, and optical ZCZ sequences have been proposed. Ternary ZCZ set have larger zero-zones in the correlation functions than binary ZCZ set for a given length while using the same hardware.

The contribution of this thesis is as follows. In the first chapter, it is proposed to analyze several bipolar sequences associated with radiofrequency systems such as the Walsh-Hadamard sequences, pseudo-random, complementary and ZCZ. Optical sequences such as optical ZCZ and ZCC sequences have also been presented. The characteristics and constraints that these sequences must respect are given. The conditions set on the correlation properties make it possible to control or even minimize the effect of the MUIs on the bit error rate (BER). In order to clarify the choice of the type of sequence to be implemented, it is important to know the different ways to generate them and to highlight the advantages and disadvantages of each one. It should be noted that two proposals for new optical ZCZ and ZCC codes have been presented.

The second chapter aims to present the first elements needed to understand the study conducted in this thesis. A brief overview of CDMA and some of its key features and highlights the particularities of the CDMA technique is presented. We recall the basic principles of spread spectrum and multicarrier modulations. The notions of selectivity and diversity were presented.

In the third chapter, we will analyze the performances of sequences in a quasi-synchronous DS-CDMA system (DS: Direct-Sequence). Here, we directly multiply the message to be transmitted by a sequence. The spectral spread of the coded signal comes from the fact that the frequency of sequences is much greater than the frequency of data. We will develop a theoretical model describing their statistics. We will determine the signal-to-noise plus interference ratio (SINR: Signal to Interference plus Noise Ratio) in the uplink. The latter makes it possible to define new correlation criteria, in particular the even and odd correlation functions, which will make it possible to choose the right set of sequences to be used in the system. It should be noted that the ZCZ sequences have transmission performance that is much greater than Gold sequences when the delay between users is within their zero-correlation zone. We also note that some ZCZ sequences maintain better performance beyond their zero-correlation zone.

In the fourth chapter, we will analyze the performances of sequences in a quasi-synchronous MC-CDMA system (MC: Multi Carrier). The MC-CDMA technique is based on the concatenation of spread spectrum and multicarrier modulation. Unlike the previous technique (DS-CDMA), MC-CDMA modulation spreads the data of each user in the frequency domain. The major advantage of this technique is that it allows multiple access with a transmitted signal having all the characteristics and advantages of multicarrier modulation. In addition, the frequency diversity of the channel is fully exploited. However, the MC-CDMA technique did not inherit only the advantages of multicarrier modulation and CDMA technique. Indeed, the MC-CDMA signal, by its multi-carrier nature, has a large amplitude fluctuation that can lead to performance degradation due to the power amplification function, amplification which is by nature non-linear. In addition, after transmission on a channel, the MC-CDMA receiver must fight against MUI. First, we compare the influence of ZCZ sequences with conventional sequences on Crest Factor (CF) variation. In addition to their low CF values, ZCZ sequences also have stable CF, which is a major advantage in MC-CDMA systems. The second contribution of this chapter focuses on the optimization of the uplink using spreading sequences. The BER of the quasi-synchronous MC CDMA system, uplink, is generalized to include the case of ternary sequences. According to the BER criterion, the best results are obtained when the ZCZ sequences are used. These latter sequences

eliminate interference and provide BER performance similar to the AWGN channel. We conclude that ZCZ sequences have low CF and interference-free communication.

In the fifth chapter, the transmission of CDMA signals on an optical channel is approached and the performance of the optical system using different optical sequences is studied. The objective is to find optical sequences allowing a significant increase of performance. It is shown that the optical ZCZ sequences used in the case of the uplink quasi synchronous SAC-OCDMA system, eliminate the MUI, if the maximum delay between user is at inside the zero-correlation zone, but their performance remains low compared to ZCC codes with the same parameters (number of sequences and weight).

Finally, a general conclusion summarizes the main contributions of this thesis and some perspectives to this work are then presented.

Chapter 1: Sequence Design

1.1 Introduction

Sequences (codes) with good correlation properties are extensively applied in communication systems. There are various kinds of sequences, binary and non-binary sequences, unipolar and bipolar sequences, periodic and aperiodic sequences, complementary pairs and complementary sets etc. The focus of this chapter is on the properties of digital sequences that will be used in the succeeding chapters. This chapter also includes new constructions of optical zero correlation zone (ZCZ) and zero cross-correlation (ZCC) sequences.

1.2 Sequence Operations

The term "sequence" will be used to describe a digital signal. A sequence $\boldsymbol{a} = (a_1, \dots, a_n, \dots, a_N)$ of length N is called binary if its elements a_n take only two values. We will refer to binary sequences with elements from $\{0,1\}$ as unipolar sequences and those with elements from $\{-1,1\}$ as bipolar sequences. Ternary sequences have elements from $\{-1,0,1\}$. Table 1-1 gives some sequence operations.

Table 1-1 Sequence operations

$-\boldsymbol{a} =$	$(-a_1, \dots, -a_n, \dots, -a_N)$
$\overline{\boldsymbol{a}} =$	$(a_1, \dots, a_{N/2}, -a_{(N/2)+1}, \dots, -a_N)$
$\boldsymbol{aa} =$	$(a_1, \dots, a_n, \dots, a_N, a_1, \dots, a_n, \dots, a_N)$
$\boldsymbol{a}\otimes\boldsymbol{a} =$	$(a_1, a_1, \dots, a_n, a_n, \dots, a_N, a_N)$
$\boldsymbol{T^n a} =$	$(a_{1+n}, \dots, a_N, \dots, a_n)$

Where $\boldsymbol{aa}$ and $\boldsymbol{a}\otimes\boldsymbol{a}$ are called respectively the concatenation and interleaving operations. The operator T^n performs n cyclic shifts of $\boldsymbol{a}$ to the right, where $n \geq 0$.

If $\boldsymbol{a}$ is a unipolar sequence, the corresponding bipolar sequence $\boldsymbol{b}$ is obtained using the following formula

$$b_n = (-1)^{a_n} \tag{1-1}$$

1.3 Correlation Functions

The CCF is a measure of similarity, or relatedness, between two different signals. When properly normalized, the CCF of bipolar sequences is a real number between -1 and 1, where a correlation value of 1 indicates that the two signals are identical, a CCF value of -1 means they are opposite, and a correlation value of 0 means that they are uncorrelated (orthogonal). On the other hand, ACF measures the similarity of a signal and time-delayed version of itself. The aperiodic CCF $\theta_{\boldsymbol{ab}}(l)$ of a pair of bipolar sequences $\boldsymbol{a}$ and $\boldsymbol{b}$ is defined in Eq. 1-2 and illustrated in Figure 1-1.

$$\theta_{\boldsymbol{ab}}(l) = \begin{cases} \sum_{n=1}^{N-l} a_n b_{n+l} & 0 \le l \le N-1 \\ \sum_{n=1}^{N+l} a_{n-l}\, b_n & -N+1 \le l < 0 \\ 0 & N < |l| \end{cases} \tag{1-2}$$

Where l is the shifting variable. When $\boldsymbol{a} = \boldsymbol{b}$, the CCF becomes the ACF and will be denoted simply by $\theta_{\boldsymbol{a}}(l)$.

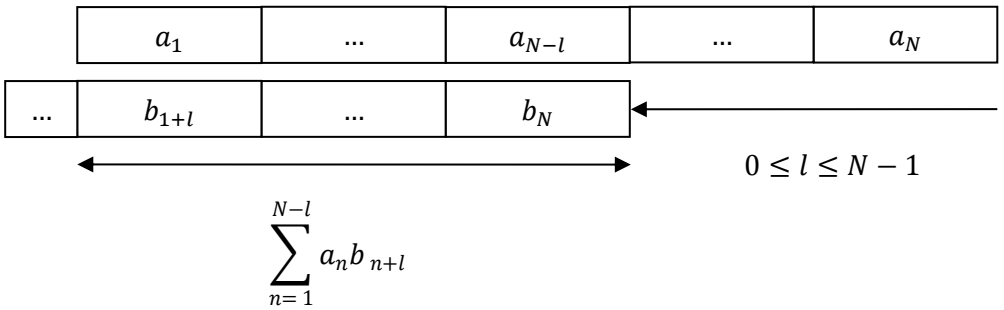

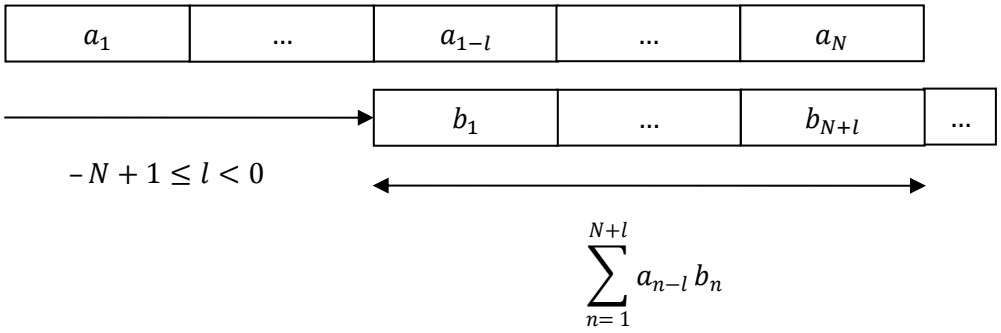

Figure 1-1 Discrete aperiodic CCF

The even and odd periodic correlation functions are related to the aperiodic correlations function as follows [1]

$$E_{ab}(l) = \theta_{ab}(l) + \theta_{ba}(N-l) \quad (1\text{-}3)$$

$$O_{ab}(l) = \theta_{ab}(l) - \theta_{ba}(N-l) \quad (1\text{-}4)$$

The designations even and odd are due to $E_{ab}(N-l) = E_{ba}(l)$ and $O_{ab}(N-l) = -O_{ba}(l)$.The sequence's energy is calculated as

$$\varepsilon_a = \sum_{n=1}^{N} a_n^2 \quad (1\text{-}5)$$

The classification of periodic correlation functions is given in Figure 1-2.

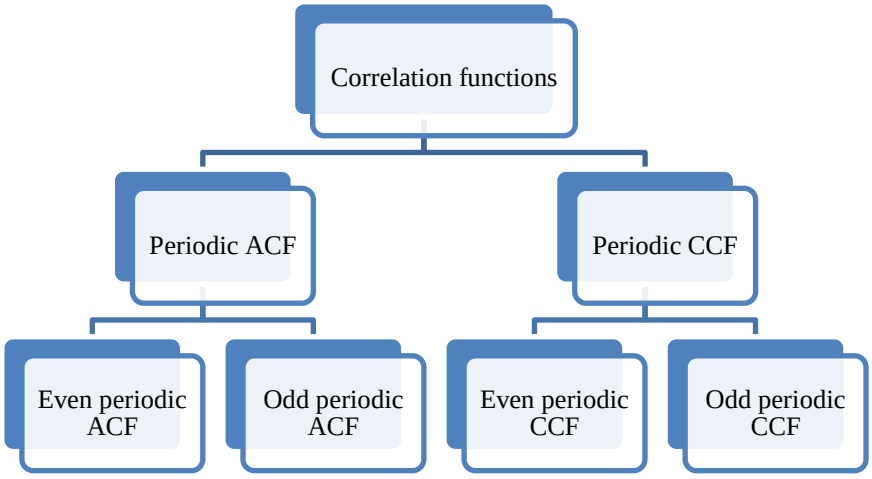

Figure 1-2 Classification of periodic correlation functions

The ACF and CCF properties are related according to the Sarwate's bound [2]

$$\frac{E_{max\ CCF}^2}{N} + \frac{N-1}{N(K-1)}\frac{E_{max\ ACF}^2}{N} \geq 1 \tag{1-6}$$

Where $E_{max\ ACF}$ and $E_{max\ CCF}$ are respectively the maximum out-of-phase ACF and CCF values, N is the sequence length and K is the number of sequences in the set (set's size).

The Sarwate bound stipulates that it is not possible to achieve low values for both ACF and CCF simultaneously. Thus, a good trade-off must be found. Another bound was derived by Welch in [3] where the peak value of periodic correlation function $E_{max} = max\{E_{max\ ACF}, E_{max\ CCF}\}$ is lower bounded as

$$E_{max} \geq N\sqrt{\frac{K-1}{KN-1}} \tag{1-7}$$

1.4 Perfect Sequences

A bipolar sequence of length N is called a perfect sequence if

$$E_{\boldsymbol{a}}(l) = \begin{cases} \varepsilon_{\boldsymbol{a}} & l = 0 \\ 0 & l \neq 0 \end{cases} \tag{1-8}$$

According to [4], the only bipolar perfect sequence is $\{1\ 1\ 1\ -1\}$. Some ternary perfect sequences are given in Table 1-2.

Table 1-2 Ternary perfect sequences [5]

N	$\mu_{\boldsymbol{a}}$	Sequences
7	0.57	$\{1,1,0,1,0,0,-1\}$
13	0.69	$\{-1,1,-1,0,1,1,1,1,-1,0,1,0,0\}$
21	0.76	$\{-1,1,1,-1,0,1,0,1,-1,1,1,1,1,1,-1,-1,0,-1,1,0,0\}$
31	0.80	$\{-1,-1,-1,-1,1,1,-1,1,1,1,1,-1,0,1,1,1,-1,1,0,-1,1,1,0,-1,1,-1,1,0,1,0,0\}$

Where μ_a is the energy per element ratio (EER) defined as

$$\mu_a = \frac{\varepsilon_a}{N} \leq 1 \tag{1-9}$$

The equality $\mu_a = 1$ is achieved when the sequence is bipolar.

1.5 Walsh-Hadamard Sequences

Walsh-Hadamard (WH) sequences are created out of Hadamard matrix $\boldsymbol{H_N} = \left[\boldsymbol{h_1}, \ldots, \boldsymbol{h_n} \ldots, \boldsymbol{h_N}\right]^{\boldsymbol{T}}$ of order N. Any pair of bipolar WH sequences $\boldsymbol{h_i}$ and $\boldsymbol{h_j}$ is orthogonal that is

$$E_{\boldsymbol{h_i h_j}}(0) = \begin{cases} N & i = j \\ 0 & i \neq j \end{cases} \tag{1-10}$$

Higher order Hadamard matrices are generated recursively using

$$\boldsymbol{H_{2N}} = \begin{bmatrix} \boldsymbol{H_N} & \boldsymbol{H_N} \\ \boldsymbol{H_N} & -\boldsymbol{H_N} \end{bmatrix} \tag{1-11}$$

Example 1 of **Annex A** shows the construction of Hadamard matrices. The ACF of WH sequences do not have good characteristics; it can have more than one peak. The CCF can also have peaks in the out-of-phase shifts $(l \neq 0)$. Therefore, WH sequences do not have the best correlation properties.

1.6 Pseudo-Noise Sequences

A pseudo-noise (PN) sequence is a deterministic periodic sequence with properties associated with randomness. For example, when an ideal coin is tossed, the result is obviously either head 1 or tail 0. The sequence obtained by repeatedly tossing an ideal coin has the following properties [4]

1. Balance property: the number of $1s$ is approximately equal to the number of 0s.

2. Run property: a run is defined as a consecutive occurrence of $1s$ or $0s$. Short runs are more probable than long runs.

3. Correlation property: PN sequence and its cyclically shifted version have very low correlation values. The ACF general form of any PN sequence $\boldsymbol{a}$ is

$$E_{\boldsymbol{a}}(l) = \begin{cases} N & l = 0 \\ k & l \neq 0 \end{cases} \tag{1-12}$$

Where k is preferably zero. These ideal properties can only be approximated in practice since the smallest possible values of k are ± 1 [4].

1.6.1 *M*-sequences

One type of PN sequences is the so called maximum length sequence (*m*-sequence). It has a length of $N = 2^m - 1$ and can be generated by m-stage linear feedback shift registers ($LFSR$) [4]. The generic form of $LFSR$ is depicted in Figure 1-3.

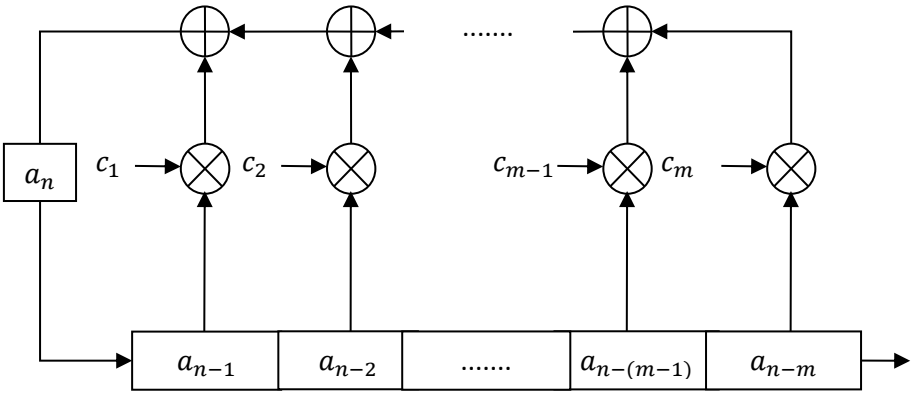

Figure 1-3 Generic $LFSR$ generator [6]

Where $(a_{n-1}, a_{n-2}, \dots, a_{n-m})$ are the contents (memory elements) of the LFSR and $(c_1, c_2, \dots, c_m)$ are the feedback connection coefficients.

The addition of elements is performed modulo-2 defined by $0 \oplus 0 = 1 \oplus 1 = 0$ and $0 \oplus 1 = 1 \oplus 0 = 1$. Table 1-3 lists the feedback connections for *m*-sequence and the number of available sequences for a given length, where the rest of m-sequences can be derived by means of sampling [4].

Table 1-3 Feedback taps for *m*-sequence [7]

Number of shift registers m	Sequence length $N = 2^m - 1$	Family size K	Feedback taps [4]
3	7	2	[2, 3]
4	15	2	[3, 4]
5	31	6	[3,5]
6	63	6	[5, 6]
7	127	18	[6, 7]

Example 2-a) in **Annex A** details the generation of an *m*-sequence of length $N = 7$. A subset of *m*-sequence set can exhibit three-valued periodic CCF. This subset is composed of a pair of sequences referred to as *preferred pair*. For the preferred pair of *m*-sequences of order m, the periodic CCF and ACF side-lobe values are restricted to the values given by $(-t\,(m),\ -1,\ t\,(m)-2)$, where [8]

$$t(m) = \begin{cases} 2^{\frac{m+1}{2}} + 1 & m\ odd \\ 2^{\frac{m+2}{2}} + 1 & m \equiv 2\ mod\ 4 \end{cases} \quad (1\text{-}13)$$

Note that preferred sequences *do not exist* for lengths where m is a multiple of four [8]. The Feedback taps for preferred pairs of m-sequence are given in Table 1-4.

Table 1-4 Preferred pairs of *m*-sequences

Number of shift registers m	Sequence length $N = 2^m - 1$	Feedback taps for preferred pairs of m-sequence
3	7	[1, 3], [2, 3]
4	–	–
5	31	[3, 5], [2, 3, 4 ,5]
6	63	[5, 6], [1, 6]
7	127	[6, 7] [1, 2, 3, 7]

1.6.2 **Gold Sequences**

Despite the nearly optimal ACF property of *m*-sequences, they present some weaknesses; The CCF peak values increase quite rapidly with the increase in sequence length. In addition, the number of sequences is rather small for practical purposes. Therefore, Gold sequences were proposed to provide sets of sequences with large number and lower cross-correlation values. In Table 1.5, Gold sequences properties are compared to *m*-sequences.

Table 1-5 Comparison between Gold sequence *m*-sequences [7]

Sequence length	m-sequences		Gold sequences	
	Family size	CCF Peak	Family size	CCF Peak
7	2	5	9	5
15	2	9	-	-
31	6	11	33	9
63	6	23	65	17
127	18	41	129	17

To generate Gold sequences, preferred pair of *m*-sequences is used. New sequences can be added by a process of modulo-2 addition as illustrated in Figure 1-4. Each successive shift produces a new Gold sequence. Gold sequences set can be written as $\{\boldsymbol{a}, \hat{\boldsymbol{a}}, \boldsymbol{a} \oplus \hat{\boldsymbol{a}},\ \boldsymbol{a} \oplus T^1\hat{\boldsymbol{a}}, \dots,\ \boldsymbol{a} \oplus T^{N-1}\hat{\boldsymbol{a}}\}$ [8].

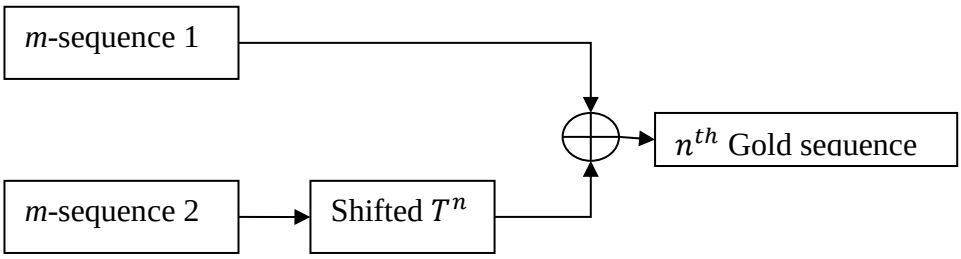

Figure 1-4 Gold sequence generator

Since there are N possible cyclic shifts ($n = 0,1, \dots, N-1$) between the preferred pairs of m-sequences of length N, the available set size for the Gold sequence family is $N +$

$2 = 2^m + 1$. Example 2-b) in **Annex A** details the generation of $K = 9$ Gold sequences each with length $N = 7$.

1.6.3 Orthogonal Gold Sequences

Experiments results show that CCF values of the Gold sequences are "-1" for many sequence shifts [4]. This suggests that it may be possible to turn the "-1" CCF values to "0" by attaching an additional "0" to the original unipolar Gold sequences. In fact, $K = 2^m$ orthogonal sequences (except $\hat{\boldsymbol{a}}$) can be obtained by this simple zero-padding [9]. These sequences referred to as orthogonal Gold sequences (OG) show reasonable cross-correlation and off-peak autocorrelation values. Example 2-c) in **Annex A** details the generation of $K = 8$ orthogonal Gold sequences each with length $N = 8$.

1.7 Complementary Sequences

1.7.1 Complementary Pairs

Complementary pairs (CPs) were first introduced by Golay [10]. A set of CPs is defined as a pair of equally long which have the property that the number of pairs of like elements with any given separation in one sequence is equal to the number of pairs of unlike elements with the same separation in the other sequence [10]. The latter property can also be expressed in aperiodic ACF terms; A pair of two bipolar sequences ($\boldsymbol{a}$, $\boldsymbol{b}$) is a CP if the sum of their aperiodic ACFs is [10]

$$\theta_{\boldsymbol{a}}(l) + \theta_{\boldsymbol{b}}(l) = \begin{cases} 2N, & l = 0 \\ 0, & l \neq 0 \end{cases} \tag{1-14}$$

Example 3-a) in **Annex A** analyze the properties an CP each with length $N = 8$. A complementary set of M sequences is a set where the sum of aperiodic ACFs of all its sequences is zero. Table 1-6 shows complementary sets of lengths 3,5, and 7.

Table 1-6 Complementary sets [10]

Length N	Complementary sets
3	$(1\ 1\ 1;\ -1\ 1\ 1;\ 1\ -1\ 1;\ 1\ 1\ -1)$
5	$(1-1-1-1-1;\ -1\ 1\ 1-1\ 1;\ 1-1-1-1\ 1;\ -1-1-1\ 1-1)$
7	$(111-1111;\ 1-1111-1-1;\ 1-1-11-111;\ 11-11-1-1-1)$

To extend the length of a CP we use the following property [10].

Property: let $(\boldsymbol{a},\ \boldsymbol{b})$ be an CP each of length L, an extended pair of two concatenated sequences such as $(\boldsymbol{ab},\ (-\boldsymbol{a})\boldsymbol{b})$ is also a CP. Applying the latter operation m times results in a pair of sequences each of length $N = 2^m L$.

1.7.2 Orthogonal Golay Complementary Sequences

Orthogonal Golay complementary (OGC) sequences set can be recursively obtained in [11] as

$$\boldsymbol{H}_{2N}^{CP} = \begin{bmatrix} \boldsymbol{H}_N^{CP} & \overline{\boldsymbol{H}}_N^{CP} \\ \boldsymbol{H}_N^{CP} & -\overline{\boldsymbol{H}}_N^{CP} \end{bmatrix} \tag{1-15}$$

Where $\boldsymbol{H}_N^{CP} = [\boldsymbol{A} \quad \boldsymbol{B}]$, $\boldsymbol{A}$ and $\boldsymbol{B}$ are a CP, and $\overline{\boldsymbol{H}}_N^{CP} = [\boldsymbol{A} \quad -\boldsymbol{B}]$ (the right half columns are reversed). Example 3-b) in **Annex A** details the generation of $K = 4$ OGC sequences each with length $N = 4$.

1.7.3 Mutually Orthogonal Complementary Sets

We define a matrix $\boldsymbol{F}$ where each element is a sequence of length L. The number of rows is K each contains M elements as

$$\boldsymbol{F} = \begin{bmatrix} \boldsymbol{F_{11}} & \boldsymbol{F_{12}} & \cdots & \boldsymbol{F_{1M}} \\ \boldsymbol{F_{21}} & \boldsymbol{F_{22}} & & \boldsymbol{F_{2M}} \\ \vdots & & \ddots & \vdots \\ \boldsymbol{F_{K1}} & \boldsymbol{F_{K2}} & \cdots & \boldsymbol{F_{KM}} \end{bmatrix} \tag{1-16}$$

The sequence length is $N = ML$. $\boldsymbol{F}$ is defined as Mutually Orthogonal Complementary Set (MOCS) if elements belonging to the same column form a complementary set sequences from the same row are orthogonal that is [12]

$$\sum_{k=1}^{K} \theta_{\boldsymbol{F_{km}}}(l) = 0, \quad \forall m, \forall\, l \neq 0 \tag{1-17}$$

$$\sum_{k=1}^{K} \theta_{\boldsymbol{F_{km}F_{kn}}}(l) = 0, \ \ \forall m \neq n\,, \forall l \tag{1-18}$$

Matrices $\boldsymbol{F_1'}$ and $\boldsymbol{F_2'}$ generated respectively by interleaving and concatenation are also a MOCS [12]

$$\boldsymbol{F_1'} = \begin{bmatrix} \boldsymbol{F}\otimes\boldsymbol{F} & (-\boldsymbol{F})\otimes\boldsymbol{F} \\ (-\boldsymbol{F})\otimes\boldsymbol{F} & \boldsymbol{F}\otimes\boldsymbol{F} \end{bmatrix} \tag{1-19}$$

$$\boldsymbol{F_2'} = \begin{bmatrix} \boldsymbol{FF} & (-\boldsymbol{F})\boldsymbol{F} \\ (-\boldsymbol{F})\boldsymbol{F} & \boldsymbol{FF} \end{bmatrix} \tag{1-20}$$

Note that $\boldsymbol{F}\otimes\boldsymbol{F}$ denotes the matrix whose ith row is obtain by interleaving the ith row of F and the ith row of $\boldsymbol{F}$ whereas $\boldsymbol{FF}$ denotes the matrix whose ith row is obtain by concatenating the ith row of F and the ith row of $\boldsymbol{F}$ [12]. Example 3-b) in **Annex A** gives a basic MOCS and details the generation of $K = 4$ MOCS sequences each with length $N = 8$.

1.8 Zero Correlation Zone Sequences

Let a set $\boldsymbol{Z}$ with K sequences where $\boldsymbol{Z} = \{\boldsymbol{z_1}, \dots, \boldsymbol{z_k}, \dots, \boldsymbol{z_K}\}$ each with length N where $\boldsymbol{z_k} = \{z_{k,1}, \dots, z_{k,n}, \dots, z_{k,N}\}$. The set $\boldsymbol{Z}$ can also be written in matrix form as

$$\boldsymbol{Z} = \begin{bmatrix} z_{11} & \dots & z_{1,n} & \dots & z_{1,N} \\ \vdots & \ddots & \vdots & \ddots & \vdots \\ z_{k1} & \dots & z_{k,n} & \dots & z_{k,N} \\ \vdots & \ddots & \vdots & \ddots & \vdots \\ z_{K1} & \dots & z_{K,n} & \dots & z_{K,N} \end{bmatrix} \tag{1-21}$$

A ZCZ sequence set is denoted by $ZCZ(N, K, Z_0)$, where N is the sequence length, K the number of sequences, and Z_0 is the zero-zone length. Any pair of ZCZ sequences $(\boldsymbol{z_i} \quad \boldsymbol{z_j})$ in a set has the following correlation property [13]

$$E_{\boldsymbol{z_i z_j}}(l) = \begin{cases} \mu_i N & l = 0, \ \ i = j \\ 0 & l = 0, \ \ i \neq j \\ 0 & 0 < |l| \leq Z_0 \end{cases} \tag{1-22}$$

The following bound has been set on the parameters of ZCZ sequence set [14]

$$Z_0 \ \leq \ \frac{N}{K} - 1 \tag{1-23}$$

From equation above, note that there is a tradeoff between the Z_0 width and the family size K. For a fixed length N, increasing K size must be achieved at the cost of reduced Z_0 and vice versa. A ZCZ sequences set that satisfies the theoretical limit is called an optimal ZCZ set. For bipolar sequence set, ZCZ bound becomes even tighter [15]

$$Z_0 \leq \frac{N}{2K} \tag{1-24}$$

1.8.1 Binary ZCZ Sequences

1.8.1.1 Fan et al [13]

Let a MOCS matrix $\boldsymbol{F}^{(n)}$ with K rows each of length N. Using the concatenation operation in Eq. 1-20, we can obtain a matrix $\boldsymbol{F}^{(n+1)}$ with $2K$ rows each of length $2N$. If the basic starter $\boldsymbol{F}^{(0)}$ is a Hadamard matrix of order 2 ($K = N = 2$), the rows of MOCS $\boldsymbol{F}^{(n)}$ extended n times form ZCZ sequences of $ZCZ(2^{2n+1}, 2^{n+1}, 2^{n-1})$, where $n \geq 1$. CPs of length $L = 2^m$ each can also be used to generate $ZCZ(2^{2n+m+1}, 2^{n+1}, 2^{n+m-1})$ using the concatenation operation. Example 4-a) in **Annex A** details the generation of Fan et al binary ZCZ sequences set of size $K = 4$, sequence length $N = 8$, and zero-zone $Z_0 = 1$.

1.8.1.2 Maeda et al [16]

A set of ZCZ sequences can be constructed from WH matrix $\boldsymbol{H}_L$ and interleaving technique. The starter matrix is obtained as follows

$$\boldsymbol{F} = \begin{bmatrix} \boldsymbol{F^1} \\ \boldsymbol{F^2} \end{bmatrix} = \begin{bmatrix} -\boldsymbol{H_L} & +\boldsymbol{H_L} & +\boldsymbol{H_L} & +\boldsymbol{H_L} \\ +\boldsymbol{H_L} & +\boldsymbol{H_L} & -\boldsymbol{H_L} & +\boldsymbol{H_L} \end{bmatrix} \tag{1-25}$$

There are $K = 2L$ sequences in $\boldsymbol{F}$ each of length $N = 4L$.We use the interleaving operation of $\boldsymbol{F^1}$ and $\boldsymbol{F^2}$ to obtain

$$\boldsymbol{Z^{(0)}} = \begin{bmatrix} \boldsymbol{F^1} \otimes \boldsymbol{F^2} \\ \boldsymbol{F^1} \otimes (-\boldsymbol{F^2}) \end{bmatrix} \tag{1-26}$$

The set $\boldsymbol{Z^{(0)}}$ is a ZCZ sequences set with $ZCZ(8L,\ 2L, 1)$. In general, an extended set $\boldsymbol{Z^{(m)}}$ with $ZCZ(2^{m+3}L,\ 2L,\ 2^{m+1}-1)$ can be recursively constructed by interleaving ZCZ sequence set $\boldsymbol{Z^{(m-1)}}$ as

$$\boldsymbol{Z^{(m)}} = \begin{bmatrix} \boldsymbol{Z^{(m-1)}} \otimes \boldsymbol{Z^{(m-1)}} \\ \boldsymbol{Z^{(m-1)}} \otimes (-\boldsymbol{Z^{(m-1)}}) \end{bmatrix} \tag{1-27}$$

Example 4-b) in Annex A details the generation of Maeda et al ZCZ sequences set of size $K = 4$, sequence length $N = 16$, and zero-zone $Z_0 = 1$.

1.8.1.3 Cha et al [17]

A set of ZCZ sequences can be constructed from binary perfect sequence $\boldsymbol{p^{(0)}}$ of length 4. First, the perfect sequence is extended as

$$\boldsymbol{p^{(n)}} = [\boldsymbol{p^{(n-1)}} \quad \overline{\boldsymbol{p}}^{(n-1)}] \tag{1-28}$$

Where $n \geq 1$ and $\overline{\boldsymbol{p}}$ means that the right half columns of $\boldsymbol{p}$ are reversed. The length of $\boldsymbol{p^{(n)}}$ is $N = 4{\times}2^n$. Another sequence $\boldsymbol{g^{(n)}}$ can be generated as

$$g_i^{(n)} = (-1)^i p_i^{(n)} \tag{1-29}$$

Where $p_i^{(n)}$ is an element of $\boldsymbol{p^{(n)}}$ and $i = 1, \ldots, N$.

The pair $(\boldsymbol{p^{(n)}}, \boldsymbol{g^{(n)}})$ is called *binary preferred pair*. The number of sequences in the set can be further increased as

$$\boldsymbol{Z} = \left\{\boldsymbol{p^{(n)}}, \boldsymbol{g^{(n)}},\ \boldsymbol{T^{\Delta}p^{(n)}}, \boldsymbol{T^{\Delta}g^{(n)}}, \ldots, \boldsymbol{T^{s\Delta}p^{(n)}}, \boldsymbol{T^{s\Delta}g^{(n)}}\right\} \tag{1-30}$$

Where $\Delta > 0$ is a shift increment and $s > 0$ is the maximum shift related as follows

$$(s+1)\Delta \leq \frac{N}{4} + 1 \tag{1-31}$$

The ZCZ set size is given as follows

$$K = \quad 2(s+1) \tag{1-32}$$

And Z_0 length is given as

$$Z_{cz} = \quad |2\Delta - 1| \tag{1-33}$$

Where $Z_{cz} = 2Z_0 + 1$. Example 4-c) in Annex A details the generation of Cha et al ZCZ sequences set of size $K = 4$, sequence length $N = 16$, and zero-zone $Z_0 = 1$.

1.8.2 Ternary ZCZ Sequences

1.8.2.1 Hayashi [18]

From a Hadamard matrix $\boldsymbol{H_L}$, a ternary set $\boldsymbol{F}$ of $K = 2L$ sequences each of length $N = 2(L+1)$ can be obtained by adding columns of zero elements as

$$\boldsymbol{F} = \begin{bmatrix} \boldsymbol{F^1} \\ \boldsymbol{F^2} \end{bmatrix} = \begin{bmatrix} +\boldsymbol{H}_L & \boldsymbol{0} & +\boldsymbol{H_L} & \boldsymbol{0} \\ +\boldsymbol{H}_L & \boldsymbol{0} & -\boldsymbol{H_L} & \boldsymbol{0} \end{bmatrix} \tag{1-34}$$

A ternary ZCZ sequence set $\boldsymbol{Z^{(0)}}$ is obtained by interleaving rows from $\boldsymbol{F^1}$ and $\boldsymbol{F}^2$ as

$$\boldsymbol{Z^{(0)}} = \begin{bmatrix} \boldsymbol{F^1} \otimes \boldsymbol{F^2} \\ \boldsymbol{F^1} \otimes (-\boldsymbol{F^2}) \end{bmatrix} \tag{1-35}$$

The set $\boldsymbol{Z^{(0)}}$ constitutes a starter set. In general, an extended set $\boldsymbol{Z^{(m)}}$ can be recursively constructed by interleaving ZCZ sequence set $\boldsymbol{Z^{(m-1)}}$ as

$$\boldsymbol{Z^{(m)}} = \begin{bmatrix} \boldsymbol{Z^{(m-1)}} \otimes \boldsymbol{Z^{(m-1)}} \\ \boldsymbol{Z^{(m-1)}} \otimes (-\boldsymbol{Z^{(m-1)}}) \end{bmatrix} \tag{1-36}$$

Thus, we obtain ternary ZCZ sequence set of $ZCZ(2^{m+2}(L+1), 2L, 2^{m+1} - 1)$. Example 5-a) in Annex A details the generation of Hayashi's ternary ZCZ sequences set of size $K = 8$, sequence length $N = 20$, and zero-zone $Z_0 = 1$.

1.8.2.2 Takatsukasa et al [5]

This construction is based on a ternary perfect sequence $\boldsymbol{t} = (t_1, \dots, t_n, \dots, t_{N_1})$ and binary orthogonal set $\boldsymbol{H}_{N_2} = \left[\boldsymbol{h_1}, \dots, \boldsymbol{h_i} \dots, \boldsymbol{h_{N_2}}\right]^T$. If the greatest common divisor $\gcd(N_1, N_2) = 1$, a ternary ZCZ sequence set $\boldsymbol{Z}$ with $ZCZ(N_1N_2, N_2, N_1 - 1)$ can be constructed as follows

$$z_{i,k} = \quad t_{k \bmod N_1} h_{i,k \bmod N_2} \tag{1-37}$$

Where $k = 1, \dots, N_1N_2$, for ZCZ sequence element $z_{i,k}$.
The ZCZ sequence obtained from Eq. 1-37 is

$$\boldsymbol{z_i} = \quad \left\{z_{i,1}, \dots, z_{i,k} \dots, z_{i,N_1N_2}\right\} \tag{1-38}$$

Example 5-b) in Annex A details the generation of Takatsukasa et al ternary ZCZ sequences set of size $K = 4$, sequence length $N = 28$, and zero-zone $Z_0 = 6$.

1.8.3 Optical ZCZ Sequences

Let a set $\boldsymbol{C}$ with K sequences each of length N where each element $c_{k,n} \in \{0,1\}$ as

$$\boldsymbol{C} = \begin{bmatrix} \boldsymbol{c_1} \\ \vdots \\ \boldsymbol{c_k} \\ \vdots \\ \boldsymbol{c_K} \end{bmatrix} = \begin{bmatrix} c_{1,1} & \dots & c_{1,n} & \cdots & c_{1,N} \\ \vdots & \ddots & \vdots & \ddots & \vdots \\ c_{k,1} & \dots & c_{k,n} & \cdots & c_{k,N} \\ \vdots & \ddots & \vdots & \ddots & \vdots \\ c_{K,1} & \dots & c_{K,n} & \cdots & c_{K,N} \end{bmatrix} \tag{1-39}$$

The set $\boldsymbol{C}$ is called optical ZCZ set if the correlation functions satisfy [19]

$$E_{\boldsymbol{c_i c_k}}(l) = \sum_{n=1}^{N} c_{i,n} c_{k,(n+l) mod N} = \begin{cases} w & i = k, l = 0 \\ 0 & i \neq k, l = 0 \\ 0 & 0 < |l| \leq Z_0 \end{cases} \tag{1-40}$$

Where w is the sequence Hamming weight (number of ones in in the sequence).

A system referred to as optical ZCZ-CDMA was proposed in [20]. Only few constructions of OZCZ sequences were proposed for this system. In this section, a new construction

method of OZCZ sequences family is proposed. Compared to other OZCZ sequences, the new set is easy to generate, has a large Hamming weight and a flexible zero-zone.

1.8.3.1 Proposed constructions

First, we define a bipolar matrix denoted by $\boldsymbol{F}$ of M rows each row of length N written as

$$\boldsymbol{F} = \begin{bmatrix} \boldsymbol{f^1} \\ \vdots \\ \boldsymbol{f^m} \\ \vdots \\ \boldsymbol{f^M} \end{bmatrix} = \begin{bmatrix} f_1^1 & \dots & f_n^1 & \dots & f_N^1 \\ \vdots & \ddots & \vdots & \ddots & \vdots \\ f_1^m & \dots & f_n^m & \dots & f_N^m \\ \vdots & \ddots & \vdots & \ddots & \vdots \\ f_1^M & \dots & f_n^M & \dots & f_N^M \end{bmatrix} \tag{1-41}$$

Where $f_n^m \in \{1, -1\}$ is the element of $\boldsymbol{F}$. Next, balanced sequences that satisfy $\sum_{n=1}^{N-1} f_n^m = 0$ are selected and denoted by $\boldsymbol{f^k}$ where $k = 1,2, \dots, K \leq M$. A unipolar sequence set $\boldsymbol{G^d}$ can be obtained using the following operation on $\boldsymbol{F}$

$$g_n^{k,d} = \frac{(-1)^d f_n^k + 1}{2} \tag{1-42}$$

Where $g_n^{k,d} \in \{0, 1\}$ is the element of $\boldsymbol{G^d}$ and $d \in \{1,0\}$.
The optical sequence set is a collection of pairs of bipolar and unipolar sequences

$$\{(\boldsymbol{f^1} \quad \boldsymbol{g^{1,d}}) \quad \dots \quad (\boldsymbol{f^k} \quad \boldsymbol{g^{k,d}}) \quad \dots \quad (\boldsymbol{f^K} \quad \boldsymbol{g^{K,d}})\} \tag{1-43}$$

Theorem [21]**:** A set of sequences obtained by applying Eq. 1-42 on any bipolar ZCZ sequences set that satisfies the balance condition is an OZCZ set; that is all the bipolar ZCZ sequences can be used to constructed OZCZ sequences for ZCZ-CDMA system if they satisfy the balance condition.

Example 5-b) in Annex A details the generation of two new constructions of OZCZ sequences set of size $K = 2$, sequence length $N = 8$, and zero-zone $Z_0 = 1$.

1.9 Zero Cross Correlation Sequences

The sequence set $\boldsymbol{C}$ of the previous section is called zero cross correlation (ZCC) set if the correlation functions satisfy [22]

$$E_{c_i c_k}(0) = \begin{cases} w & i = k \\ 0 & i \neq k \end{cases} \tag{1-44}$$

The code length for ZCC codes is $N = Kw$.

1.9.1 New ZCC sequences [23]

In this section, a simple and flexible construction method of ZCC sequences is presented. The construction procedure is as follows. For $w = 2$, a starter ZCC set of size $K = 2$ and sequence length $N = 4$ is given as follows

$$\boldsymbol{ZCC} = \begin{bmatrix} 1\,1 & 0\,0 \\ 0\,0 & 1\,1 \end{bmatrix} \tag{1-45}$$

To increase the number of codes to $K' = K + 1$, the following mapping technique is used

$$\boldsymbol{ZCC} = \begin{bmatrix} \boldsymbol{A} & \boldsymbol{B} \\ \boldsymbol{C} & \boldsymbol{D} \end{bmatrix} \tag{1-46}$$

Where $\boldsymbol{A}$ is the original ZCC set of $[K,\ N]$, $\boldsymbol{B}$ consists of $[K,\ w]$ zeros, $\boldsymbol{C}$ consists of $[1, N]$ zeros, and $\boldsymbol{D}$ of a $[1, w]$ ones.

For example, we can obtain a ZCC set of size $K = 3$, sequence length $N = 6$, and weight $w = 2$ by using the mapping technique of Eq. 1-46 on ZCC starter of Eq. 1-45 as

$$\boldsymbol{ZCC}_{\boldsymbol{w=2}}^{\boldsymbol{K=3}} = \begin{bmatrix} 1\,1\,0\,0 & 0\,0 \\ 0\,0\,1\,1 & 0\,0 \\ 0\,0\,0\,0 & 1\,1 \end{bmatrix} \tag{1-47}$$

In general, the ZCC sequence length is $N = Kw$.

1.9.2 Abd et al [22]

The construction procedure of Abd et al ZCZ set is as follows. For a given number of users K, a starter identity matrix is generated

$$\boldsymbol{I_K} = \begin{bmatrix} 1 & \dots & 0 & \dots & 0 \\ \vdots & \ddots & \vdots & \ddots & \vdots \\ 0 & \dots & 1 & \dots & 0 \\ \vdots & \ddots & \vdots & \ddots & \vdots \\ 0 & \dots & 0 & \dots & 1 \end{bmatrix}_K \tag{1-48}$$

Obviously, the set $\boldsymbol{I_K}$ is a ZCC set with sequence length $N = K$ and a Hamming weight $w = 1$. To increase the sequence weight to $w = 2$, a mapping technique is used as follows

$$\boldsymbol{ZCC} = \begin{bmatrix} \boldsymbol{I_K} & \vec{\boldsymbol{I}}_{\boldsymbol{K}} \end{bmatrix} \tag{1-49}$$

Where $\vec{\boldsymbol{I}}_{\boldsymbol{K}}$ is the reverse of $\boldsymbol{I_K}$ given bellow

$$\vec{\boldsymbol{I}}_{\boldsymbol{K}} = \begin{bmatrix} 0 & \dots & 0 & \dots & 1 \\ \vdots & \ddots & \vdots & \ddots & \vdots \\ 0 & \dots & 1 & \dots & 0 \\ \vdots & \ddots & \vdots & \ddots & \vdots \\ 1 & \dots & 0 & \dots & 0 \end{bmatrix}_K \tag{1-50}$$

ZCC sets with bigger Hamming weight can be obtained by alternating between $\boldsymbol{I_K}$ and $\vec{\boldsymbol{I}}_{\boldsymbol{K}}$.

1.10 Conclusion

This chapter has presented some basic concepts which will be used in succeeding chapters. The most important concept is the correlation function. Theoretical correlation limits were presented. It was shown that it is generally not possible to achieve good ACF and CCF simultaneously. Thus, a good compromise must be found. In addition, various construction of sequences with specific correlation properties were discussed: perfect sequences, WH sequences, PN sequences, complementary sets, ZCZ, and ZCC sequences. Extensive design examples presented in Annex A allow constructions to be explained in a straightforward manner. In the next chapter, an overview of spread spectrum modulation and CDMA technique is given.

Chapter 2: An overview of Spread Spectrum and CDMA

2.1 Introduction

The spectrum available for radio communication is a limited resource which calls for optimal allotment to various services. In a multiuser system, efficient assignment of the transmitting bandwidth to each user becomes necessary. Spread spectrum (SS) is a mature technology that being applied in various communications systems such as non-cooperative surveillance [24], underwater wireless communications [25], navigation [26], and Ad-hoc network [27]. Direct sequence (DS) SS is being considered as a potential candidate for future 5G networks [28] such as coded non-orthogonal multiple access (NOMA) systems [29].

2.2 Spread Spectrum Modulation

Spread Spectrum is a modulation technique that uses a bandwidth well beyond what is necessary for the data rate. The spreading is accomplished using a spreading sequence. Direct-sequence spread spectrum DSSS is perhaps the most common form of spread spectrum. The simplest form of DSSS uses binary phase shift keying (BPSK) modulation. DSSS transmitter is illustrated in Figure 2-1.

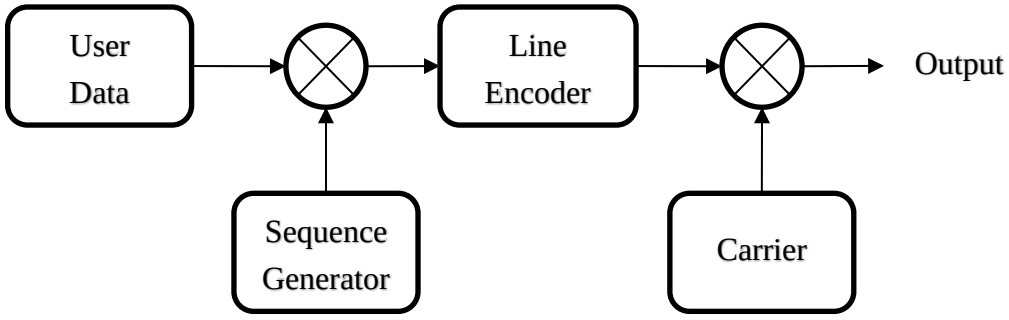

Figure 2-1 Direct-sequence transmitter

An illustration of the power spectral density (PSD) of the original information signal and the spread signal is plotted in Figure 2-2.

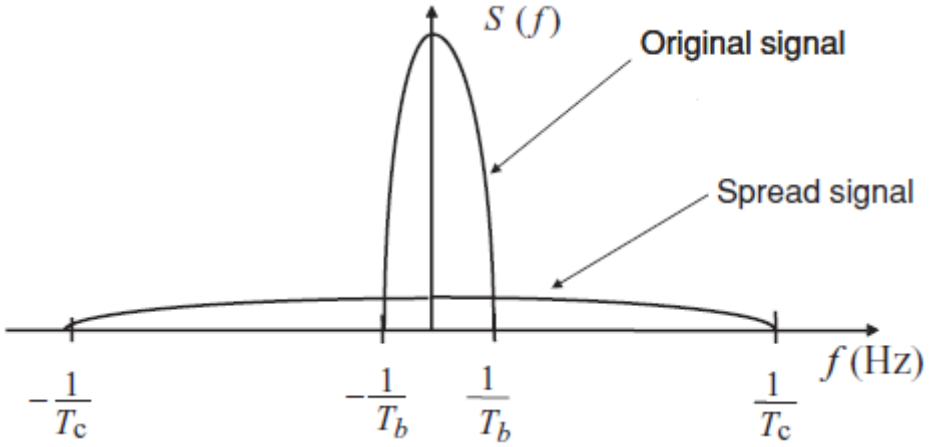

Figure 2-2 PSD of original and spread signals [30]

Where T_b and T_c are respectively the bit and chip durations.

2.3 Multiple access and multiplexing

Multiple access refers to multiple transmitters sending information to one or more receivers. Multiplexing refers to a single transmitter sending information to one or more receivers. Direct-sequence Code division multiple access (DS-CDMA) is one class of spread spectrum multiple access (SSMA) techniques in which many users access a common channel simultaneously using encoding. The other types of CDMA are given in Figure 2-3.

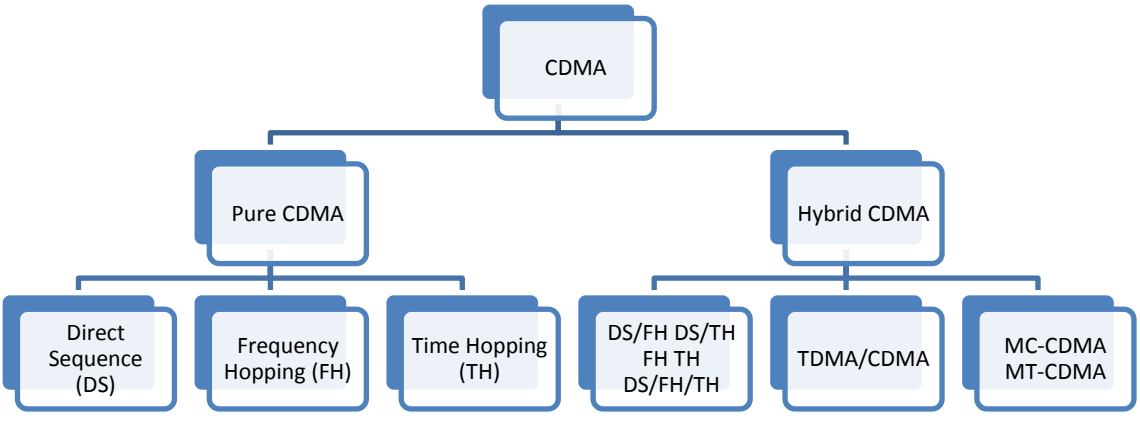

Figure 2-3 Various CDMA technologies [31]

The concept of CDMA can be simply explained by the following analogy [32]. Assume we have a few students gathered in a classroom who would like to talk to each other simultaneously. Either they must take turns to speak or use different languages to communicate. The latter option is similar to CDMA, student speaking the same language can understand each other while other student with different languages are perceived as noise and rejected. Similarly, in CDMA each user is assigned a unique spreading sequence. Many users occupy the radio channel but only those with a particular sequence can communicate. The bits of a CDMA sequence are called chips, and the chip rate is always greater than data rate.

Spreading sequence must have certain properties that facilitate demodulation by the intended receiver and make it as hard as possible for the unintended receiver. The DS-CDMA spreading operation is illustrated in Figure 2-4 a). The despreading of the received data is achieved by correlation with same sequence used at the transmitter (the mapping $1 \rightarrow -1$ and $0 \rightarrow 1$ is adopted) as shown in Figure 2-4 b).

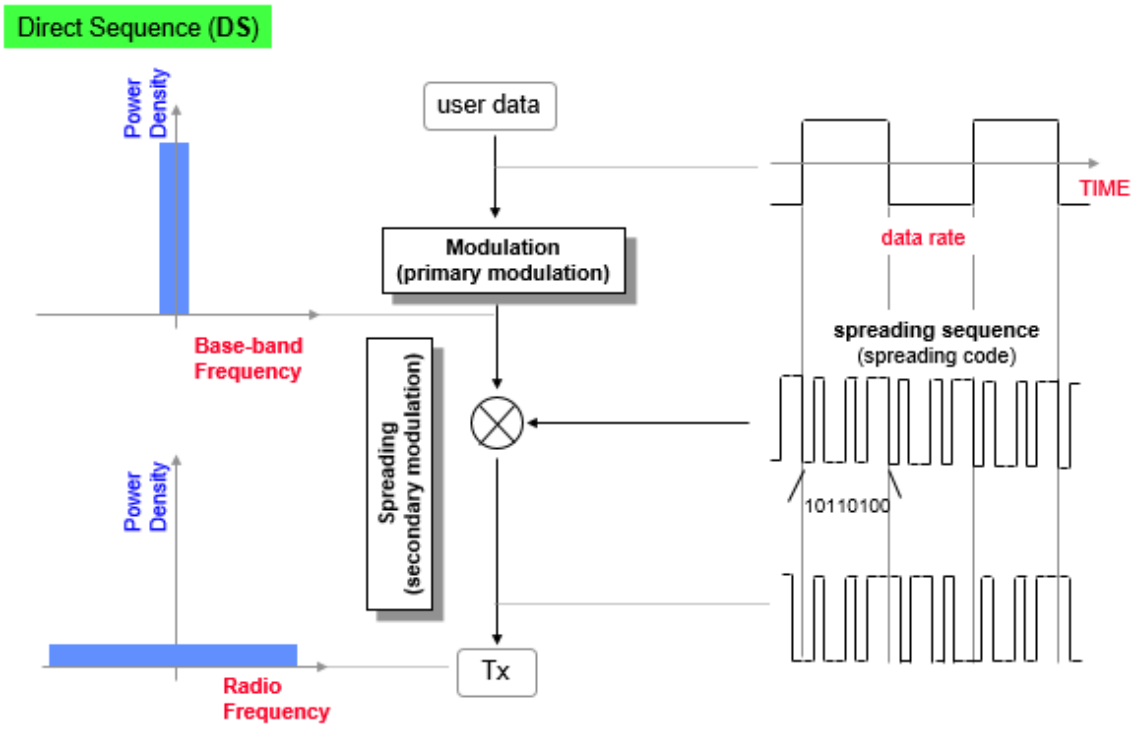

a)

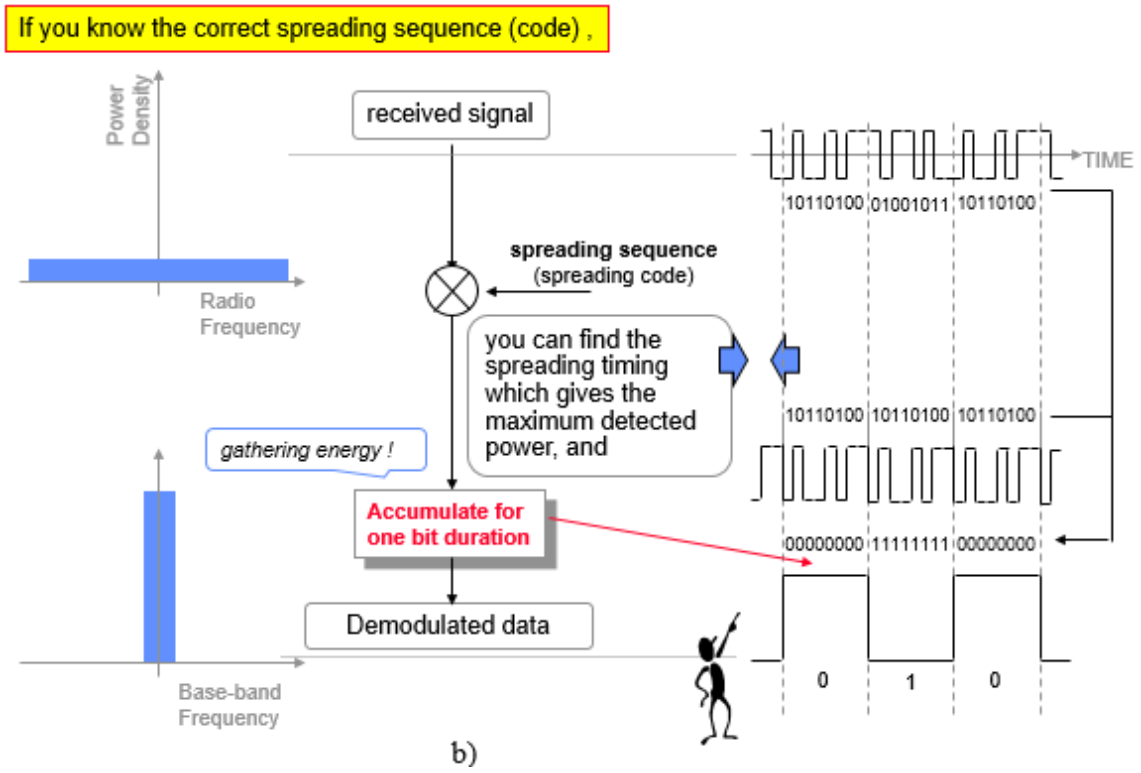

Figure 2-4 a) Spreading in DS-CDMA; b) Dispreading in DS-CDMA [32]

Unauthorized receiver cannot detect the signal as illustrated in Figure 2-5.

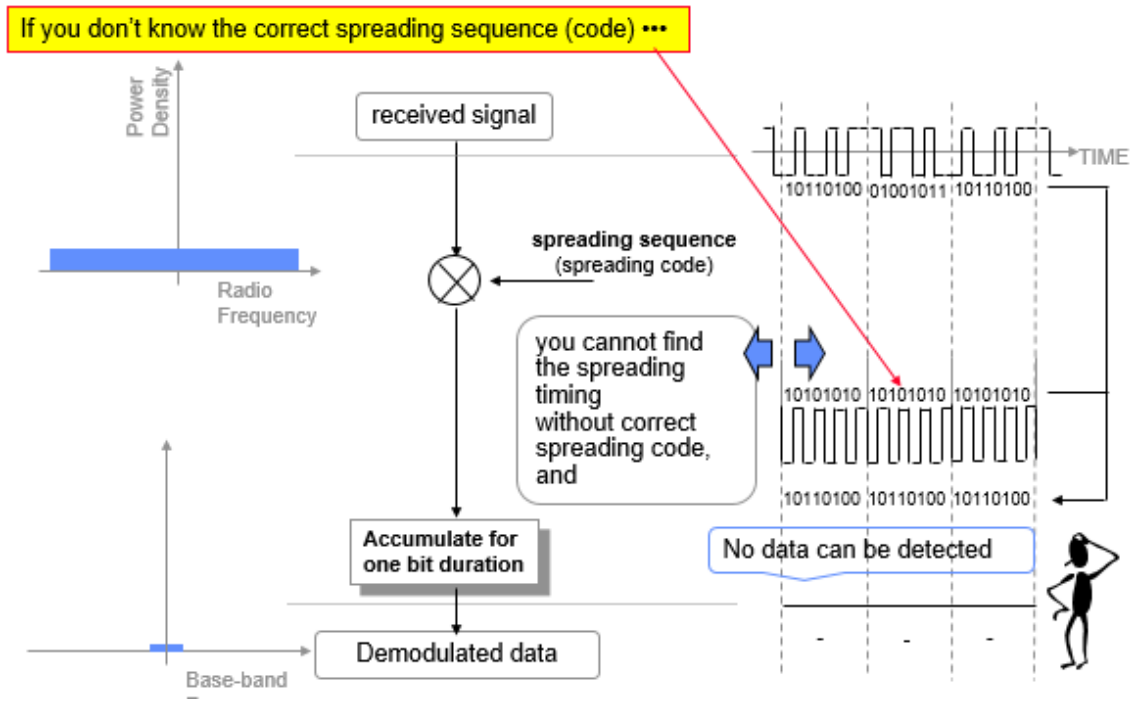

Figure 2-5 Dispreading at unauthorized receiver [32]

2.4 Noise and Interference

All wireless communication systems are subject to performance degradation caused by unknown signal superimposed on the signal of interest. Such intrusive additive radio frequency (RF) signals are generally classified as either noise or interference. The term noise usually refers to signals that are well characterized as random processes (such as the thermal noise in electronic circuits). The term interference, on the other hand, usually refers to signals that are more deterministic (such as signals from other wireless communication systems). Multiuser communications systems that employ CDMA exhibit a user capacity limit in the sense that there exists a maximum number of users that can simultaneously communicate over the channel for a specific level of performance per user [33]. This limitation brought about by the domination of the other users' interference over additive thermal noise. The multiuser interference (MUI) is illustrated in Figure 2-6.

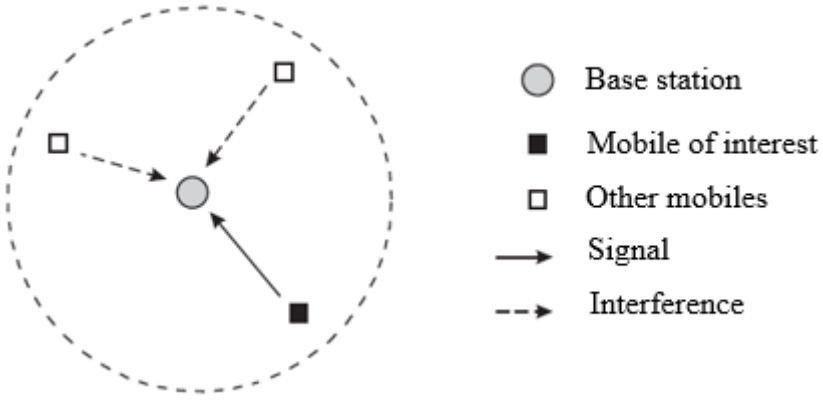

Figure 2-6 MUI in cellular systems

In addition, multipath is a phenomenon that happens when a signal arrives at the receiver via different paths and possibly at different times because of reflections as shown in Figure 2-7.

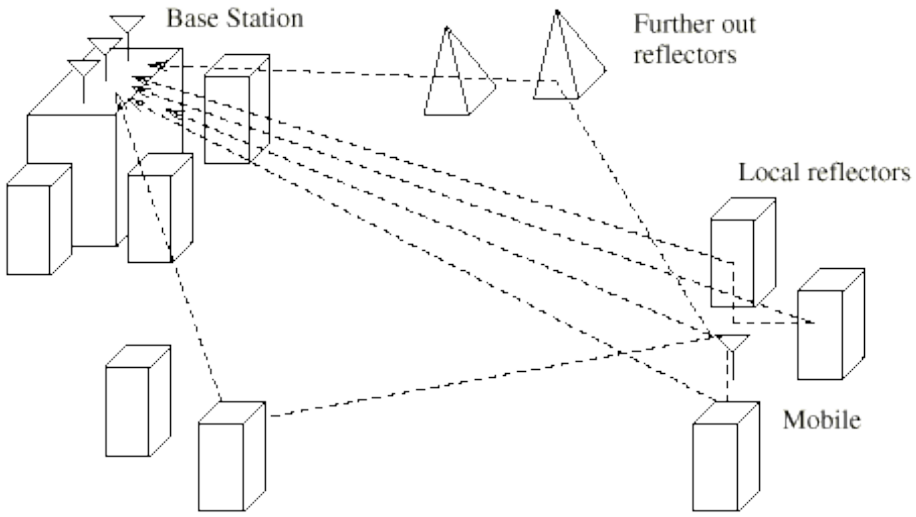

Figure 2-7 Wireless channel with multipath propagation [34].

CDMA system has the capacity of overcoming multipath interference (MPI) by using a rake receiver. It does this by using several sub-receivers (baseband correlators) each tuned (slightly delayed) to the individual multipath components. The correlators' outputs are then combined to achieve improved communication, higher signal-to-noise ratio (SNR). Figure 2-8 illustrates the rake receiver structure.

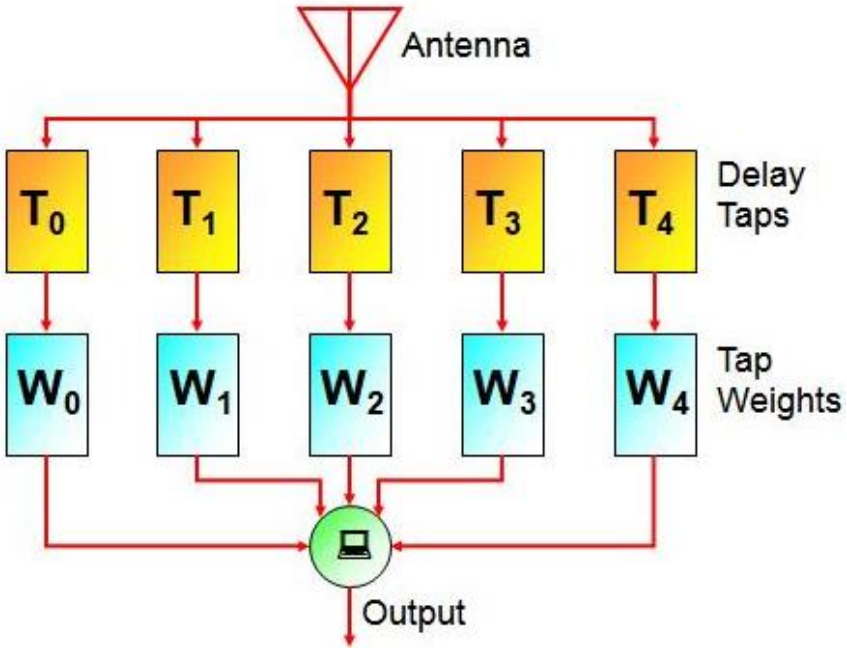

Figure 2-8 Generic Rake receiver [35]

There are two primary ways to combine the rake finger outputs. The first method called equal gain combining (EGC) weighs each output equally. The second method called maximum ratio combining (MRC) uses data to estimate weights coefficients that maximize SNR [31]. As for the improvement in performance, Table 2-1 gives the effect of rake receiver for $BER = 10^{-3}$.

Table 2-1 Rake receiver improvement [36]

System	Modulation	Rake (branches)	$SNR\ (dB)$
W-CDMA	BPSK	1	24
		2	14
		3	10

Where W-CDMA means wideband CDMA.

2.5 Delay Spread

Knowledge of the propagation characteristics of the medium is essential to the understanding and design of any communication system. A channel can be characterized as being either frequency-selective or frequency nonselective (fading affects all frequencies equally). Such characterization is based on the channel parameters, namely the delay spread T_d which is the time interval between the arrival of the first and last significant multipath signals seen by the receiver. Delay spread for different environments is given in Table 2-2.

Table 2-2 Delay spread of different environments [31]

Environment	Max path length (m)	Delay spread T_d
Indoor	$12 - 60$	$40 - 200\ nsec$
Outdoor	$300 - 6000$	$1 - 20\ \mu sec$

A flat fading channel has a coherence bandwidth greater than the transmitted signal bandwidth where the coherence bandwidth W_c of a multipath channel is defined as

$$W_c = \frac{1}{2\pi T_d} \tag{2-1}$$

2.6 Power control

2.6.1 Uplink and downlink

Synchronized communication is used typically when a single station transmits to mobiles as in the forward link of cellular networks while asynchronous transmission is used when mobiles independently transmits to a station such as the reverse link of cellular networks. Figure 2-9 shows forward and reverse links for cellular network.

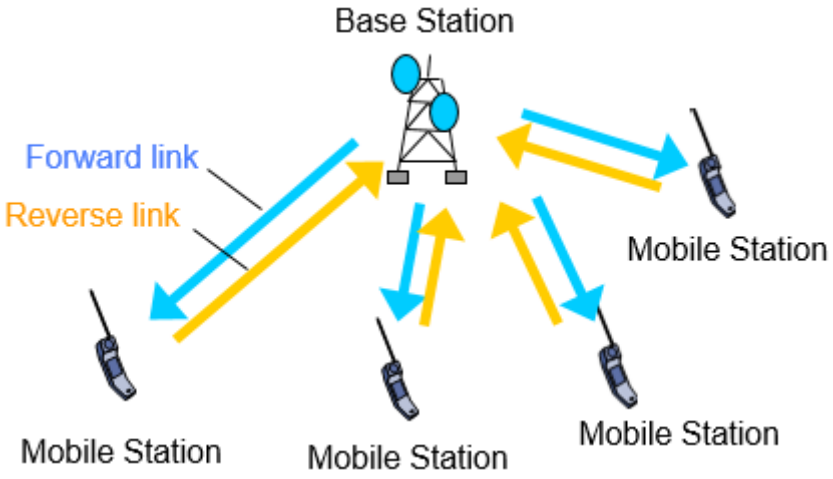

Figure 2-9 Multiple access in cellular networks [32]

2.6.2 Power Control

When a base station (BS) is receiving signals simultaneously from two mobiles, one close to the BS and the other far from it the near-far problem occurs. Let's suppose that the second mobile is the desired transmitter. If both mobiles transmit at the same power level, the interferer (mobile closest to the BS) will be the predominant signal at the BS receiver. Therefore, the detection of the desired signal will be subject to high BER. To solve this problem, the BS measures the signal from a mobile, and if it is above a threshold, it sends a command to that station to reduce its power to a level equals to the other mobiles. This is called *power control*.

2.7 Multicarrier Modulation

The multicarrier (MC) modulation involves a multitude of parallel *subcarriers* to transmit symbols of the same data stream. Unlike DS-CDMA, where an appropriate signature

time-domain spreading sequence provide separation of user signals, in multicarrier CDMA (MC-CDMA) signatures are formed in the frequency domain, by controlling amplitudes and phases of subcarriers in a user-specific manner. Figure 2-10 illustrates the transmitter diagram of MC-CDMA.

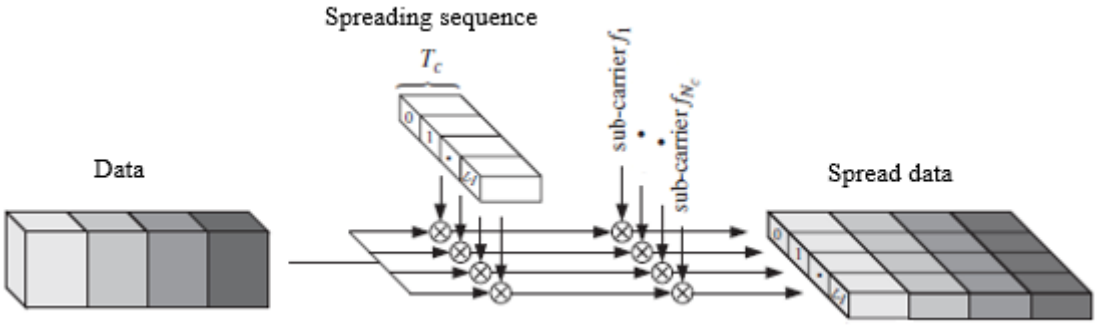

Figure 2-10 MC-CDMA Transmitted signal [37]

Where T_c is the spreading sequence element duration and $f_1, \dots, f_N$ are subcarriers frequencies. Note that this scheme does not include serial to parallel data conversion, therefore the data rate on each of the subcarrier is the same as the input data rate.

2.8 Applications

2.8.1 Ad-hoc Networks

An ad-hoc network is a group of devices communicating with each other directly. If two devices cannot communicate directly, an intermediate device (s) is used to relay from the source to the destination. DS-CDMA is advantageous for ad-hoc networks where it imposes no sharp upper bound on the number of mobiles and directly benefits from inactive terminals in the network [27]. Ad-hoc networks have the following features

- *No centralized access point:* many Ad-hoc networks are local area networks where computers or other devices are enabled to send data directly to one another rather than going through a base station.
- *Dynamic topology:* The problem of changing network topology occurs in, for example, in sensor-laden cars exchanging data about traffic conditions as they weave among each other on a busy state highway.

- *Limited power and capacity (memory and processing):* The need to maximize the efficiency of data exchange — in order to minimize energy consumption — makes designing communications protocols for ad-hoc networks a challenging task.

2.8.2 Underwater Communications

Underwater acoustic communication (UAC) is the wireless communication in which acoustic waves carry digital signal through an underwater channel. UAC has been receiving intention due to its application in [38]

- *Marine research:* collection of scientific data recorded at ocean-bottom stations to monitor pollution and climate environmental systems
- *Marine commercial operations:* remote control in off-shore oil and gas industry, unmanned underwater vehicles, speech transmission between divers, and mapping of the ocean floor for detection of objects and discovery of new resources.
- *Defense:* submarines and autonomous underwater vehicles (AUVs).

2.8.3 Satellite communication

Satellites are used as signal relaying stations to convey communications to and from different mobiles to the outside networks as shown in Figure 2-11.

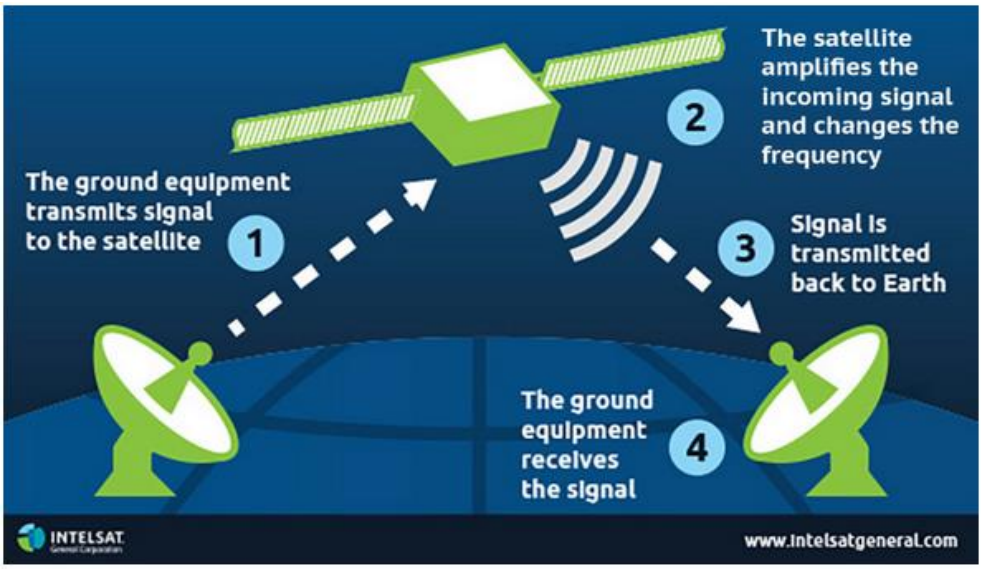

Figure 2-11 CDMA-based Satellite system

Because their applications are not limited by the geographical locations, satellite-based communications play an important role in disaster relief and military operations. CDMA is used in satellite-based global navigation systems (GNSS) such as [39] the navigation satellite timing and Ranging System (NAVSTAR) which is a constellation of 27 satellites deployed around the earth and managed by the United States Air Force (USAF).

2.9 Conclusion

In this chapter, we gave an overview on spread spectrum modulation and CDMA technique. The propagation characteristics of an RF channel was also addressed. Various operations such as rake receiver, power control, and multicarrier modulation were discussed. Lastly, some important applications of CDMA were mentioned. In the next chapter, we will investigate spreading sequences and their application to DS-CDMA system.

Chapter 3: On ZCZ Sequences and their Application to DS-CDMA

3.1 Introduction

In the previous chapter, we reviewed the basic concepts of multiple access spread spectrum and CDMA systems. The analysis in this chapter identifies parameters of the spreading sequence that influence CDMA system performance. Firstly, we will develop analytical approaches to derive the BER for quasi-synchronous and asynchronous DS-CDMA over multipath channels. Secondly, both binary and ternary spreading sequences will be evaluated. Lastly, it is point out that interference-free communication can be obtained only if both zero even and odd CCFs of binary ZCZ sequences are verified.

3.2 DS-CDMA System Model

Our goal in this section is to describe a communication link with several active transmitters and a single receiver. One of the transmitted signals is intended for the receiver and the rest produce undesired MUI. The basic model of DS-CDMA system in frequency non-selective fading channel of K users is illustrated in Figure 3-1.

3.2.1 Transmitter

For each user k, bipolar binary data $d_k(t)$ of duration T_b is multiplied by a spreading sequence $c_k(t)$ of duration T_c and length $N = T_b/T_c$.

$$d_k(t) = \sum_m d_{k,m} W(t - mT_b) \tag{3-1}$$

$$c_k(t) = \sum_n c_{k,n} W(t - nT_c) \tag{3-2}$$

Where $W(t)$ is the rectangular pulse waveform.

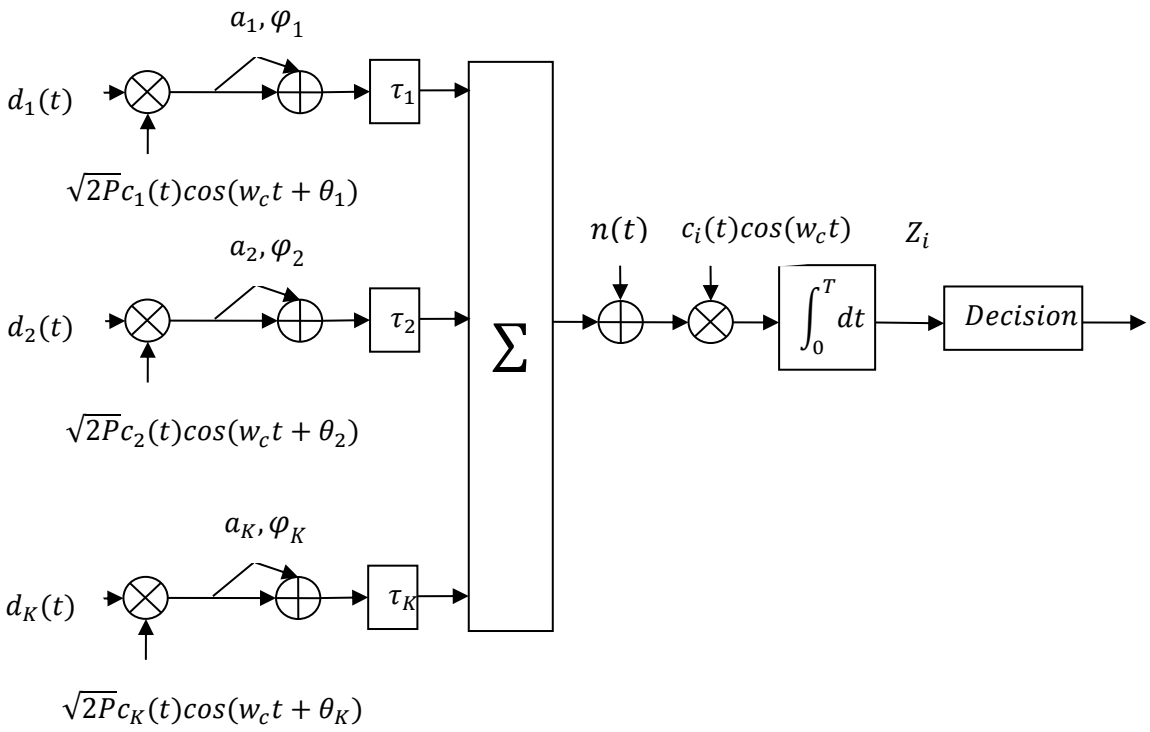

Figure 3-1 Generic DS-CDMA system [40]

After spreading, the k^{th} user's signal is modulated onto a carrier with initial phase θ_k, where θ_k is a random variable uniformly distributed over $[0, 2\pi]$. The common signal power and the center frequency are respectively denoted by P and w_c. The k^{th} transmitted signal can be expressed as

$$s_k(t) = Re\left\{\sqrt{2P}d_k(t)c_k(t)e^{j(w_c t+\theta_k)}\right\} \tag{3-3}$$

Where$Re\{.\}$ denotes the real part.

3.2.2 **Channel**

In quasi-synchronous systems, the relative time delay between different users T_q is restricted within few chips. Generally, the transmitted signals go through a multipath channel with random (or unknown) path characteristics, and which has additive white Gaussian noise (AWGN) present at the receiver. A path is defined as a group of sub-paths whose delays differ from one another by amounts much less than reciprocal of the transmission bandwidth [41]. The noise $n(t)$ is statistically independent of the multipath

medium, stationary, Gaussian, with two-sided flat power-density spectrum $N_0/2$ (at least over the transmission bandwidth). This noise model might correspond to thermal noise in the receiver. The channel output signal is a sum of L delayed, phase-shifted, and attenuated replicas of the transmitted signal [42]

$$y(t) = \sum_{k=1}^{K} \sum_{m=0}^{L-1} Re\{g_{k,m} s_k(t - \tau_{k,m})\} \tag{3-4}$$

Where $\tau_{k,m}$ is the m^{th} random delay of the k^{th} user uniformly distributed over $[0, T_q]$ and $g_{k,m}$ is complex gain coefficient that combines the m^{th} scatter path attenuation and phase-shifted components of the k^{th} user [43]

$$\begin{gathered} g_{k,0} = 1 + a_{k,0} e^{j\varphi_{k,0}} \\ \text{and } g_{k,m} = a_{k,m} e^{j\varphi_{k,m}} \text{ for } 1 \leq m \leq L-1 \end{gathered} \tag{3-5}$$

Where $a_{k,m}$ is the attenuation, and $\varphi_{k,m}$ is the phase-shift of k^{th} user signal coming from the m^{th} path.

If all the interferers happen to be close to the receiver, the MUI can be very large compared to the MPI [44]. In addition, for closely spaced geographical points, two signal replicas from the same transmitter with similar delays are more likely than those with large delays [44]. Therefore, we will consider only the 0^{th} path component ($m = 0$) and its sub-paths. The overall amplitude of the signal $g_{k,0}$ could be characterized by a Rician distribution [42]. The signal at the channel output is modeled as follows

$$y(t) = \sum_{k=1}^{K} Re\{g_{k,0} s_k(t - \tau_{k,0})\} \tag{3-6}$$

In the remaining analysis, we will drop the subscript 0.

3.2.3 **Derivation of a New BER in terms of ECF and OCF**

The received signal can be expressed as [42]

$$r(t) = \sum_{k=1}^{K} Re\{(1 + a_k e^{j\varphi_k}) s_k(t - \tau_k) + n(t)\} = y(t) + n(t) \quad (3\text{-}7)$$

Where $y(t)$ is the sum of signals from all transmitters.

As was stated earlier, for closely spaced geographical points, the MPI is small compared to MUI. Therefore, the DS-CDMA system under consideration will simply employ a conventional matched filter (correlator). The i^{th} correlator's output is

$$Z_i = \int_0^{T_b} r(t) c_i(t) \cos(w_c t)\, dt = D_i + I_i + N_i \quad (3\text{-}8)$$

Where D_i is the desired signal given as (see **Annex B.1**)

$$D_i = \sqrt{P/2}\, \mu_i T_b [1 + a_i \cos(\varphi_i)] \quad (3\text{-}9)$$

And the interference term is (see **Annex B.1**)

$$I_i = \sqrt{\frac{P}{2}} \sum_{\substack{k=1 \\ k \neq i}}^{K} \left[d_{k,-1} R_{c_k c_i}(\tau_k) + d_{k,0} \hat{R}_{c_k c_i}(\tau_k) \right] [\cos(\vartheta_k) + a_k \cos(\vartheta_k + \varphi_k)] \quad (3\text{-}10)$$

Where the data bits $d_{k,-1}$ and $d_{k,0}$ are respectively the previous and current symbols of the k^{th} user and $\vartheta_k = \theta_k - w_c \tau_k$. $R_{c_k c_i}(\tau_k)$ and $\hat{R}_{c_k c_i}(\tau_k)$ are called the continuous-time partial CCFs expressed in terms of even and odd correlation function as follows (see **Annex B.2**)

$$\hat{R}_{c_k c_i}(lT_c) = T_c \left(E_{c_k c_i}(l) + O_{c_k c_i}(l) \right)/2 \quad (3\text{-}11)$$

$$R_{c_k c_i}(lT_c) = T_c \left(E_{c_k c_i}(l) - O_{c_k c_i}(l) \right)/2 \quad (3\text{-}12)$$

The noise component is

$$N_i = \int_0^{T_b} n(t) c_i(t) \cos(w_c t)\, dt \quad (3\text{-}13)$$

The $SINR$ of user i is defined as [43]

$$SINR_i = \frac{E\{Z_i\}}{\sqrt{Var\{Z_i\}}} \tag{3-14}$$

Where $E\{.\}$ and $Var\{.\}$ are respectively the mathematical expectation (or mean) and the variance of a random variable.

It can be shown (see **Annex B.3**) that the mean of the desired signal component is

$$E\{D_i\} = \sqrt{P/2}\,\mu_i T_b \tag{3-15}$$

The interference and the noise signals are

$$E\{I_i\} = E\{N_i\} = 0 \tag{3-16}$$

And the correlator's output mean is

$$E\{Z_i\} = \sqrt{P/2}\,\mu_i T_b \tag{3-17}$$

As for the variances derivation, it can be shown (see **Annex B.4**) that

$$Var\{D_i\} = P\mu_i^2 T_b^2 \gamma/4 \tag{3-18}$$

Where $\gamma = E\{a_k^2\}$.

And the interference variance (see **Annex B.4**)

$$Var\{I_i\} = \frac{PT_c^2(1+\gamma)}{8N_q} \sum_{\substack{k=1 \\ k\neq i}}^{K} \sum_{l=0}^{N_q-1} \left(E_{c_k c_i}^2(l) + O_{c_k c_i}^2(l)\right) \tag{3-19}$$

Where $N_q = T_q/T_c$.

Also with a straightforward development, we can obtain the noise variance (see **Annex B.4**)

$$Var\{N_i\} = \mu_i T_b N_0/4 \tag{3-20}$$

The correlator's output variance is

$$Var\{Z_i\} = \frac{P\mu_i^2 T_b^2 \gamma}{4} + \frac{PT_b^2(1+\gamma)}{8N_q N^2} \sum_{\substack{k=1 \\ k\neq i}}^{K} \sum_{l=0}^{N_q-1} \left(E_{c_k c_i}^2(l) + O_{c_k c_i}^2(l) \right) + \frac{\mu_i T_b N_0}{4} \quad (3\text{-}21)$$

Where $T_c^2 = T_b^2/N^2$.

In [45], the authors state that when a transmitter and receiver use a DS-BPSK waveform to communicate, all the interference in the channel can be approximated as AWGN which justify the use of the Gaussian approximation to obtain the following $BER = Q(SINR_i)$. After simplification, we obtain [46]

$$BER_i = Q\left(\frac{1}{\sqrt{\frac{\gamma}{2} + \frac{(1+\gamma)}{4N_q N^2 \mu_i^2} \sum_{\substack{k=1 \\ k\neq i}}^{K} \sum_{l=0}^{N_q-1} \left(E_{c_k c_i}^2(l) + O_{c_k c_i}^2(l) \right) + \frac{N_0}{2E_b \mu_i}}} \right) \quad (3\text{-}22)$$

Where $Q(.)$ is the complementary error function and $E_b = T_b P$ is the data bit energy. Note that the above equation can easily be generalized to asynchronous case by letting $N_q = N$ as follows

$$BER_i = Q\left(\frac{1}{\sqrt{\frac{\gamma}{2} + \frac{(1+\gamma)}{4N^3 \mu_i^2} \sum_{\substack{k=1 \\ k\neq i}}^{K} \sum_{l=0}^{N-1} \left(E_{c_k c_i}^2(l) + O_{c_k c_i}^2(l) \right) + \frac{N_0}{2E_b \mu_i}}} \right) \quad (3\text{-}23)$$

A more appropriate performance measure is the averaged BER overall users

$$BER = \frac{1}{K} \sum_{i=1}^{K} BER_i \quad (3\text{-}24)$$

3.3 Numerical Results

The *BER* obtained in the previous section provides important criteria for the design of suitable spreading sequences for both quasi-synchronous and asynchronous DS-CDMA

systems. In this section, the obtained BER will be used to evaluate the performance of binary and ternary ZCZ sequences compared to the well-known Gold sequences. Note that ZCZ sequences are designed with zero even correlation functions (see Eq. 1-22 in chapter 1). This will reduce the amount of MUI which results in an improved BER as follows

$$BER_i = Q\left(\frac{1}{\sqrt{\frac{\gamma}{2} + \frac{(1+\gamma)}{4N_q N^2 \mu_i^2}\sum_{\substack{k=1 \\ k\neq i}}^{K}\sum_{l=0}^{N_q-1} O_{c_k c_i}^2(l) + \frac{N_0}{2E_b\mu_i}}}\right) \tag{3-25}$$

However, MUI still exists and can affect communication quality. To the best of our knowledge, only one construction of ternary ZCZ sequences proposed by Hayashi's [18] has both zero even and odd correlation functions. The latter sequences set eliminate MUI which results in an interference-free communication as follows

$$BER_i = Q\left(\frac{1}{\sqrt{\frac{\gamma}{2} + \frac{N_0}{2E_b\mu_i}}}\right) \tag{3-26}$$

In case of transmission in an AWGN channel where $\gamma = 0$, we have

$$BER_i = Q\left(\frac{1}{\sqrt{\frac{N_0}{2E_b\mu_i}}}\right) = Q\left(\sqrt{\frac{2E_b\mu_i}{N_0}}\right) \tag{3-27}$$

3.3.1 **Interference vs. Chip delay**

The MUI term is present in Eq.3-22 as a cumulative sum of CCFs. Here, we will evaluate the cumulative CCF (CCCF) of various binary ZCZ sequences (see section 1.8.1) and compare them to that of Gold sequence set. By letting $n = 2$ and $m = 1$ in Fan et al. construction (see section 1.8.1.1) we can obtain a binary ZCZ sequences set with $K = 8$ sequences each of length $N = 64$ that have a zero-zone of $Z_0 = 4$. Similarly, Maeda et al. construction (see section 1.8.1.2) can obtained by using a Hadamard matrix of order 4 and using interleaving once $m = 1$. The latter set has $K = 8$ sequences each of length

$N = 64$ with $Z_0 = 3$. Lastly, Cha et al binary ZCZ set obtained also by choosing $N = 64$ and $K = 8$ in Eqs. 1-31 and 1-32. The latter parameters can be used to determine the corresponding zero-zone $Z_0 = 3$ (see section 1.8.1.3). Gold sequences of length $N = 63$ are generated using the method given in section 1.6.2. The performance of various sequences in terms of CCCF is illustrated in Figure 3-2.

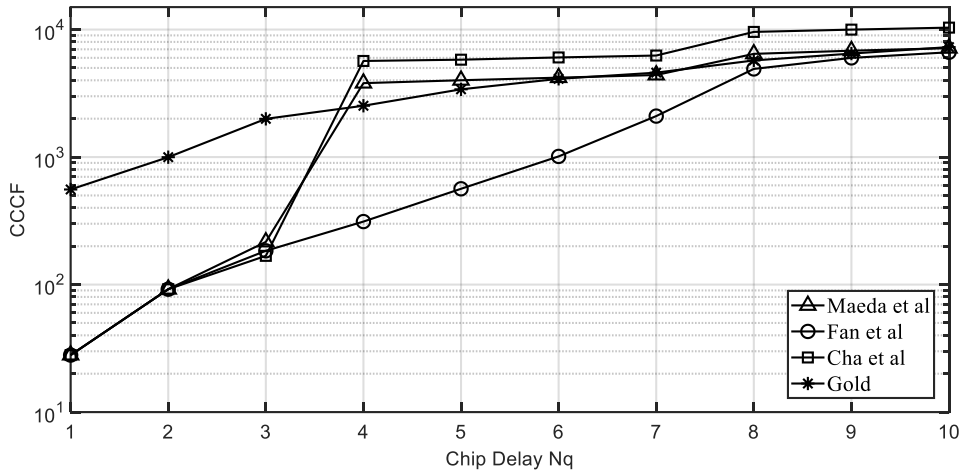

Figure 3-2 Performance of various sequences in terms of CCCF

Some interesting remarks can be deduced from Figure 3-2. It is shown that ZCZ sequences have significantly lower CCF values than Gold sequences when the delay is inside the zero-zone $Z_0 = 3$. However, outside the zero-zone $(N_q = 4)$, CCCF values of Maeda and Cha binary ZCZ sequences increases rapidly to a level higher than Gold sequences. The best performance is provided by Fan's binary ZCZ sequences. Although Fan's sequences have a zero-zone of only $Z_0 = 4$, they maintain low correlation well beyond that value.

3.3.2 **BER vs. SNR for different types of sequences**

Gold sequences of length $N = 63$ are generated using the method given in section 1.6. We have already given the parameters of Fan et al. construction to obtain a binary ZCZ set of $ZCZ(N, K, Z_0) = ZCZ(64,8,4)$ in the previous section. Similarly, by letting $N = 4$ and $m = 2$ in Hayashi's construction (see section 1.8.2.1) we can obtain a ternary ZCZ sequences set with $K = 8$ sequences each of length $N = 80$ (a sequence length close to 64 can't be obtained) that have a zero-zone of $Z_0 = 7$ and energy per chip ratio $\mu_i = 0.8$.

Note that, according to Eq. 3-26, the sequence length of Hayashi's construction has no effect on the BER performance. Our focus is the MUI, therefore, in what follows, we will assume that the transmitted signal undergoes light fading $\gamma = 0.01$ [47]. The number of active users in the system is chosen to be $K = 8$ and the maximum time delay between users is $N_q = 4$ chips. The performance of various spreading sequences is plotted in Figure 3-3 by using Eq.3-22.

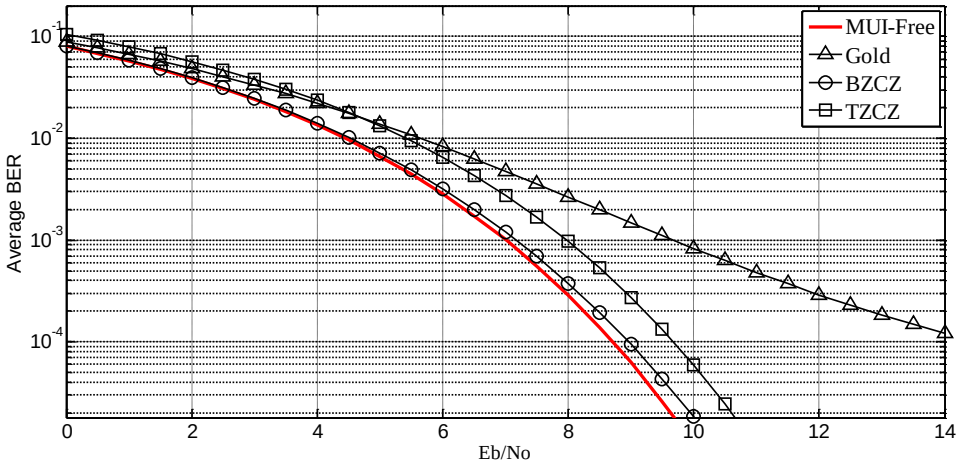

Figure 3-3 BER comparison between various spreading sequences

Although binary ZCZ sequences (denoted by "BZCZ" in Figure 3-3) can provide much better BER performance than Gold sequences, the interference effect still exists (see Eq.3-25). Ternary ZCZ sequences with zero even and odd CCFs (denoted by TZCZ in Figure 3-3) eliminate MUI and provide better performance than Gold sequences for $SNR > 6$. However, their performance remains lower than binary ZCZ sequences. This is due to lower enery per chip ratio $\mu_i = 0.8$ that affect transmission power ($\mu_i = 1$ for binary ZCZ sequences).

In communication systems, the BER must be kept below a certain level otherwise the quality of communication may be poor. For diversity sake, we will analyze the performance of $K = 8$ sequences for three BER levels $10^{-2}, 10^{-3}$, and 10^{-4}. Table 3-1 gives SNR values for different BER levels of various sequences.

Table 3-1 SNR values for different BER levels

BER	Sequences types SNR (dB)		
	Gold	TZCZ	BZCZ
$\sim 10^{-2}$	5.5	5.5	4.25
$\sim 10^{-3}$	9.5	7.75	7
$\sim 10^{-4}$	13.75	9.5	9

For a BER level 10^{-2}, Gold and Ternary ZCZ (TZCZ) sequences require roughly the same SNR $(5.5\ dB)$ whereas binary ZCZ (BZCZ) requires lower $(\sim 22\%)$ SNR. If the QS-DS-CDMA system requires BER level of 10^{-3}, the corresponding SNR values for Gold is $9.5\ dB$ whereas it is lower by $(\sim 18\%)$ for TZCZ, and $(\sim 26\%)$ for BZCZ sequences. If the system requires lower BER level (10^{-4}), the corresponding SNR values for Gold sequences is $13.75\ dB$ whereas it is lower by $(\sim 30\%)$ for TZCZ, and $(\sim 34\%)$ for BZCZ sequences. We conclude that, if a low level of BER is required, it is clear that QS-DS-CDMA system using Gold sequences is severely affected by MUI.

It is also interesting to see the BER performance of various binary ZCZ sequences (see section 3.2.4.1). In Figure 3-4, the BER vs. chip delay is plotted for an $SNR = 9\ dB$.

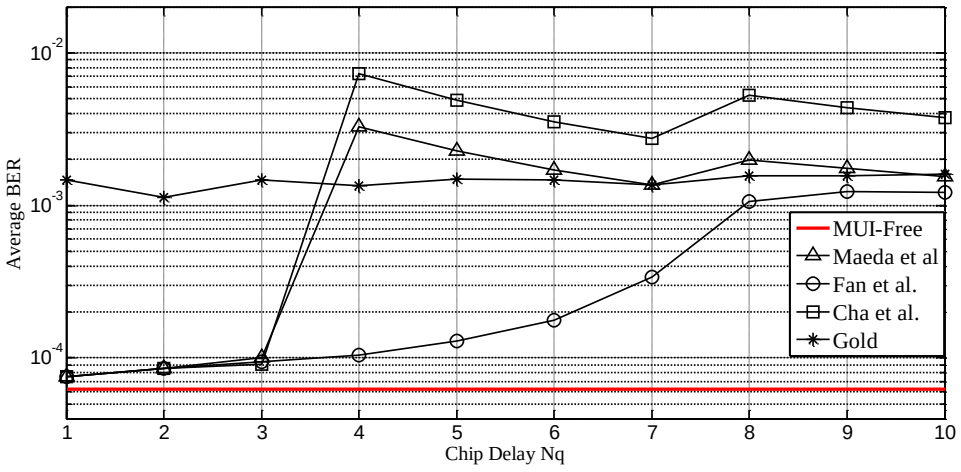

Figure 3-4 BER vs. chip delay

The same analysis of Figure 3-2 can also be used for Figure 3-4. Note that the two Figures 3-2 and 3-4 are proportional to each other in terms of variations. The BER of Gold sequences remain approximately the same for all chip delays. ZCZ sequences provide lower BER when the chip delay is inside the zero-zone $Z_0 = 3$. For a chip delay larger than zero-zone $N_q > Z_0$, Maeda et al and Cha et al BERs increase to levels higher than that of Gold sequences. Note that, in some intervals, the BER decreases (Maeda et al and Cha et al), this is due to the fact that CCCF remains constant in those intervals while the denominator ($4N_q N^2 \mu_i^2$ in Eq. 3-22) increases with N_q. It is concluded that the best performance can be obtained by Fan et al sequences since they have the lowest BER for delays well beyond there zero-zones.

3.3.3 **BER vs. Chip delay of a ZCZ set with zero even and odd CCFs**

In Figure 3-5, the BER vs. chip delay of ternary ZCZ sequences set is plotted for different number of users. The same ternary ZCZ sequences set considered in the previous section (Hayashi's construction) with $K = 8$ sequences each of length $N = 80$ that have a zero-zone of $Z_0 = 7$ and energy per chip ratio is $\mu_i = 0.8$ is used in this section. The signal to noise ratio is taken $SNR = 9\ dB$. Note that adding more users to the system will not affect ZCZ sequences performance as long as the maximum time delay between users is less than the set's zero-zone.

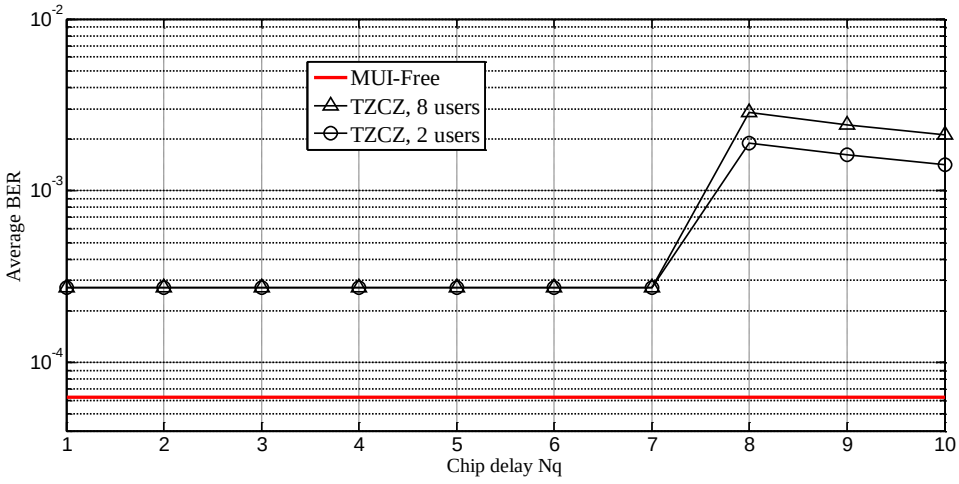

Figure 3-5 BER vs. chip delay of a ZCZ set with zero even and odd CCFs

We conclude that MUI-free QS-DS-CDMA can be obtained by using binary ZCZ sequences with zero even and odd CCFs.

3.4 Conclusion

A new expression of BER for quasi-synchronous and asynchronous DS-CDMA system in Rician fading channel was derived. The new BER allows the evaluation of both binary and ternary sequences. The obtained results show that ZCZ sequences do effectively reduce MUI. However, to ensure interference-free reliable communication, binary ZCZ sequences with both zero even and odd PCFs must be designed.

Chapter 4: On ZCZ Sequences and their Application to MC-CDMA

4.1 Introduction

Multi-carrier (MC) transmission is the predominant transmission technique in today's communication systems. The MC-CDMA transmission scheme combines orthogonal frequency division multiplexing (OFDM) and CDMA. The main advantages of the combined system are variable data rate, high spectral efficiency, and robustness against frequency selective fading [9]. However, high crest factor (CF) is one of the major drawbacks of MC transmission [11]. Thus, CF reduction is one of the most important research areas in MC-CDMA systems. In addition, asynchronous MC-CDMA suffers from the effect of MUI caused by all active users in the system. The degradation of system's BER caused by MUI must also be taken into consideration [48]. Spreading sequences in MC-CDMA have an effective role in CF and MUI reduction [9], [48]. Hence, spreading sequences should be selected to simultaneously ensure low CF and low BER values. Therefore, the effect of correlation properties of sequences on CF is investigated. Furthermore, a new BER as a function of SNR is derived. In this chapter, conventional sequences and ZCZ sequences are analyzed in terms of CF and BER. First, we evaluate the CF values of various sequences and then evaluate their performance in quasi-synchronous and asynchronous MC-CDMA systems.

4.2 CF Analysis

In this study, we consider crest factor (CF) as a measure of signal envelope compactness. Its relation to peak-to-average power ratio (PAPR) is given as follows [48]

$$CF = \sqrt{PAPR} \tag{4-1}$$

The CF of an MC-CDMA signal must satisfy the following inequality [48]

$$CF(\boldsymbol{c}) \leq \frac{max\{|S_C(f)|\}}{\sqrt{E_c/2}} \tag{4-2}$$

Where $S_c(f)$ and E_c are respectively the Fourier transform and the energy of sequence $\boldsymbol{c}$. The Fourier transform of the sequence can be calculated by applying the well-known auto-correlation theorem given by [48]

$$|S_c(f)|^2 = \sum_{l=-N+1}^{N-1} \theta_{\boldsymbol{c}}(l) e^{-j2\pi lf} \tag{4-3}$$

The evaluation procedure of CF values is performed as follows. First, different kinds of sequence sets each of lengths $N = 8, 16, 32, 64,$ and 128 are generated. Walsh-Hadamard (WH) sequences are obtained from Hadamard matrix method given in section 1.5. The generation method of orthogonal Gold (O. Gold) is given in section 1.6.3. The generation method of orthogonal Golay complementary (OGC) sequences is given in section 1.7.2. Various lengths of Fan *et al.* construction are obtained by setting the values of n and m as given in Table 4-1 (see also section 1.8.1.1 for more details).

Table 4-1 Parameters of Fan's construction

Parameters		ZCZ		
n	m	Length N	Family size K	Zero-zone Z_0
1	0	8	4	1
1	1	16	4	2
2	0	32	8	2
2	1	64	8	4
3	0	128	16	4

Similarly, various lengths of Maeda *et al.* construction are obtained by setting the values of N and m as given in Table 4-2 (see also section 1.8.1.2 for more details).

Table 4-2 Parameters of Maeda's construction

Parameters		ZCZ		
WH length N	Interleaving m	Length N	Family size K	Zero-zone Z_0
1	0	8	2	0
2	0	16	4	1
4	0	32	8	1
4	1	64	8	3
8	1	128	16	3

Various lengths of Cha *et al.* construction are obtained by setting the values of N and K as given in Table 4-3 (see also section 1.8.1.3 for more details).

Table 4-3 Parameters of Cha's construction

Parameters		ZCZ		
Preferred pair N	s	Length N	Family size K	Zero-zone Z_0
8	1	8	4	0
16	1	16	4	1
32	3	32	8	1
64	3	64	8	3
128	7	128	16	3

Second, the CF is computed for each sequence in the set, then all values are averaged. The family size of sequences used in CF analysis are given in Table 4-4.

Table 4-4 Family size of sequences with lengths $N = 8, 16, 32, 64$, and 128

Sequences	Family sizes K				
Walsh-Hadamard (WH)	8	16	32	64	128
Orthogonal Gold (O. Gold)	8	–	32	64	128
O. Golay complementary (OGC)	8	16	32	64	128
Fan *et al.*	4	4	8	8	16
Maeda *et al.*	2	4	8	8	16
Cha *et al.*	4	4	8	8	16

Figure 4-1 illustrates the CF performance of various sequences [49]. Note that as the sequence's length increases, the CF also increases except for OGC and Cha *et al.* sequences ($N \geq 64$). In addition to their low CF levels, OGC and Cha *et al.* sequences have also a steady CF (remain under $CF = 3$ for all lengths) which constitutes a major advantage in MC-CDMA systems.

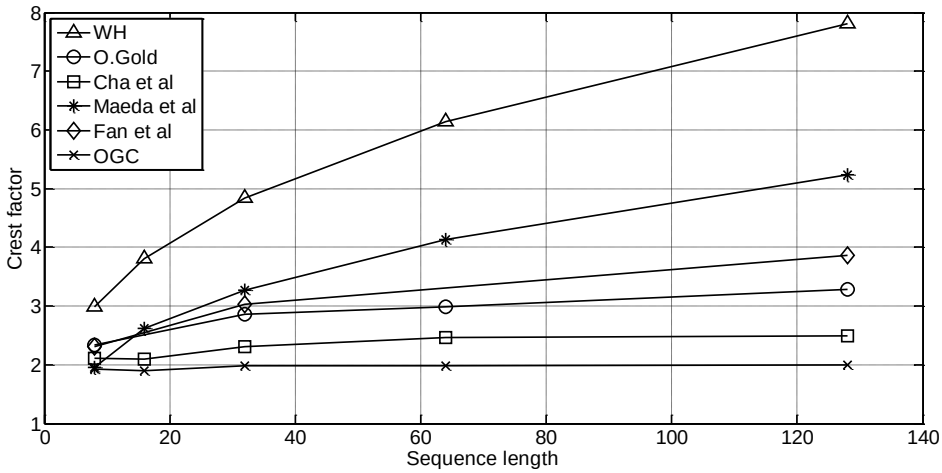

Figure 4-1 Average CF of sequences for various lengths

The second-best sequences are Fan et al and orthogonal Gold sequences. The CF level for these sequences is relatively low and slowly increases with the increase of sequence's length N. WH sequences have, by far, the highest values of CF.

4.3 BER Analysis

4.3.1 MC-CDMA System Model

The basic model of MC-CDMA system in AWGN channel is given in Figure 4-2.

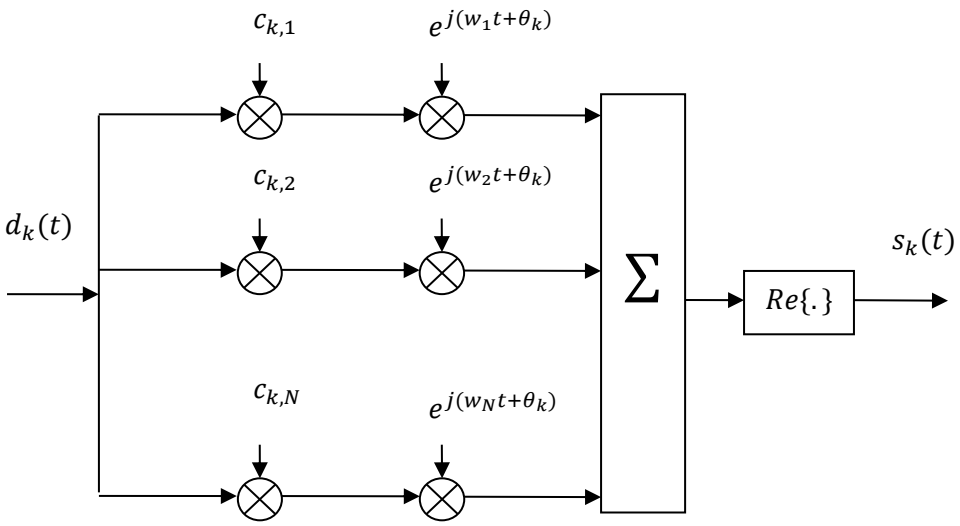

Figure 4-2 MC-CDMA transmitter for the k^{th} user

The k^{th} user's, binary data $d_k(t)$ is

$$d_k(t) = \sum_m d_{k,m} W(t - mT_b) \tag{4-4}$$

Where $W(t)$ is the pulse waveform, T_b is the data bit duration. The spreading sequence $c_k(t)$

$$c_k(t) = \sum_{n=1}^{N} c_{k,n} W(t - nT_c), \tag{4-5}$$

Where T_c is the chip duration, and the sequence length is $N = T_b/T_c$.

In an MC-CDMA scheme of K users, the same information symbol $d_{k,m}$ is spread over N carriers, each multiplied by a different element of the spreading sequence $c_{k,n}$ assigned to the k^{th} user. After spreading, the user bit is modulated onto successive subcarriers such that one information symbol is spread over several subcarriers. BPSK modulation is used. The transmitted signal for the k^{th} user is

$$s_k(t) = \sqrt{\frac{2P}{N}} \sum_{n=1}^{N} Re\{d_k(t) c_{k,n} e^{j(w_n t + \theta_k)}\} \quad (4\text{-}6)$$

Where $Re\{.\}$ denotes the real part, P is the power of data bits assumed to be equal for all users, $w_n = 2\pi n/T_b$ is the n^{th} subcarrier angular frequency, and the random phase θ_k is uniformly distributed over $[0, 2\pi]$.

A QS-MC-CDMA system in AWGN channel is considered. In quasi-synchronous systems, the relative time delay between different users T_q is restricted within few chips. We restrict our analysis to line of sight (LOS) conditions where the multipath replicas have insignificant power compared to LOS signal [36]. We consider a correlation receiver synchronized to the desired user i ($\tau_i = 0$). The random time delays are quantized to integer multiple of the sequence element (chip) duration T_c where $T_c = T_b/N$. The time delays and phase angles are measured relative to τ_i and θ_i (i.e., setting $\tau_i = 0, \theta_i = 0$). The signal at the i^{th} receiver can be written as

$$r(t) = s_i(t) + \sum_{\substack{k=1 \\ k \neq i}}^{K} s_k(t - \tau_k) + n(t) \quad (4\text{-}7)$$

Where τ_k is the random time delay of user k assumed uniformly distributed over $[0, T_q]$, and $n(t)$ is a zero-mean bandpass white noise with equivalent low pass signal that has a power spectral density N_0.

4.3.2 Derivation of a new BER for ternary sequences in MC-CDMA system

The MC-CDMA receiver for the i^{th} user is shown in Figure 4-3.

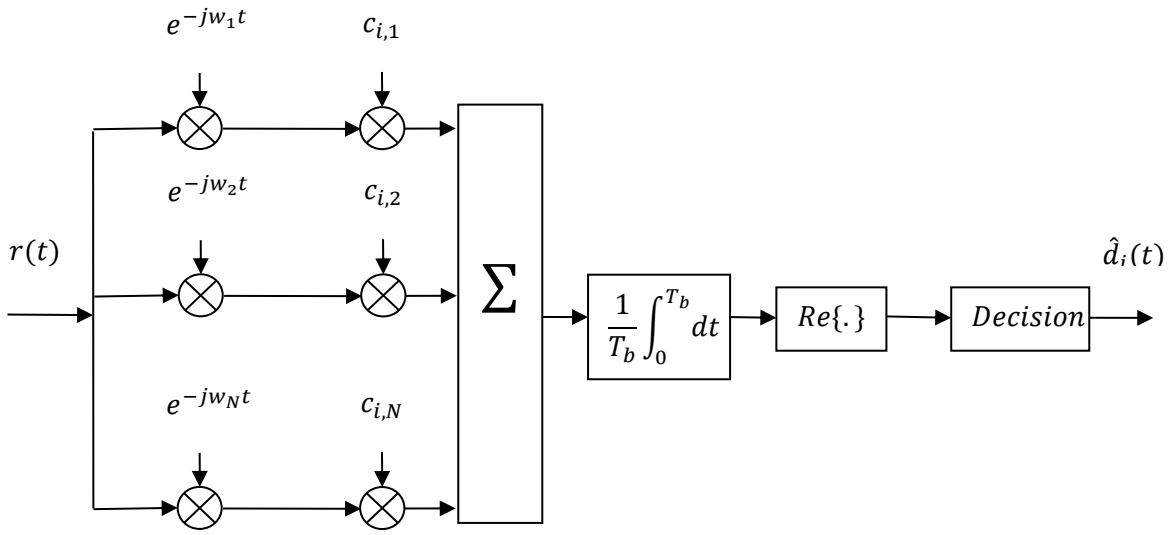

Figure 4-3 MC-CDMA receiver for the i^{th} user

The decision variable of the $m = 0$ data bit of user i is given by

$$Z_i = Re\left\{\frac{1}{T_b}\int_0^{T_b} r(t)\sum_{n'=1}^{N} c_{i,n'}\mathrm{e}^{-jw_{n'}t}\,dt\right\} \tag{4-8}$$

Eq. 4-8 can also be written as (see **Annexes C.1 and C.2)**

$$Z_i = \sqrt{\frac{2P}{N}}(D_i + MUI_i + N_i) \tag{4-9}$$

Where D_i, MUI_i and N_i are respectively the desired signal, the MUI, and the noise terms. In what follows, we will normalize the decision variable by a factor $\sqrt{2P/N}$. It can be shown that signal component (see **Annex C.1**) is

$$D_i = N\mu_i \tag{4-10}$$

For a time delay τ_k, the desired symbol $b_{i,0}$ is affected by the corresponding $b_{k,0}$ and previous symbols $b_{k,-1}$ of each interferer k, thus the MUI_i term is (see **Annex C.1**)

$$MUI_i = \frac{1}{T_b}\sum_{\substack{k=1\\k\neq i}}^{K}\sum_{n=1}^{N}\sum_{n'=1}^{N} c_{k,n}c_{i,n'}\int_0^{T_b} d_k(t-\tau_k)cos\left[(w_n - w_{n'})t + \vartheta_{k,n}\right]dt \quad (4\text{-}11)$$

Where $\vartheta_{k,n} = \theta_k - w_n\tau_k$

In the case where $n' = n$, interference from the same subcarriers of user k is called inter-symbol interference (ISI) equals to (see **Annex C.1**)

$$ISI_i = \frac{1}{T_b}\sum_{\substack{k=1\\k\neq i}}^{K}\sum_{n=1}^{N}\left[\tau_k d_{k,-1} + (T_b - \tau_k)d_{k,0}\right]c_{k,n}c_{i,n'}cos\left(\vartheta_{k,n}\right) \quad (4\text{-}12)$$

If $n' \neq n$, interference from other subcarriers of user k is called inter-channel interference (ICI) equal to (see **Annex C.1**)

$$ICI_i = \frac{1}{T_b}\sum_{\substack{k=1\\k\neq i}}^{K}\sum_{n=1}^{N}\sum_{\substack{n'=1\\n'\neq n}}^{N} c_{k,n}c_{i,n'}\int_0^{T_b} d_k(t-\tau_k)cos\left[(w_n - w_{n'})t + \vartheta_{k,n}\right]dt \quad (4\text{-}13)$$

The noise term is (see **Annex C.2**)

$$N_i = \frac{1}{T_b}\sqrt{\frac{N}{2P}}\int_0^{T_b} n(t)\sum_{n'=1}^{N} c_{i,n'}cos(w_{n'}t)\,dt \quad (4\text{-}14)$$

It is deduced from [50] that the signal-to-noise ratio (SNR_i) for MC-CDMA is defined as

$$\sqrt{SNR_i} = \frac{D_i + MUI_i}{\sqrt{2Var\{N_i\}}} \quad (4\text{-}15)$$

Where the variance of the noise $Var\{N_i\}$ is (see **Annex C.2**)

$$Var\{N_i\} = N_0 N^2 \mu_i / 4E_b \quad (4\text{-}16)$$

The SNR_i becomes

$$\sqrt{SNR_i} = \frac{\mu_i N + MUI_i}{N\sqrt{N_0\mu_i/2E_b}}$$
$$= \sqrt{\frac{2E_b}{N_0\mu_i}}\left[\mu_i + \frac{MUI_i}{N}\right] \quad (4\text{-}17)$$

Since we considered AWGN channel, the decision variable can be regarded as a Gaussian random variable [50]. The BER_i of user i, conditioned on $\{\tau_k\}, \{\theta_k\}, \{b_{k,-1}\}$, and $\{b_{k,0}\}$, is

$$BER_i = \frac{1}{2}erfc\left(\sqrt{SNR_i}\right) = \frac{1}{2}erfc\left(\sqrt{\frac{2E_b}{N_0\mu_i}\left[\mu_i + \frac{MUI_i}{N}\right]}\right) \quad (4\text{-}18)$$

In the case of binary spreading sequences ($\mu_i = 1$), BER_i becomes

$$BER_i = \frac{1}{2}erfc\left(\sqrt{\frac{2E_b}{N_0}\left[1 + \frac{MUI_i}{N}\right]}\right) \quad (4\text{-}19)$$

An expression similar to Eq. 4-19 was obtained in [50] as

$$BER_i = \frac{1}{2}erfc\left(\sqrt{\frac{E_b}{N_0}\left[1 + \frac{MUI_i}{N}\right]}\right) \quad (4\text{-}20)$$

Note that a factor of 2 is missing, this is due to an error in calculation of noise term in [50]. The correct noise variance analysis is given in **Annex C.2**. To obtain the unconditional BER for user i, we average BER_i over all variables via Monte Carlo integration. A more appropriate performance measure is the averaged BER over all users [50]

$$BER = \frac{1}{K}\sum_{i=1}^{K} BER_i \quad (4\text{-}21)$$

4.4 Numerical Results

This section emphasizes interference related issues in quasi-synchronous and asynchronous MC-CDMA systems. The performance of MC-CDMA system using various spreading sequences in the presence of MUI in AWGN channel is evaluated. We have considered an MC-CDMA system where several mobile users transmit their signal to a common receiver such as the uplink cellular system. In this section, a comparative study of various spreading sequences is performed.

4.4.1 BER vs. Chip delay

Here, we will evaluate the BER of various binary ZCZ sequences and compare them to that of O. Gold and OGC sequences. By letting $n = 2$ and $m = 1$ in Fan et al. construction (see Table 4-1) we can obtain a binary ZCZ sequences set with $K = 8$ sequences each of length $N = 64$ that have a zero-zone of $Z_0 = 4$. Similarly, Maeda et al. construction (see Table 4-2) can obtained by using a Hadamard matrix of order 4 and using interleaving once $m = 1$. The latter set has $K = 8$ sequences each of length $N = 64$ with $Z_0 = 3$. Lastly, Cha et al binary ZCZ set obtained also by choosing $N = 64$ and $K = 8$ (see Table 4-3). The latter parameters can be used to determine the corresponding zero-zone $Z_0 = 3$ (see Table 4-3). O. Gold sequences of length $N = 64$ are generated using the method given in section 1.6.3. The performance of various sequences in terms of BER is obtained after 200 000 trials and illustrated in Figure 4-4.

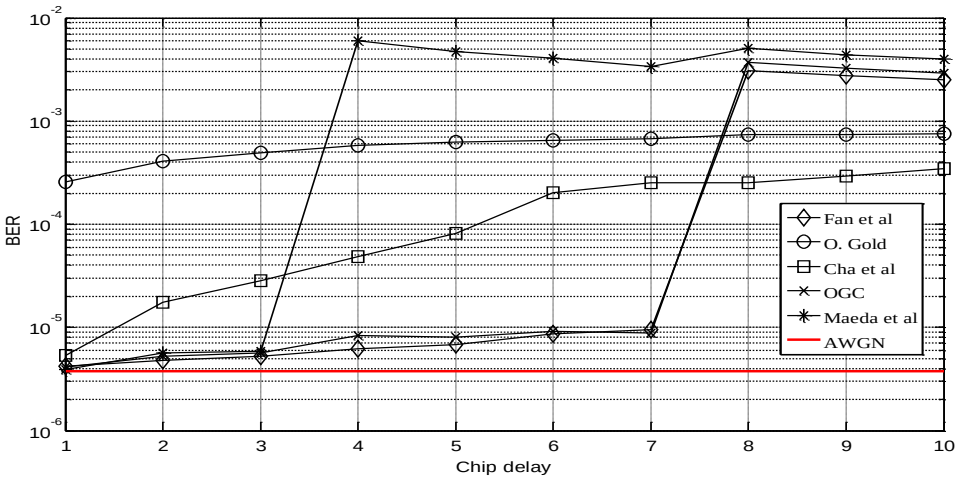

Figure 4-4 Performance of various sequences in terms of CCCF

The bit rate is taken equal to 100 $Mbps$ and the SNR is equal to 7 dB. In Figure 4-4, two BERs are taken as reference; O. Gold sequences (BER remains approximately the same for all delays) and AWGN channel (in color red) where interference from other users is forced to zero). ZCZ sequences have significantly lower BER values than O. Gold sequences and eliminate MUI when the delay is inside the zero-zone $Z_0 = 3$. However, outside the zero-zone $(N_q = 4)$, BER values of Maeda et al sequences increases rapidly to a level higher than O. Gold sequences. As for Cha et al sequences, the BER level increases gradually but maintains a lower value than O. Gold sequences for all delays. The best performance is provided by Fan et al and OGC sequences. Although Fan's sequences have a zero-zone of only $Z_0 = 4$, they maintain low correlation well beyond that value (until $N_q = 7$). The most interesting result come from OGC sequences. Although they do not have a zero-zone; they still provide a BER performance similar to that of Fan et al sequences.

4.4.2 **BER vs. SNR for different types of sequences**

It is also interesting to see the BER performance of various binary ZCZ sequences as a function of SNR. The performance of various sequences in terms of BER is obtained after 200 000 trials and illustrated in Figure 4-5. The bit rate was taken equal to 100 $Mbps$.

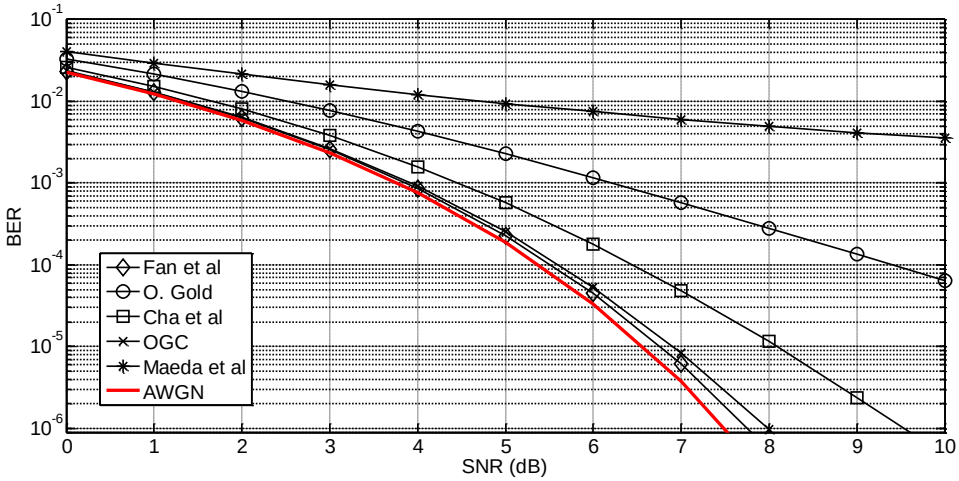

Figure 4-5 BER versus SNR of various spreading sequences

In order to analyze ZCZ sequences inside and outside their zero-zones, the maximum delay was chosen equal to $N_q = 4$. The latter delay is inside the zero-zone for Fan et al sequences ($Z_0 = 4$) and outside the zero-zone for Maeda et al and Cha et al sequences which have the same zero-zone $Z_0 = 3$. Outside the zero-zone $Z_0 = 3$; two different behaviors are noted. Maeda et al sequences exhibit the worst BER performance while Cha et al sequences maintain good performance (much better than O. Gold sequences). According to the BER criterion, the best results are obtained when Fan et al sequences are used for spreading (see Figure 4-5). The latter sequences eliminate interference and provide a BER performance similar to AWGN channel. OGC sequences performance is almost identical to Fan et al performance for $SNR \leq 5\ dB$.

From the numerical results (CF and BER), it can be observed that ZCZ sequences have both low CF and interference-free communication (see Table 4-5). Therefore, we conclude that ZCZ sequences are the suitable candidate for QS-MC-CDMA systems.

Table 4-5 BER and CF Performance comparison in QS-MC-CDMA

	Criteria	
Sequences	CF	BER ($N_q \leq Z_0$)
ZCZ (Fan et al)	Low	Low
ZCZ (Maeda et al)	Highest	Low
ZCZ (Cha et al)	Low	Low
Orthogonal Gold	Low	Highest
OGC	Lowest	Low

4.5 Conclusion

In this chapter, the CF performances of various sequences, i.e. ZCZ, orthogonal Gold, and OGC sequences were analyzed and compared. In addition, the BER performance of QS-MC-CDMA in AWGN channel was also evaluated. With the use of efficient spreading sequence, the system can operate at low CF and low BER. Based on the obtained results for different sequences, it is observed that the QS-MC-CDMA system with ZCZ sequences shows good performance in terms of both CF and BER and are suitable candidate for QS-MC-CDMA.

Chapter 5: On Optical ZCZ Sequences and their Application to OCDMA

5.1 Introduction

For short-range communication link, optical wireless communication (OWC) system is expect to be essential [51]. OWC link relies on optical radiations to convey information in free space with wavelengths ranging from infrared (IR) to ultraviolet (UV) including the visible light spectrum [51]. Figure 5-1 shows the VLC spectrum.

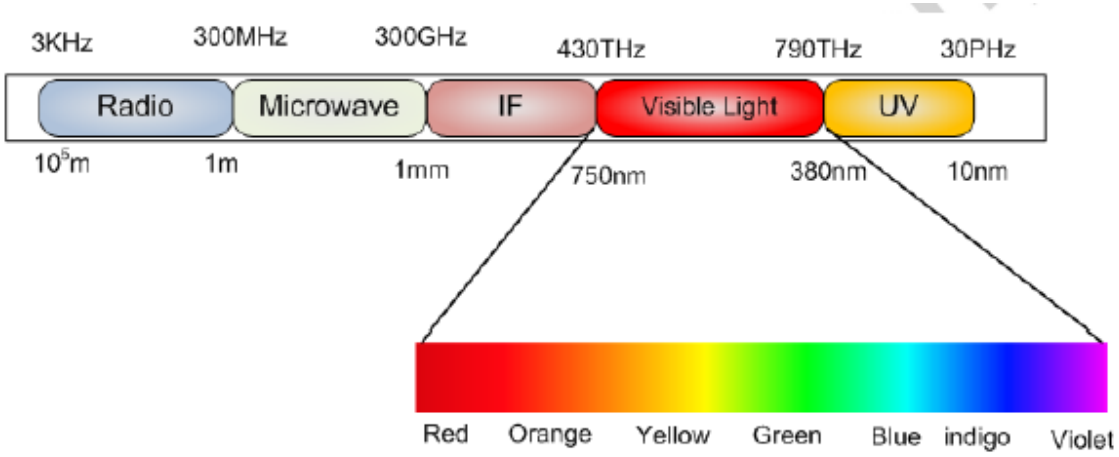

Figure 5-1 VLC spectrum [52]

OWC can be used as a complementary technology to radio frequency systems. Visible light communication (VLC) is an attractive technology due to its potential to simultaneously provide energy sufficient lighting and high-speed communication using light emitting diodes (LEDs). VLC is being adopted in, to name a few, vehicle to vehicle communication [53], indoor

positioning [54], and underwater communications [55]. In general, line of sight (LOS) configurations are commonly used for VLC as in Figure 5-2

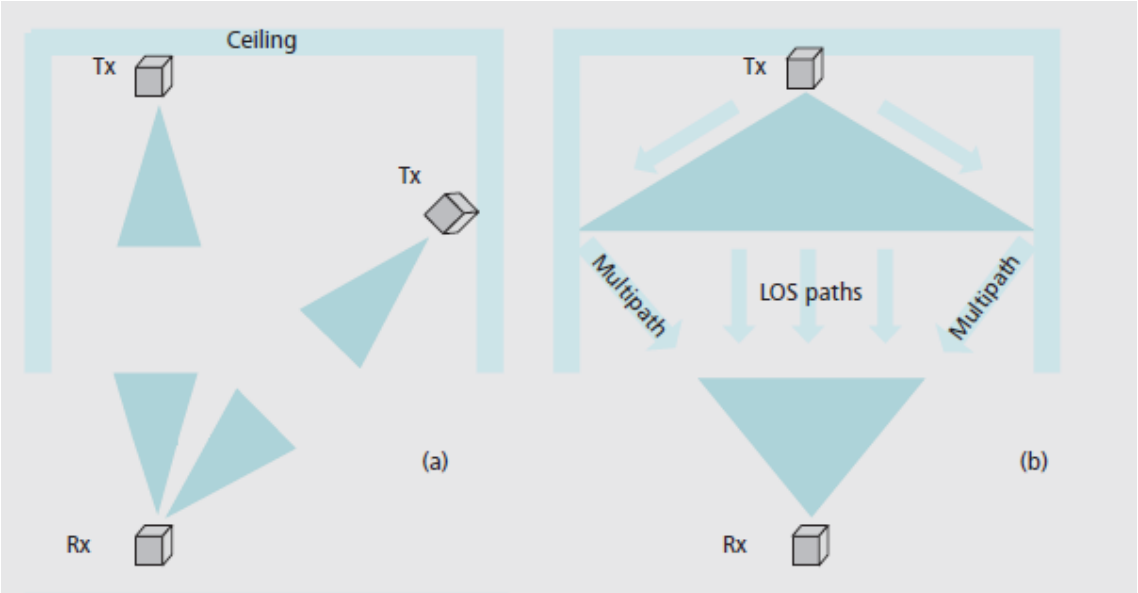

Figure 5-2 a) Direct LOS link; b) non-direct-LOS link [51]

A possible scenario for future wireless communication on airplane is depicted in Figure 5-3.

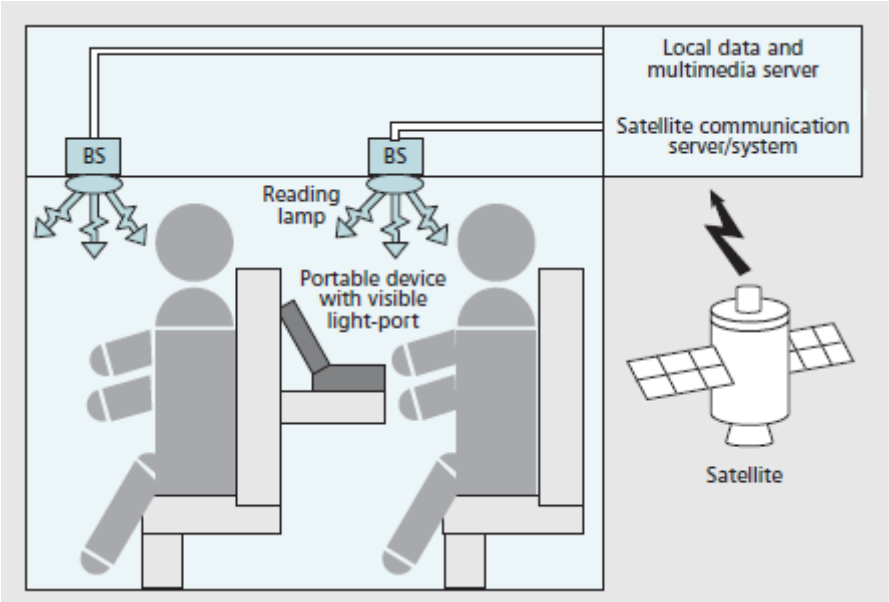

Figure 5-3 Broadband wireless network scenario [51]

Service is established through a combination of wired, wireless, and satellite technologies. Wired BSs are merged with LED-based illumination equipment (reading lamps) to provide passengers with Internet access and a range of multimedia services.

Multiple access techniques allow multiple users to access the available network services. For indoor applications, a suitable topology is chosen based on the room size, number of users, and user's mobility [51]. The three probable topologies are shown in Figure 5-4.

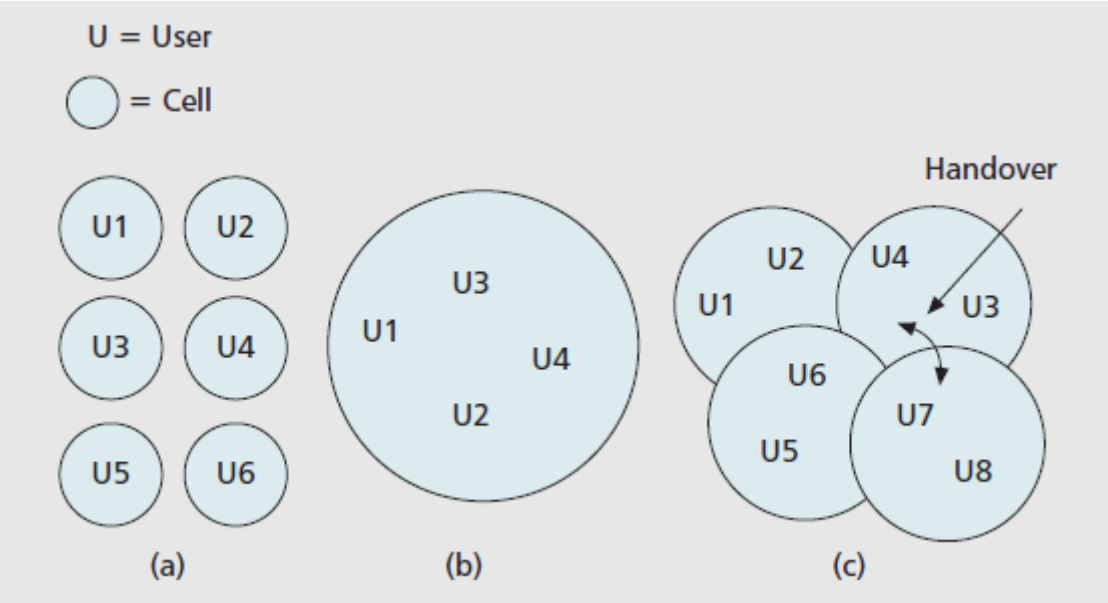

Figure 5-4 a) cell per user; b) cell per room; c) cellular topology [51]

In a single cell per user, each user has an access point (AP) and all resources are available to one user so multiple access techniques are not required. Multiple access is required for single cell per room (also per office) topology and cellular topology needed to provide coverage in, for example, a conference room. Optical CDMA (OCDMA) is a strong candidate for VLC-based applications. In OCDMA, users are able to transmit at overlapping times and wavelengths. It is also possible to implement hybrid optical systems such as wavelength division multiple access (WDMA)/CDMA and time division multiple access (TDMA)/CDMA. The design task of uplink channel remains an open issue [51]. The predominant source of bit error in uplink OCDMA is the MUI. To eliminate MUI in synchronous OCDMA, ZCC sequences have been proposed [22].

However, synchronization problems introduce relative non-zero time delays. Therefore, optical ZCZ sequences were introduced [19].

5.2 OCDMA VLC System

A spectral amplitude coding (SAC)-OCDMA for VLC system is designed in [19] to support K active users transmitting simultaneously through optical wireless channel. Each user employs a white LED for signal transmission and a photodiode for signal reception. All optical sources are assumed to be ideally flat over a bandwidth $[v_0 - \Delta_v/2 \quad v_0 + \Delta_v/2]$ where v_0 denotes the optical central frequency and Δ_v the bandwidth. Users are considered to have equal transmitted P and equal received power P_r.

5.2.1 Transmitter

At the transmitter, the k^{th} user information data $d_k(t)$ modulates the intensity of light using a modulator. Next, the spectral encoder is used to divide the LED broadband spectrum into N wavelengths where each user is assigned a set of wavelengths. All encoded data will be passed through an OWC channel. The SAC-OCDMA transmitter is shown in Figure 5-5.

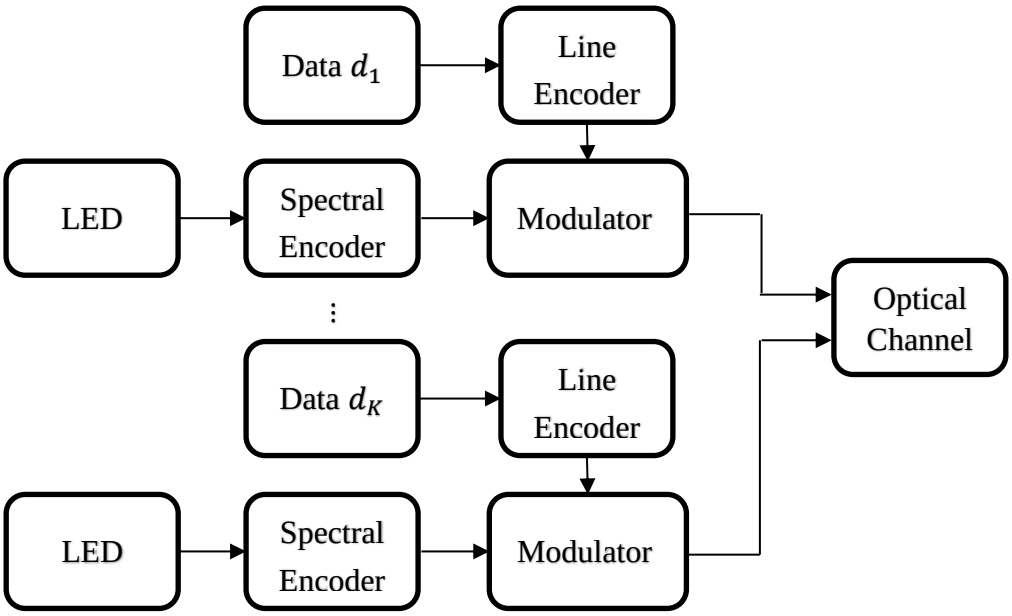

Figure 5-5 SAC-OCDMA transmitter for VLC system

The PSD of the k^{th} transmitted signal is

$$S_k(v) = \frac{P}{\Delta_v} d_k \sum_{n=1}^{N} c_{k,n} \prod(v, n) \tag{5-1}$$

Where $c_{k,n} \in \{0,1\}$ is the k^{th} user n^{th} element and $\prod(v, n)$ is a rectangular impulse defined as follows

$$\prod(v, n) = \quad u\left(v - \left[v_0 + \frac{\Delta_v}{2N}(2n - N - 2)\right]\right) - u\left(v - \left[v_0 + \frac{\Delta_v}{2N}(2n - N)\right]\right) \tag{5-2}$$

Where is $u(v)$ the unit impulse function.

5.2.2 **Receiver**

At the receiver side, the reverse process will be performed by a spectral decoder to filter out data of the intended user. Next, the data is passed through a photodetector and a low pass filter (LPF) to eliminate the undesired frequency range. The SAC-OCDMA receiver is shown in Figure 5-6.

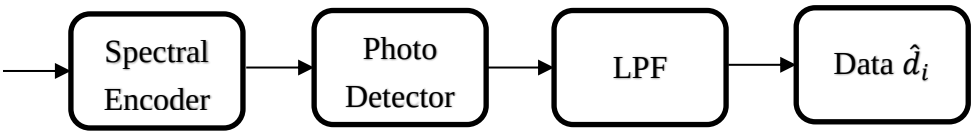

Figure 5-6 SAC-OCDMA receiver for VLC system

The received signal includes the desired signal as well as signals from other active users. The PSD of the received optical signal is

$$r_i(v) = \frac{P_r}{\Delta_v} \sum_{k=1}^{K} d_k \sum_{n=1}^{N} c_{i,n} c_{k,(n+\tau_k) mod N} \prod(v, n + \tau_k) \tag{5-3}$$

It can be shown that the received signal PSD can be written as (see **Annex D.1**)

$$r_i(v) = \frac{P_r}{\Delta_v}\sum_{k=1}^{K} d_k E_{c_i c_k}(\tau_k)\prod(v, n+\tau_k) \quad (5\text{-}4)$$

The main source of OCDMA degradation are the shot noise, thermal noise, and phase-induced intensity noise ($PIIN$). For ZCZ sequences, the PIIN is eliminated when the time delay is inside the zero-zone [19]. The current variance at the receiver can be expressed as [19]

$$Var(i) = 2eIB + 4K_b T_n B/R_L \quad (5\text{-}5)$$

Where e is the electron charge, I is the average photocurrent, B is the receiver electrical bandwidth, K_b is the Boltzmann's constant, T_n the receiver noise temperature, and R_L is the receiver load resistor.

The average photocurrent I is calculated as follows [19]

$$I = R\int_0^{\infty} r_i(v)\, dv \quad (5\text{-}6)$$

Where R is the responsivity of the photodiode given as

$$R = \frac{\eta e}{h v_0} \quad (5\text{-}7)$$

Where η is the photo detector's quantum efficiency and h is Planck's constant.

The integral part of Eq. 5-6 is calculated in **Annex D.2** and given bellow

$$\int_0^{\infty} r_i(v)\, dv = \frac{P_r}{N}\sum_{k=1}^{K} d_k\, E_{c_i c_k}(\tau_k) \quad (5\text{-}8)$$

By replacing Eq. 5-7 and Eq. 5-8 in Eq. 5-6, the average photocurrent I becomes

$$I = \frac{R P_r}{N}\sum_{k=1}^{K} d_k\, E_{c_i c_k}(\tau_k) \quad (5\text{-}9)$$

By setting $k = i$ in Eq. 5-9 and putting $\tau_i = 0$, the i^{th} user's component is

$$I_d = RP_r d_i E_{c_i}(0)/N$$
$$= RP_r d_i w/N \quad (5\text{-}10)$$

The average photocurrent of the interference signal is obtained by setting $k \neq i$ in Eq. 5-9 as follows

$$I_{MUI} = \frac{RP_r}{N} \sum_{\substack{k=1 \\ k \neq i}}^{K} d_k E_{c_i c_k}(\tau_k) \quad (5\text{-}11)$$

For worst case scenario ($d_i = d_k = 1$), Eq. 5-10 and Eq. 5-11 become respectively

$$I_d = RP_r w/N \quad (5\text{-}12)$$

$$I_{MUI} = \frac{RP_r}{N} \sum_{\substack{k=1 \\ k \neq i}}^{K} E_{c_i c_k}(\tau_k) \quad (5\text{-}13)$$

The interference current I_{MUI} can be averaged over $\tau_k \in [0 \quad N_q]$, where N_q is the maximum time delay between user as

$$\bar{I}_{MUI} = \frac{RP_r}{NN_q} \sum_{\substack{k=1 \\ k \neq i}}^{K} \sum_{\tau_k=1}^{N_q} E_{c_i c_k}(\tau_k) \quad (5\text{-}14)$$

In what follows, we will denote MUI as

$$MUI = \sum_{\substack{k=1 \\ k \neq i}}^{K} \sum_{\tau_k=1}^{N_q} E_{c_i c_k}(\tau_k) \quad (5\text{-}15)$$

The $SINR$ for optical QS-SAC-OCDMA VLC system is given as

$$SINR = \frac{I_d^2}{Var(i)}$$
$$= \frac{I_d^2}{2e(I_d + \bar{I}_{MUI})B + \frac{4K_b T_n B}{R_L}} \quad (5\text{-}16)$$

If OZCZ sequences are used for spreading where $E_{c_i c_k}(\tau_k) = 0$ for $N_q \leq Z_0$, the MUI becomes zero $\bar{I}_{MUI} = 0$ and the $SINR$ of Eq. 5-16 becomes

$$SINR = \frac{I_d^2}{2eI_dB + \frac{4K_bT_nB}{R_L}} \tag{5-17}$$

If the system is synchronous $\tau_k = 0$ and ZCC sequences are used for spreading, the $SINR$ is the same form as Eq. 5-17. Note that Eq. 5-16 cannot be used to evaluate ZCC sequences. This is because in asynchronous transmission, ZCC sequences lose their zero in-phase CCF property and the $PIIN$ occurs and must be added to Eq. 5-16. The term MUI of Eq. 5-15 remains valid and can be used to compare ZCC sequences as it is done in the following section.

5.3 Numerical Results and Analysis

The correlation properties of sequences are crucial to system's capacity to eliminate MUI and provide reliable communication. In this section, we first investigate MUI reduction of the proposed ZCC sequences based on the following parameters: time delay, sequence length, and the number of sequences. Second, the ZCC sequences are compared to ZCZ sequences.

5.3.1 MUI vs. Time Delay

To evaluate the effect of correlation properties on the sequence's performance, we compared ZCC sequences proposed by Addad et al [23] to two ZCC sequences proposed in [22] by Abd et al and [56] by Garadi et al. (see section 1.9) and plotted the results in Figure 5-7. All ZCC sequences sets have the same parameters: family size $K = 10$,

sequence length $N = 80$, and Hamming weight $w = 8$.

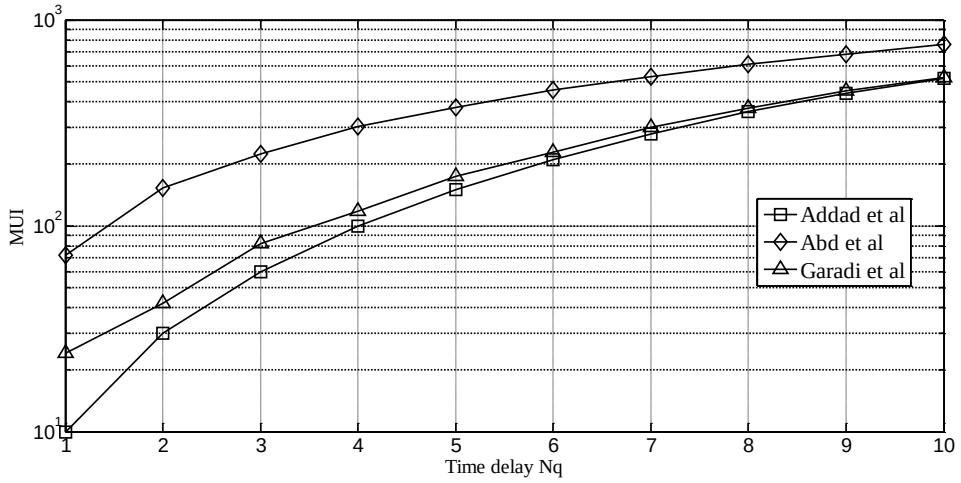

Figure 5-7 MUI vs. time delay

From Figure 5-7, when the time delay between active users increases, the MUI also increases in the system. This is because longer time delay results in higher MUI (see Eq. 5-15). With their good correlation properties, the proposed ZCC sequences provide the lowest MUI.

5.3.2 MUI vs. Sequence Length

The sequence length effect on the MUI is analyzed and plotted in Figure 5-8. ZCC sequences with $K = 10$ active users having maximum delay of $N_q = 5$ were evaluated.

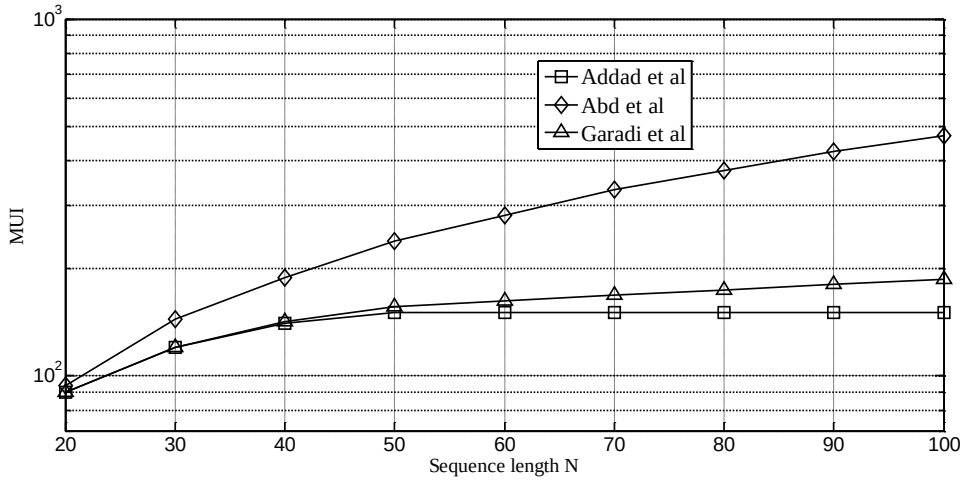

Figure 5-8 MUI vs. sequence length.

From Figure 5-8 below, the MUI level increases with the sequence length N. Since K is fixed, longer sequences can be obtained by increasing the Hamming weight w. This results in more ones "1" in the sequence and consequently higher correlation values. Note that the proposed ZCC sequences not only have the lowest MUI level but also remain constant for length higher than 50.

5.3.3 **MUI vs. Number of Active Users**

The interferer effect on the MUI is analyzed next. Figure 5-9 shows the MUI values versus the number of active users. ZCC sequences with Hamming weight $w = 8$, sequence length $N = 10$, and time delay $Z_0 = 5$ were evaluated.

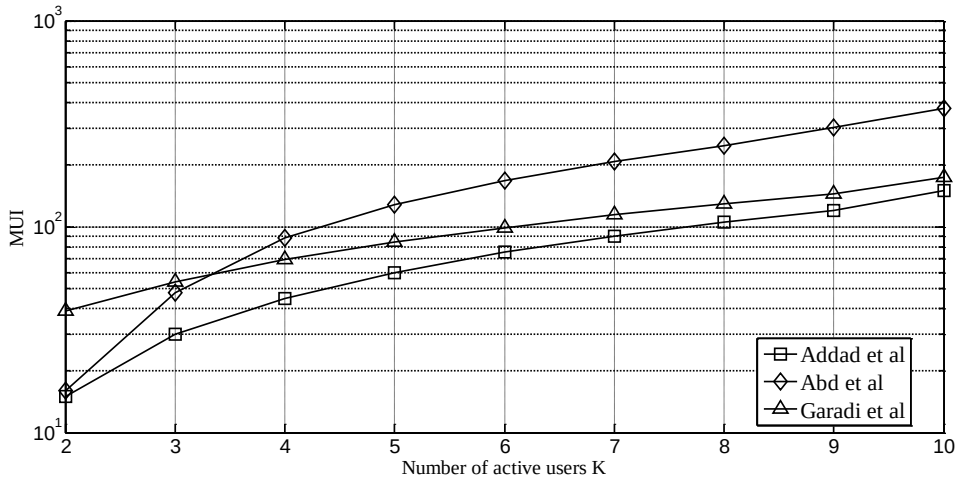

Figure 5-9 MUI vs. number of active users

From Figure 5-9, it is shown that admitting more users to the system results in high level of MUI. Note that the proposed ZCC sequences still maintain the lowest values of MUI.

5.3.4 **Comparison between ZCC and OZCZ Sequences**

Due to their zero-correlation property, ZCZ sequences have been extensively studied for radio frequency systems. In [19], authors introduced optical ZCZ sequences to eliminate MUI in optical QS-CDMA VLC system. Optical ZCZ sequences can eliminate interference $MAI(\tau_k) = 0$ for $\tau_k \leq Z_0$. Since MUI cannot be used to compare ZCC and ZCZ sequences performances, BER will be used instead. BER can be computed as follows [19]

$$BER = \frac{1}{2} erfc\left(\sqrt{\frac{SINR}{8}}\right) \quad (5\text{-}18)$$

The parameters used in the computation of analytical results are listed in Table 5-1 [19].

Table 5-1- OCDMA System's parameters

Symbol	Quantity	Value
v_0	Blue light center frequency	480 nm
η	Photo detector quantum efficiency	0.6
T_n	Receiver noise temperature	300 K
R_L	Receiver load resistor	1030 Ω
B	Receiver electrical bandwidth	311 MHz
e	Electron charge	$1.602189\times10^{-19}\ C$
K_b	Boltzmann's constant	$1.3806505\times10^{-23}\ J.K^{-1}$
h	Planck's constant	$6.626196\times10^{-34}\ J.s$

A ZCC sequences set proposed by Addad et al in [23] of size $K = 4$ and a weight of $w = 3$ is used. The sequence length is then $N = Kw = 12$. The ZCZ sequences set has the same set size and weight but different zero zones $Z_0 = 1$ and $Z_0 = 2$. The corresponding length for zero-zones $Z_0 = 1$ and $Z_0' = 2$ are respetively $N_0 = Kw(Z_0 + 1) = 24$ and $N_0' = Kw(Z_0' + 1) = 36$. The effect of sequence length is plotted in Figure 5-10.

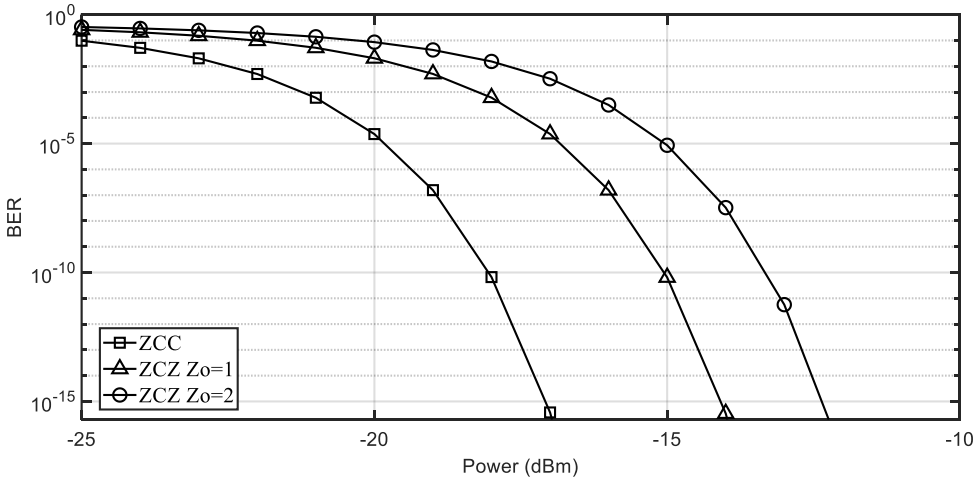

Figure 5-10 BER comparison between ZCC and ZCZ sequences

We can readily see from Figure 5-10 that ZCC sequences outperform ZCZ sequences by a large extent. Although ZCZ sequences eliminate the MUI, their sequence length is proportional to the zero zone Z_0. Large time delay require longue ZCZ sequences which results in poor BER performance. Note that using $SINR$ Eq. 5-16 to compare ZCC sequences to ZCZ sequences is not accurate. This is because ZCC sequences lose their zero correlation property in asynchronous transmission. Therefore, the $PIIN$ must be computed and added to $SINR$ of Eq. 5-16. This will require a system with balanced receiver developped in [57].

5.4 Conclusion

In this chapter, we evaluate the performance of optical QS-SAC-OCDMA for VLC system. First, MUI caused by quasi-synchronous transmission of ZCC sequences was investigated with respect correlation properties, sequence length, and number of sequences in the set. It was shown that a new ZCC sequence (see section 1.9.1) with flexible construction and good correlation properties provide the best results. It was shown also that OZCZ sequences eliminated the MUI but their length is not practical which results in poor BER performance. Therefore, we conclude that the optical ZCZ sequences are not suitable for QS-SAC-OCDMA for VLC system.

Conclusions and Future Work

This chapter concludes the thesis. A summary of the main findings and suggestions for future research is presented. This thesis has largely focused on the construction and application of ZCZ sequences to CDMA systems. two new constructions of optical ZCZ and ZCC sequences were proposed in Chapter 1. Introductory Chapter 2 is excluded from the discussion because it does not contain any new research material. In Chapter 3, a new BER for uplink QS-DS-CDMA system in nonselective Rician fading AWGN channel was derived. The new BER allows the evaluation of both binary and ternary sequences. First, MUI interference level as a function of chip delay of various binary ZCZ sequences was analysed and compared to that of Gold sequences. Second, their BER performance is investigated. The obtained results show that ZCZ sequences do effectively reduce MUI interference and provide much better BER performance, when the maximum time delay between users is inside their zero-zone. A class of ternary ZCZ sequences that eliminate interference was presented and studied. It was concluded that the best BER performance in QS-DS-CDMA could be obtained if binary ZCZ sequences with both zero even and odd periodic CCFs were designed and used. As for application, ZCZ sequences can be used to limit power consumption and prolong battery life while maintaining the robustness in CDMA-based mobile wireless communications systems such as Ad-Hoc networks.

Chapter 4 dealt with application of ZCZ sequences to QS-MC-CDMA system. The CF performances of various sequences, i.e. ZCZ, WH, orthogonal Gold, and OGC sequences were analyzed and compared. In addition, a new BER for ternary sequences in uplink QS-MC-CDMA system with an AWGN channel was derived. Based on the obtained results, a system using ZCZ sequences shows good performance in terms of both CF and BER.

In Chapter 5, attention was devoted to the application of optical ZCZ and ZCC sequences in the uplink of QS-SAC-OCDMA system. It was shown that optical ZCZ sequences eliminate the MUI interference. However, the BER turned out to be sensitive to the

sequence length which results in poor BER performance of optical ZCZ sequences compared to ZCC sequences. In addition, the MUI caused by the quasi-synchronous transmission was investigated with respect to ZCC correlation properties, sequence length, and number of sequences in the set. It was shown that the ZCC sequences proposed by the authors in Chapter 1 have the best performance.

From this work, some points deserve to be developed in the future. First, one can investigate the behavior of ZCZ sequences in presence of MPI interference for both QS-DS-CDMA and QS-MC-CDMA systems. Another possibility for contributing to the existing literature would be to investigate the performance of ZCZ sequences in QS-MC-DS-CDMA. Related to the subject of optical ZCZ sequences proposed in chapter 1, the existing model for OCDMA needs to be further developed and accurate BER could be obtained. Finally, more research must be put into the development of practical systems using ZCZ sequences and compare their performances to theoretical models studied in this thesis.

Annexes

Annex A

Example 1: Walsh-Hadamard (WH) sequences defined in section 1.5.

Generation of Hadamard matrix from a starter of order $N = 2$.

$$\boldsymbol{H_2} = \begin{bmatrix} + & + \\ + & - \end{bmatrix}$$

Using Eq. 1-11, we obtain

$$\boldsymbol{H_4} = \begin{bmatrix} + & + & + & + \\ + & - & + & - \\ + & + & - & - \\ + & - & - & + \end{bmatrix}$$

Where '$+$' and '$-$' denote 1 and -1, respectively.

The rows of $\boldsymbol{H_4}$ are WH sequences. If a larger matrix $\boldsymbol{H_8}$ is needed, apply Eq. 1-11 on $\boldsymbol{H_4}$.

Example 2: PN sequences defined in section 1.6

a) M-sequence

Figure A-1 shows A 3-stage $LFSR$.

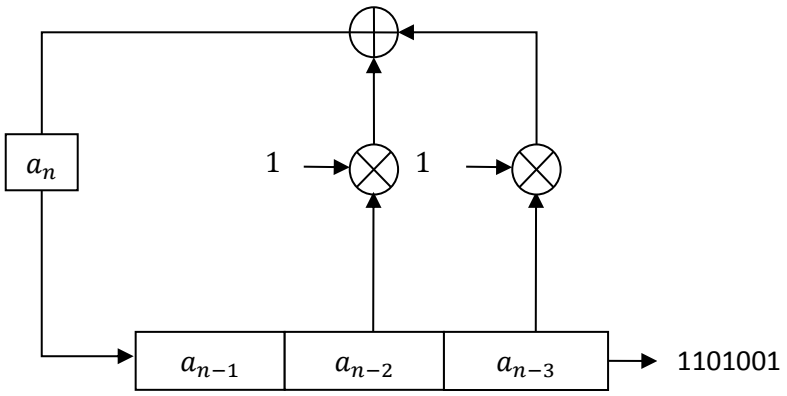

Figure A-1 Three-stages LFSR generator

Figure Above shows an m-sequence of length $N = 7$ can be generated using $m = 3$ stage $LFSR$ generator with the second and the third feedback taps [2,3] connected ($c_1 = 0, c_2 = 1$, and $c_3 = 1$). The initial state of the $LFSR$ is ($a_{n-1} = 0, a_{n-2} = 0,\ a_{n-3} = 1$). The other states are given in Table A-1 below.

Table A-1 A 3-stage $LFSR$ generator's output.

Shift	State	Output
1	001	1 (1st bit)
2	100	0
3	010	0
4	101	1
5	110	0
6	111	1
7	011	1 (7th bit)
8	001	1 (Repeat)

b) Preferred Pair

Using two LFSR generators with [2, 3] and [1, 3] taps, we obtain a preferred pair $\boldsymbol{a} = 1001011$ and $\widehat{\boldsymbol{a}} = 1001110$ with the corresponding bipolar sequences $\boldsymbol{b} = 1, -1, -1,1, -1,1,1$ and $\widehat{\boldsymbol{b}} = 1, -1, -1,1,1,1, -1$. The periodic ACF of the corresponding bipolar sequences is

$$\mathrm{E}_{\widehat{\boldsymbol{b}}}(\tau) = \{7, -1, -1 - 1, -1, -1, -1\}$$

And the CCF values are

$$\mathrm{E}_{\boldsymbol{b}\widehat{\boldsymbol{b}}}(\tau) = \{-1, -1, -5,3,3, -1, 3, -1, -1, -5,3,3, -1\}$$

Based on the preferred pair given above and the operation illustrated in Figure 1.4, we can construct a set of $K = 9$ Gold sequences each of length $N = 7$ as follows

$$\boldsymbol{G} = \begin{matrix} \boldsymbol{a} \\ \widehat{\boldsymbol{a}} \\ \boldsymbol{a} \oplus \boldsymbol{T^0}\widehat{\boldsymbol{a}} \\ \boldsymbol{a} \oplus \boldsymbol{T^1}\widehat{\boldsymbol{a}} \\ \boldsymbol{a} \oplus \boldsymbol{T^2}\widehat{\boldsymbol{a}} \\ \boldsymbol{a} \oplus \boldsymbol{T^3}\widehat{\boldsymbol{a}} \\ \boldsymbol{a} \oplus \boldsymbol{T^4}\widehat{\boldsymbol{a}} \\ \boldsymbol{a} \oplus \boldsymbol{T^5}\widehat{\boldsymbol{a}} \\ \boldsymbol{a} \oplus \boldsymbol{T^6}\widehat{\boldsymbol{a}} \end{matrix} = \begin{matrix} 1001011 \\ 1001110 \\ 0000101 \\ 1010110 \\ 1110001 \\ 0111111 \\ 0100010 \\ 0011000 \\ 1101100 \end{matrix}$$

c) Orthogonal Gold

We can construct $K = 8$ orthogonal Gold sequences of length $N = 8$ by appending "0" at to $\boldsymbol{G}$ as follows

$$OG = [\boldsymbol{G} \quad \boldsymbol{0}] = \begin{bmatrix} 10010110 \\ 00001010 \\ 10101100 \\ 11100010 \\ 01111110 \\ 01000100 \\ 00110000 \\ 11011000 \end{bmatrix}$$

Example 3: Complementary sequences defined in section 1.7

a) Complementary Pairs

The two sequences $\boldsymbol{a} = (1,1,1,-1,1,1,-1,1)$ and $\boldsymbol{b} = (1,1,1,-1,-1,-1,1,-1)$ are an CP. The aperiodic ACF of $\boldsymbol{a}$ and $\boldsymbol{b}$ are given below

$\theta_{\boldsymbol{a}}(l) =$	$+1$	0	$+1$	0	$+3$	0	-1	$+8$	-1	0	$+3$	0	$+1$	0	$+1$
$\theta_{\boldsymbol{b}}(l) =$	-1	0	-1	0	-3	0	$+1$	$+8$	$+1$	0	-3	0	-1	0	-1

b) Orthogonal Golay Complementary Sequences

Generation of an OGC set of order 4.

$$\boldsymbol{H}_2^{CP} = \begin{bmatrix} + & + \\ + & - \end{bmatrix}$$

And the orthogonal complementary set is obtained using Eq. 1-15 as

$$\boldsymbol{H}_4^{CP} = \begin{bmatrix} + & + & + & - \\ + & - & + & + \\ + & + & - & + \\ + & - & - & - \end{bmatrix}$$

The rows of $\boldsymbol{H}_4^{CP}$ are OGC sequences. If a larger matrix $\boldsymbol{H}_8^{CP}$ is needed, apply Eq. 1-15 on $\boldsymbol{H}_4^{CP}$.

c) Mutually Orthogonal Complementary Sets

The following matrix is a basic MOCS matrix where $M = K = 4$, and $L = 3$ that is the sequence length is $N = KL = 12$.

$$\boldsymbol{F} = \begin{bmatrix} - - - & - + - & + - - & + - - \\ - - + & - - + & + + + & + - + \\ + - + & - - - & + - - & - + + \\ - - + & + + - & - + - & + + + \end{bmatrix}$$

To generate MOCS of set size $K = 4$ and sequence length $N = 8$ by interleaving operation, Eq. 1-19 is applied on the following starter matrix

$$\boldsymbol{F} = \begin{bmatrix} + & + \\ + & - \end{bmatrix}$$

Which gives

$$\boldsymbol{F}_1' = \begin{bmatrix} + + & + + & - + & - + \\ + + & - - & - + & + - \\ - + & - + & + + & + + \\ - + & + - & + + & - - \end{bmatrix}$$

If the concatenation operation is used (Eq. 1-20), another MOCS is obtained as follows

$$\boldsymbol{F}_2' = \begin{bmatrix} + + & + + & - - & + + \\ + - & + - & - + & + - \\ - - & + + & + + & + + \\ - + & + - & + - & + - \end{bmatrix}$$

The rows of $\boldsymbol{F_1'}$ and $\boldsymbol{F_2'}$ are $MOCS$ sequences. If a larger matrix is needed, apply Eq. 1-19 or Eq. 1-20 on $\boldsymbol{F_1'}$ or $\boldsymbol{F_2'}$.

Example 4: Binary ZCZ sequences defined in section 1.8.1.

a) Fan et al Construction

Let's obtain a ZCZ sequence set $\boldsymbol{F^{(1)}}$ of $ZCZ(8,\ 4,\ 1)$ from Hadamard matrix a basic MOCS starter $\boldsymbol{F^{(0)}}$. The basic MOCS starter matrix chosen as

$$\boldsymbol{F^{(0)}} = \begin{bmatrix} + & + \\ + & - \end{bmatrix}$$

For the first iteration $n = 1$ and by using Eq. 1-20, a ZCZ sequence set $\boldsymbol{F^{(1)}}$ is obtained as follows

$$\boldsymbol{F^{(1)}} = \begin{bmatrix} ++ & ++ & -+ & -+ \\ ++ & -- & -+ & +- \\ -+ & -+ & ++ & ++ \\ -+ & +- & ++ & -- \end{bmatrix}$$

The rows of $\boldsymbol{F^{(1)}}$ are $MOCS$ sequences. If a larger ZCZ matrix of $ZCZ(32,\ 8,\ 2)$ is needed, apply Eq. 1-20 on $\boldsymbol{F^{(1)}}$.

b) Maeda et al Construction

A set of ZCZ sequences with $ZCZ(16,4,1)$ can be constructed as follows. We start with a Hadamard matrix of order $N = 2$ given bellow

$$\boldsymbol{H_2} = \begin{bmatrix} + & + \\ + & - \end{bmatrix}$$

The starter ZCZ matrix is obtained using Eq. 1-25 as

$$\boldsymbol{F} = \begin{bmatrix} \boldsymbol{F^1} \\ \boldsymbol{F^2} \end{bmatrix} = \begin{bmatrix} -- & ++ & ++ & ++ \\ -+ & +- & +- & +- \\ ++ & ++ & -- & ++ \\ +- & +- & -+ & +- \end{bmatrix}$$

And the ZCZ set is obtained using Eq. 1-26 as follows

$$\boldsymbol{Z}^{(\mathbf{0})} = \begin{bmatrix} -+-+ & ++++ & +-+- & ++++ \\ -++- & ++-- & +--+ & ++-- \\ ---- & +-+- & +++- & +-+- \\ --++ & +--+ & ++-- & +--+ \end{bmatrix}$$

The rows of $\boldsymbol{Z}^{(\mathbf{0})}$ are ZCZ sequences. If a larger ZCZ matrix $\boldsymbol{Z}^{(\mathbf{1})}$ of $ZCZ(32,\ 4,\ 3)$ is needed, apply Eq. 1-26 on $\boldsymbol{Z}^{(\mathbf{0})}$.

c) Cha et al Construction

A ZCZ set of parameters of $K = 4$ sequences each of length $N = 16$ is constructed from the following perfect binary sequence

$$\boldsymbol{p}^{(\mathbf{0})} = \ [+++-]$$

An extended sequence can be obtained using Eq. 1-28 $n = 2$ times as

$$\boldsymbol{p}^{(\mathbf{2})} = \ [+++- \ \ ++-+ \ \ +++- \ \ --+-]$$

The other sequence in the preferred pair is obtained using Eq. 1-29 as

$$\boldsymbol{g}^{(\mathbf{2})} = \ [+-++ \ \ +--- \ \ +-++ \ \ -+++]$$

Knowing that $K = 4$ and by using Eq. 1-32, the maximum shift is $s = 1$. Knowing that $N = 16$ and $s = 1$, we obtain the shifting increment $\Delta = 2$ by using Eq. 1-31. It follows from Eq. 1-33 that the zero-zone is $Z_0 = 1$. Using Eq. 1-30 we obtain a ZCZ set of $ZCZ(16,\ 4,\ 1)$ as

$$\boldsymbol{Z} = \begin{bmatrix} \boldsymbol{p}^{(\mathbf{2})} \\ \boldsymbol{g}^{(\mathbf{2})} \\ \boldsymbol{T}^{\Delta}\boldsymbol{p}^{(\mathbf{2})} \\ \boldsymbol{T}^{\Delta}\boldsymbol{g}^{(\mathbf{2})} \end{bmatrix} = \begin{bmatrix} +++- & ++-+ & +++- & --+- \\ +-++ & +--- & +-++ & -+++ \\ +-++ & -+++ & +--- & +-++ \\ +++- & --+- & ++-+ & +++- \end{bmatrix}$$

The rows of $\boldsymbol{Z}$ are ZCZ sequences. If a larger ZCZ matrix of $ZCZ(32,\ 4,\ 3)$ is needed, we can obtain the shifting parameters $s = 1$ and $\Delta = 4$ by using respectively Eq. 1-32 and Eq. 1-31. The zero-zone $Z_0 = 3$ by using Eq. 1-33.

Example 5: Ternary ZCZ sequences defined in section 1.8.2

a) Hayashi's construction

We start with a Hadamard matrix of order $N = 4$ as follow

$$\boldsymbol{H_4} = \begin{bmatrix} + & + & + & + \\ + & - & + & - \\ + & + & - & - \\ + & - & - & + \end{bmatrix}$$

The set $\boldsymbol{F}$ **is** obtained using Eq. 1-34 as

$$\boldsymbol{F} = \begin{bmatrix} \boldsymbol{F^1} \\ \boldsymbol{F^2} \end{bmatrix} = \begin{bmatrix} + + + + 0 + + + + 0 \\ + - + - 0 + - + - 0 \\ + + - - 0 + + - - 0 \\ + - - + 0 + - - + 0 \\ + + + + 0 - - - - 0 \\ + - + - 0 - + - + 0 \\ + + - - 0 - - + + 0 \\ + - - + 0 - + + - 0 \end{bmatrix}$$

By using the interleaving technique of Eq. 1-35, a starter ZCZ set with $ZCZ(20, 8, 1)$ can be obtain

$$\boldsymbol{Z^{(0)}} = \begin{bmatrix} + + + + + + + + 00 + - + - + - + - 00 \\ + + - - + + - - 00 + - - + + - - + 00 \\ + + + + - - - - 00 + - + - - + - + 00 \\ + + - - - - + + 00 + - - + - + + - 00 \\ + - + - + - + - 00 + + + + + + + + 00 \\ + - - + + - - + 00 + + - - + + - - 00 \\ + - + - - + - + 00 + + + + - - - - 00 \\ + - - + - + + - 00 + + - - - - + + 00 \end{bmatrix}$$

The rows of $\boldsymbol{Z^{(0)}}$ are ternary ZCZ sequences. If a larger ZCZ matrix $\boldsymbol{Z^{(1)}}$ of $ZCZ(40, 8, 3)$ is needed, apply Eq. 1-36 on $\boldsymbol{Z^{(0)}}$.

b) Takatsukasa et al construction

From a ternary perfect sequence (see Table 1-2), such as $\boldsymbol{t} = (1, 1, 0, 1, 0, 0, -1)$ of length $N_1 = 7$ and a Hadamard matrix $\boldsymbol{H}_4$ as follows

$$\boldsymbol{H}_4 = \begin{bmatrix} \boldsymbol{h_1} \\ \boldsymbol{h_2} \\ \boldsymbol{h_3} \\ \boldsymbol{h_4} \end{bmatrix} = \begin{bmatrix} + & + & + & + \\ + & - & + & - \\ + & + & - & - \\ + & - & - & + \end{bmatrix}$$

We can obtain a $ZCZ = (28, 4, 6)$ set by using Eq. 1-37 as follows

$$\boldsymbol{z_1} = \{+ + 0 + 00 - + + 0 + 00 - + + 0 + 00 - + + 0 + 00 -\}$$
$$\boldsymbol{z_2} = \{+ - 0 - 00 - - + 0 + 00 + + - 0 - 00 - - + 0 + 00 +\}$$
$$\boldsymbol{z_3} = \{+ + 0 - 00 + - + 0 - 00 - - - 0 + 00 - + - 0 + 00 +\}$$
$$\boldsymbol{z_4} = \{+ - 0 + 00 + + + 0 - 00 + - + 0 - 00 - - - 0 + 00 -\}$$

If a larger ZCZ set of is needed, two method can be used. First, we can choose longer ternary perfect sequence from Table 1-2 for example $N_1 = 13$. By using Eq. 1-37, a ternary ZCZ sequence set of $ZCZ = (52, 4, 12)$. Second, we can construct a larger Hadamard matrix $\boldsymbol{H}_8$ of size $N = 8$. By using Eq. 1-37, a ternary ZCZ sequence set of $ZCZ = (56, 8, 6)$.

Example 6: New constructions of OZCZ sequences

a) Construction 1

The MOCS matrices are known to have a zero-zone property (see Fan et al construction). We choose a starter MOCS $\boldsymbol{F^{(0)}}$ of set size $M_0 = 2$ and sequence length $N_0 = 2$ as

$$\boldsymbol{F^{(0)}} = \begin{bmatrix} - & + \\ - & - \end{bmatrix}$$

Where $+$ and $-$ denote 1 and -1, respectively.

Using Eq. 1-20, an extended set $\boldsymbol{F^{(1)}}$ of $M_1 = 4$ and $N_1 = 8$ can be obtained

$$\boldsymbol{F^{(1)}} = \begin{bmatrix} \boldsymbol{f^1} \\ \boldsymbol{f^2} \\ \boldsymbol{f^3} \\ \boldsymbol{f^4} \end{bmatrix} = \begin{bmatrix} - - & + + & + - & - + \\ - - & - - & + - & + - \\ + - & - + & - - & + + \\ + - & + - & - - & - - \end{bmatrix}$$

Using the balance condition, the sequences that satisfy $\sum_{n=1}^{N_1} f_n^m = 0$ are selected. Then, the bipolar sequences of OZCZ set is

$$\boldsymbol{F} = \begin{bmatrix} \boldsymbol{f^1} \\ \boldsymbol{f^2} \end{bmatrix} = \begin{bmatrix} -- & ++ & +- & -+ \\ +- & -+ & -- & ++ \end{bmatrix}$$

Using Eq. 1-42, the corresponding unipolar sequences when $d = 0$ is

$$\boldsymbol{G} = \begin{bmatrix} \boldsymbol{g^{1,0}} \\ \boldsymbol{g^{2,0}} \end{bmatrix} = \begin{bmatrix} 00 & ++ & +0 & 0+ \\ +0 & 0+ & 00 & ++ \end{bmatrix}$$

Combining the two sets we obtain an OZCZ set of pairs of bipolar and unipolar sequences with $ZCZ(8,2,1)$as follows

$$\boldsymbol{OZCZ} = \{(\boldsymbol{f^1} \quad \boldsymbol{g^{1,0}}), (\boldsymbol{f^2} \quad \boldsymbol{g^{2,0}})\}$$

The ACF and CCF of OZCZ sequences obtained above are given below

Correlation functions	Shifting variable							
	$l = 0$	$l = 1$	$l = 2$	$l = 3$	$l = 4$	$l = 5$	$l = 6$	$l = 7$
$E_{f^1,g^{1,0}}$	4	0	-2	0	0	0	-2	0
$E_{f^1,g^{2,0}}$	0	0	-2	0	4	0	-2	0
$E_{f^2,g^{2,0}}$	4	0	-2	0	0	0	-2	0
$E_{f^2,g^{1,0}}$	0	0	-2	0	4	0	-2	0

Following the same procedure, we can obtain OZCZ sequences with sequence length $N = 2^{2n+1}$ and zero-zones $Z_0 = 2^{n-1}$ by generating larger MOCS matrices using Eq. 1-20. The set size depends on the balance property.

b) Construction 2

We start with a Hadamard matrix of order $L = 4$ given bellow

$$\boldsymbol{H_4} = \begin{bmatrix} \boldsymbol{H^1} \\ \boldsymbol{H^2} \end{bmatrix} = \begin{bmatrix} + & + & + & + \\ + & - & + & - \\ + & + & - & - \\ + & - & - & + \end{bmatrix}$$

The starter ZCZ matrix is obtained using the interleaving operation from Eq.1-26

$$\boldsymbol{F} = \begin{bmatrix} \boldsymbol{f^1} \\ \boldsymbol{f^2} \\ \boldsymbol{f^3} \\ \boldsymbol{f^4} \end{bmatrix} = \begin{bmatrix} + + + + + - + - \\ + + - - + - - + \\ + - + - + + + + \\ + - - + + + - - \end{bmatrix}$$

Using the balance condition, a bipolar sequence set of OZCZ pair is selected

$$\boldsymbol{F} = \begin{bmatrix} \boldsymbol{f^2} \\ \boldsymbol{f^4} \end{bmatrix} = \begin{bmatrix} + + - - + - - + \\ + - - + + + - - \end{bmatrix}$$

Using Eq. 1-42, the corresponding unipolar sequences for each user $d = 0$ is

$$\boldsymbol{G} = \begin{bmatrix} \boldsymbol{g^{2,0}} \\ \boldsymbol{g^{4,0}} \end{bmatrix} = \begin{bmatrix} + + 00 + 00 + \\ + 00 + + + 00 \end{bmatrix}$$

Combining the two sets we obtain an OZCZ set of pairs of bipolar and unipolar sequences as follows

$$\boldsymbol{OZCZ} = \{(\boldsymbol{f^2} \quad \boldsymbol{g^{2,0}}), (\boldsymbol{f^4} \quad \boldsymbol{g^{4,0}})\}$$

The ACF and CCF of OZCZ sequences obtained above are given below

Correlation functions	Shifting variable							
	$l = 0$	$l = 1$	$l = 2$	$l = 3$	$l = 4$	$l = 5$	$l = 6$	$l = 7$
$E_{f^2,g^{2,0}}$	4	0	-2	0	0	0	-2	0
$E_{f^2,g^{4,0}}$	0	0	-2	0	4	0	-2	0
$E_{f^4,g^{4,0}}$	4	0	-2	0	0	0	-2	0
$E_{f^4,g^{2,0}}$	0	0	-2	0	4	0	-2	0

Following the same procedure, we can obtain OZCZ sequences with length $N = 2^m L$ and zero-zones $Z_0 = 2^{m-1}$, where $m \geq 1$ is the number of interleaving operation, by generating larger ZCZ starter matrices using Eq. 1-26. The set size depends on the balance property.

Annex B

Annex B.1: Received signal component

From section 3.2.1 of Chapter 3, we have

$$s_k(t) = \sqrt{2P}Re\{d_k(t)c_k(t)e^{j(w_c t+\theta_k)}\} \quad \text{(B-1)}$$

And from section 3.2.3, we have

$$r(t) = \sum_{k=1}^{K} Re\{(1 + a_k e^{j\varphi_k})s_k(t-\tau_k) + n(t)\} = y(t) + n(t) \quad \text{(B-2)}$$

We can extract

$$y(t) = \sum_{k=1}^{K} Re\{(1 + a_k e^{j\varphi_k})s_k(t-\tau_k)\} \quad \text{(B-3)}$$

By replacing Eq. B-1 in Eq. B-3, we obtain

$$y(t) = \sqrt{2P}\sum_{k=1}^{K} Re\{d_k(t-\tau_k)c_k(t-\tau_k)[e^{j(w_c t+\vartheta_k)} + a_k e^{j(w_c t+\vartheta_k+\varphi_k)}]\} \quad \text{(B-4)}$$

Where $\vartheta_k = \theta_k - w_c\tau_k$.

The exponential form of the i^{th} signal's component at the receiver output is

$$\begin{aligned} y_i &= \int_0^{T_b} y(t)c_i(t)cos(w_c t)\,dt \\ &= \frac{1}{2}\int_0^{T_b} (y(t)c_i(t)e^{jw_c t}) + (y(t)c_i(t)e^{-jw_c t})\,dt \end{aligned} \quad \text{(B-5)}$$

The left term of the right side of Eq. B-5 is

$$L = \sqrt{\frac{P}{2}}\int_0^{T_b}\sum_{k=1}^{K} Re\{d_k(t-\tau_k)c_i(t)c_k(t-\tau_k)[e^{j(2w_c t+\vartheta_k)} + a_k e^{j(2w_c t+\vartheta_k+\varphi_k)}]\}\,dt \quad \text{(B-6)}$$

And the right term is

$$R = \sqrt{\frac{P}{2}}\int_0^{T_b}\sum_{k=1}^{K} Re\{d_k(t-\tau_k)c_i(t)c_k(t-\tau_k)[e^{j\vartheta_k} + a_k e^{j(\vartheta_k+\varphi_k)}]\}\,dt \quad \text{(B-7)}$$

If we assume $f_c \gg T_b^{-1}$, we can then ignore term L. Then y_i becomes

$$y_i = \sqrt{\frac{P}{2}}\sum_{k=1}^{K} Re\left\{\int_0^{T_b} d_k(t-\tau_k)c_i(t)c_k(t-\tau_k)[e^{j\vartheta_k} + a_k e^{j(\vartheta_k+\varphi_k)}]\,dt\right\} \quad \text{(B-8)}$$

Since $d_k(t)$ is of the following form

$$d_k(t-\tau_k) = \begin{cases} d_{k,-1} & 0 \le t \le \tau_k \\ d_{k,0} & \tau_k \le t \le T_b \end{cases} \quad \text{(B-9)}$$

Where the data bits $d_{k,-1}$ and $d_{k,0}$ are respectively the previous and current symbols of the k^{th} user.

It can be used to simplify the following term in y_i as

$$\int_0^{T_b} d_k(t-\tau_k)c_i(t)c_k(t-\tau_k)dt = d_{k,-1}R_{c_k c_i}(\tau_k) + d_{k,0}\hat{R}_{c_k c_i}(\tau_k) \quad \text{(B-10)}$$

Where $R_{c_k c_i}(\tau_k)$ and $\hat{R}_{c_k c_i}(\tau_k)$ are called the continuous-time partial CCFs defined in [43] as

$$R_{c_k c_i}(\tau_k) = \int_0^{\tau_k} c_k(t-\tau_k)c_i(t)\,dt \quad \text{(B-11)}$$

$$\hat{R}_{c_k c_i}(\tau_k) = \int_{\tau_k}^{T_b} c_k(t-\tau_k)c_i(t)\,dt \quad \text{(B-12)}$$

And Eq. B-8 becomes

$$y_i = \sqrt{\frac{P}{2}} \sum_{k=1}^{K} Re\{[d_{k,-1} R_{c_k c_i}(\tau_k) + d_{k,0} \hat{R}_{c_k c_i}(\tau_k)][e^{j\vartheta_k} + a_k e^{j(\vartheta_k + \varphi_k)}]\} \quad \text{(B-13)}$$

a) Desired signal

The i^{th} receiver (setting $k = i$ in Eq. B-13) can acquire time and phase synchronization from the i^{th} non-faded transmitted signal. Therefore, time delays and phase angles are measured relative to τ_i and θ_i (we take $\tau_i = \theta_i = \vartheta_i = 0$). Putting $\tau_i = 0$ in Eq. B-11, we obtain $R_{c_i}(0) = 0$.The i^{th} user's component is

$$D_i = \sqrt{P/2}\, d_{i,0} \hat{R}_{c_i}(0)(1 + a_i \cos(\varphi_i)) \quad \text{(B-14)}$$

We can express $\hat{R}_{c_i}(0)$ as

$$\hat{R}_{c_i}(0) = \int_0^{T_b} c_i^2(t)\, dt = \sum_{n=1}^{N} \int_{(n-1)T_c}^{nT_c} c_i^2(t)\, dt = \sum_{n=1}^{N} c_{i,n}^2 T_c = \mu_i T_b \quad \text{(B-15)}$$

Where $c_{i,n}$ is the spreading sequence element $\in \{-1,0,1\}$ and $\mu_i = \left(\sum_{n=1}^{N} c_{i,n}^2\right)/N$ is the energy per chip ratio defined in Chapter 1, Eq. 1-9.

We consider only the case of $d_{i,0} = 1$ [43], the i^{th} user's component is

$$D_i = \sqrt{P/2}\, \mu_i T_b (1 + a_i \cos(\varphi_i)) \quad \text{(B-16)}$$

b) Interference

Setting $k \neq i$ in Eq. B-13 yields the MUI term as follows

$$I_i = \sqrt{\frac{P}{2}} \sum_{\substack{k=1 \\ k \neq i}}^{K} [d_{k,-1} R_{c_k c_i}(\tau_k) + d_{k,0} \hat{R}_{c_k c_i}(\tau_k)][\cos(\vartheta_k) + a_k \cos(\vartheta_k + \varphi_k)] \quad \text{(B-17)}$$

Annex B.2: Partial CCFs

For $\tau_k = lT_c, (0 \le l \le N_q - 1)$ where $N_q = T_q/T_c$, the continuous-time partial CCFs are illustrated in Figure B-1.

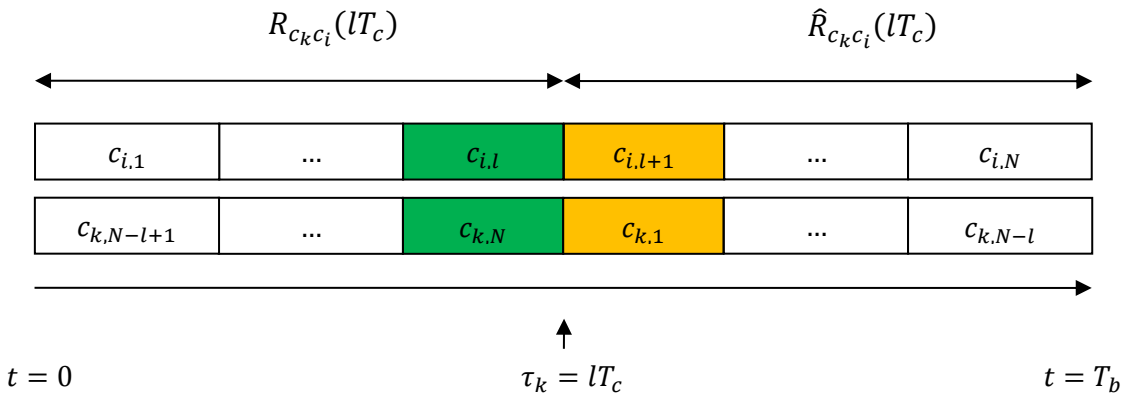

Figure B-1 Continuous-time partial CCFs.

From Figure B-1, $\hat{R}_{c_k c_i}(lT_c)$ and $R_{c_k c_i}(lT_c)$ can be written as discrete-time periodic even and odd CCFs

$$\begin{aligned}
\hat{R}_{c_k c_i}(lT_c) &= \int_{lT_c}^{T_b} c_k(t - lT_c)c_i(t)\,dt \\
&= \sum_{n=1}^{N-l} \int_{(n-1+l)T_c}^{(n+l)T_c} c_k(t - lT_c)c_i(t)\,dt \\
&= \sum_{n=1}^{N-l} \int_{(n-1+l)T_c}^{(n+l)T_c} c_{k,n}c_{i,l+n}\,dt \\
&= \sum_{n=1}^{N-l} c_{k,n}c_{i,l+n} \int_{(n-1+l)T_c}^{(n+l)T_c} dt \\
&= \sum_{n=1}^{N-l} (c_{k,n}c_{i,l+n})T_c
\end{aligned} \tag{B-18}$$

Knowing that the aperiodic CCF between two sequences $\boldsymbol{a}$ and $\boldsymbol{b}$ is (see Eq. 1-2 in Chapter 1)

$$\theta_{\boldsymbol{ab}}(l) = \sum_{n=1}^{N-l} a_n b_{n+l} \qquad 0 \le l \le N-1 \tag{B-19}$$

We can write

$$\hat{R}_{c_k c_i}(lT_c) = T_c \theta_{c_k c_i}(l) \tag{B-20}$$

Similarly, we can obtain as

$$\begin{aligned} R_{c_k c_i}(lT_c) &= \int_0^{lT_c} c_k(t - lT_c) c_i(t)\, dt \\ &= \sum_{n=1}^{l} \int_{(n-1)T_c}^{nT_c} c_{k,(N-l)+n} c_{i,n}\, dt \\ &= \sum_{n=1}^{l} \left(c_{k,(N-l)+n} c_{i,n}\right) T_c \end{aligned} \tag{B-21}$$

Replacing l by $N - l$ in Eq. B-19, we obtain

$$\theta_{\boldsymbol{ab}}(N-l) = \sum_{n=1}^{l} a_n b_{n+(N-l)} \qquad 0 \le l \le N-1 \tag{B-22}$$

Which gives

$$R_{c_k c_i}(lT_c) = T_c \theta_{c_i c_k}(N-l) \tag{B-23}$$

By using Eq. 1-3 and Eq. 1-4 from Chapter 1

$$\hat{R}_{c_k c_i}(lT_c) = T_c \left(E_{c_k c_i}(l) + O_{c_k c_i}(l)\right)/2 \tag{B-24}$$

$$R_{c_k c_i}(lT_c) = T_c \left(E_{c_k c_i}(l) - O_{c_k c_i}(l)\right)/2 \tag{B-25}$$

Annex B.3: Mean calculations

The following mean and variance properties will be need for the calculation of $E\{Z_i\}$.

Linearity: let X and Y be two random variables and c a constant, we have

$$E\{X+Y\} = E\{X\} + E\{Y\} \quad \text{(B-26)}$$

$$E\{cX\} = cE\{X\} \quad \text{(B-27)}$$

If X and Y are independent, we have

$$E\{XY\} = E\{X\}E\{Y\} \quad \text{(B-28)}$$

$$E\{f_1(X)f_2(Y)\} = E\{f_1(X)\}E\{f_2(Y)\} \quad \text{(B-29)}$$

Let X be a uniformly distributed random variable then we have

$$E\{\cos(X)\} = E\{\sin(X)\} = E\{\cos(X)\sin(X)\} = 0 \quad \text{(B-30)}$$

$$E\{\cos^2(X)\} = E\{\sin^2(X)\} = 1/2 \quad \text{(B-31)}$$

The mean of the correlator's output is

$$E\{Z_i\} = E\{D_i + I_i + N_i\} \quad \text{(B-32)}$$

Using the linearity properties of the mean

$$E\{Z_i\} = E\{D_i\} + E\{I_i\} + E\{N_i\} \quad \text{(B-33)}$$

1) Desired signal mean

The mean of the desired signal component (from Eq. B-16)

$$E\{D_i\} = E\left\{\sqrt{P/2}\,\mu_i T_b(1 + a_i\,cos(\varphi_i))\right\} \quad \text{(B-34)}$$

We assume that the random variables $d_{k,}, \theta_k, \varphi_k, \tau_k$, and a_k are mutually independent. By using Eq. B-26 to Eq. B-28 we obtain

$$E\{D_i\} = \sqrt{P/2}\,\mu_i T_b(1 + E\{a_i\}E\{cos(\varphi_i)\}) \quad \text{(B-35)}$$

Using Eq. B-30, the remaining term is

$$E\{D_i\} = \sqrt{P/2}\,\mu_i T_b \quad \text{(B-36)}$$

2) Interference mean

The mean of the interference signal component from Eq. B-17 is

$$E\{I_i\} = E\left\{\sqrt{\frac{P}{2}}\sum_{\substack{k=1\\k\neq i}}^{K}\left[d_{k,-1}R_{c_k c_i}(\tau_k) + d_{k,0}\hat{R}_{c_k c_i}(\tau_k)\right][cos(\vartheta_k) + a_k\, cos(\vartheta_k + \varphi_k)]\right\} \quad \text{(B-37)}$$

It can be readily shown using Eq. B-30 that

$$E\{cos(\vartheta_k)\} = E\{cos(\vartheta_k + \varphi_k)\} = 0 \quad \text{(B-38)}$$

Therefore,

$$E\{I_i\} = 0 \quad \text{(B-39)}$$

3) Noise mean

The noise has zero mean $E\{n(t)\} = 0$, therefore

$$E\{N_i\} = \int_0^T E\{n(t)\}c_i(t)\, cos(w_c t)\, dt = 0 \quad \text{(B-40)}$$

Finally, the correlator's out mean is

$$E\{Z_i\} = \sqrt{P/2}\,\mu_i T_b \quad \text{(B-41)}$$

Annex B.4: Variance calculation

The following mean and variance properties will be need for the calculation of $Var\{Z_i\}$.

The variance of a random variable X is defined as follows

$$Var[X] = \quad E\{X^2\} - (E\{X\})^2 \tag{B-42}$$

If X and Y are independent, we have

$$Var\{X + Y\} = \quad Var\{X\} + Var\{Y\} \tag{B-43}$$

The correlator's output variance is

$$Var\{Z_i\} = \quad Var\{D_i + I_i + N_i\} \tag{B-44}$$

We assume that the random variables $d_{k,}, \theta_k, \tau_k,$ and a_k have mutually independent components that is θ_i and θ_k are independent if $i \neq k$. And the noise is statistically independent of the multipath medium. Then, we can write

$$Var\{Z_i\} = \quad Var\{D_i\} + Var\{I_i\} + Var\{N_i\} \tag{B-45}$$

1) Desired signal variance

The desired signal variance is

$$\begin{aligned} Var\{D_i\} = \quad & E\left\{\left(\sqrt{P/2}\,\mu_i T_b(1 + a_i\, cos(\varphi_i))\right)^2\right\} - \left(\sqrt{P/2}\,\mu_i T_b\right)^2 \\ = \quad & \frac{P\mu_i^2 T_b^2}{2}(1 + E\{a_i^2 cos^2(\varphi_i)\} + 2E\{a_i\, cos(\varphi_i)\}) - \frac{P\mu_i^2 T_b^2}{2} \end{aligned} \tag{B-46}$$

By using Eq. B-30 and B-31, we obtain

$$Var\{D_i\} = \frac{P\mu_i^2 T_b^2}{2}\left(1+\frac{E\{a_i^2\}}{2}\right) - \frac{P\mu_i^2 T_b^2}{2}$$

$$= P\mu_i^2 T_b^2 \gamma/4 \quad \text{(B-47)}$$

Where $\gamma = E\{a_k^2\}, \forall k$.

2) Interference variance

Since $E\{I_i\} = 0$, the interference variance is computed as follows

$$Var\{I_i\} = E\left\{\left(\sqrt{\frac{P}{2}}\sum_{\substack{k=1\\k\neq i}}^{K}\left[d_{k,-1}R_{c_k c_i}(\tau_k) + d_{k,0}\hat{R}_{c_k c_i}(\tau_k)\right]\left[cos(\vartheta_k) + a_k\, cos(\vartheta_k+\varphi_k)\right]\right)^2\right\}$$

$$= E\left\{\frac{P}{2}\sum_{\substack{k=1\\k\neq i}}^{K}\sum_{\substack{s=1\\s\neq i}}^{K}\left[d_{k,-1}R_{c_k c_i}(\tau_k) + d_{k,0}\hat{R}_{c_k c_i}(\tau_k)\right]\left[d_{s,-1}R_{c_s c_i}(\tau_s) + d_{s,0}\hat{R}_{c_s c_i}(\tau_s)\right]\left[cos(\vartheta_k) + a_k\, cos(\vartheta_k+\varphi_k)\right]\left[cos(\vartheta_s) + a_s\, cos(\vartheta_s+\varphi_s)\right]\right\} \quad \text{(B-48)}$$

The random variable d_k has mutually independent elements that is

$$E\{d_{k,n}d_{s,m}\} = \begin{cases}1 & k=s, n=m\\ 0 & otherwise\end{cases} \quad \text{(B-49)}$$

We obtain

$$Var\{I_i\} = \frac{P}{2}\sum_{\substack{k=1\\k\neq i}}^{K} E\left\{\left(\left[d_{k,-1}R_{c_k c_i}(\tau_k) + d_{k,0}\hat{R}_{c_k c_i}(\tau_k)\right]\left[cos(\vartheta_k) + a_k\, cos(\vartheta_k+\varphi_k)\right]\right)^2\right\} \quad \text{(B-50)}$$

The following relations can be readily obtained from the means properties

$$E\{cos^2(\vartheta_k)\} = \quad E\{cos^2(\vartheta_k + \varphi_k)\} = 1/2 \tag{B-51}$$

Using Eq. B-51 and B-50, we can write

$$Var\{I_i\} = \quad \frac{P(1+\gamma)}{4} \sum_{\substack{k=1 \\ k \neq i}}^{K} E\left\{R^2_{c_k c_i}(\tau_k) + \hat{R}^2_{c_k c_i}(\tau_k)\right\} \tag{B-52}$$

Where

$$E\left\{R^2_{c_k c_i}(\tau_k) + \hat{R}^2_{c_k c_i}(\tau_k)\right\} = \quad \frac{1}{T_q} \int_0^{T_q} R^2_{c_k c_i}(lT_c) + \hat{R}^2_{c_k c_i}(lT_c) d\tau_k \tag{B-53}$$

Therefore

$$Var\{I_i\} = \quad \frac{P(1+\gamma)}{4T_q} \sum_{\substack{k=1 \\ k \neq i}}^{K} \int_0^{T_q} R^2_{c_k c_i}(lT_c) + \hat{R}^2_{c_k c_i}(lT_c) d\tau_k \tag{B4-54}$$

The integral part can be written as

$$\int_0^{T_q} R^2_{k,i}(lT_c) + \hat{R}^2_{k,i}(lT_c) d\tau_k = \quad \sum_{l=0}^{N_q - 1} \int_{lT_c}^{(l+1)T_c} R^2_{c_k c_i}(lT_c) + \hat{R}^2_{c_k c_i}(lT_c) d\tau_k \tag{B-55}$$

Using Eq. 3-11 and Eq. 3-12 from chapter 3, we obtain

$$\begin{aligned} \int_0^{T_q} R^2_{k,i}(lT_c) + \hat{R}^2_{k,i}(lT_c) d\tau_k &= \quad \frac{T_c^2}{2} \int_0^{T_q} E^2_{k,i}(l) + O^2_{k,i}(l) d\tau_k \\ &= \quad \frac{T_c^2}{2} \sum_{l=0}^{N_q - 1} \int_{lT_c}^{(l+1)T_c} E^2_{k,i}(l) + O^2_{k,i}(l) d\tau_k \\ &= \quad \frac{T_c^3}{2} \sum_{l=0}^{N_q - 1} \left(E^2_{k,i}(l) + O^2_{k,i}(l)\right) \end{aligned} \tag{B-56}$$

Where $N_q = T_q / T_c$.

The interference term (Eq. B-54) can be written as

$$Var\{I_i\} = \frac{PT_c^3(1+\gamma)}{8T_q}\sum_{\substack{k=1\\k\neq i}}^{K}\sum_{l=0}^{N_q-1}\left(E_{k,i}^2(l)+O_{k,i}^2(l)\right)$$

$$= \frac{PT_c^2(1+\gamma)}{8N_q}\sum_{\substack{k=1\\k\neq i}}^{K}\sum_{l=0}^{N_q-1}\left(E_{k,i}^2(l)+O_{k,i}^2(l)\right) \quad \text{(B-57)}$$

3) Noise variance

The noise variance is calculated as follows

$$Var\{N_i\} = E\left\{\left(\int_0^{T_b} n(t)c_i(t)\,cos(w_c t)\,dt\right)^2\right\}$$

$$= E\left\{\int_0^{T_b} n(t)c_i(t)\cos(w_c t)\,dt\int_0^{T_b} n(\alpha)c_i(\alpha)\cos(w_c\alpha)\,d\alpha\right\}$$

$$= E\left\{\int_0^{T_b}\int_0^{T_b} n(t)n(\alpha)c_i(t)\,c_i(\alpha)\cos(w_c t)\cos(w_c\alpha)\,dtd\alpha\right\}$$

$$= \int_0^{T_b}\int_0^{T_b} E\{n(t)n(\alpha)\}\,c_i(t)c_i(\alpha)\cos(w_c t)\cos(w_c\alpha)\,dtd\alpha \quad \text{(B-58)}$$

If the noise is wide-sense stationary random process, then

$$Var\{N_i\} = \int_0^{T_b}\int_0^{T_b} \theta_n(\alpha-t)\,c_i(t)c_i(\alpha)\cos(w_c t)\cos(w_c\alpha)\,dtd\alpha \quad \text{(B-59)}$$

Knowing that the white noise has power spectral density (PSD) of $S_n(f) = N_0/2$ and using the inverse Fourier transform of the noise's PSD, we obtain the noise ACF function

$$\theta_n(\alpha-t) = \int_{-\infty}^{+\infty} S_n(f)e^{j2\pi f(\alpha-t)}df = \frac{N_0}{2}\delta(\alpha-t) \quad \text{(B-60)}$$

We obtain

$$Var\{N_i\} = \int_0^{T_b}\int_0^{T_b} \frac{N_0}{2}\delta(\alpha-t)c_i(t)c_i(\alpha)\cos(w_c t)\cos(w_c\alpha)\,dtd\alpha \quad \text{(B-61)}$$

Where $\delta(t)$ is Dirac delta function defined as follows

$$\int_{-\infty}^{+\infty} \phi(t)\delta(t-t_0)dt = \quad \phi(t_0) \tag{B-62}$$

Where $\phi(t)$ is a regular function continuous at $t = t_0$.

It follows that

$$\int_0^{T_b} c_i(\alpha)\cos(w_c\alpha)\delta(\alpha - t)\, d\alpha = \quad c_i(t)\cos(w_c t) \tag{B-63}$$

And the noise variance becomes

$$\begin{aligned} Var\{N_i\} = & \quad \frac{N_0}{2}\int_0^{T_b} c_i^2(t)(\cos(w_c t))^2\, dt \\ = & \quad \frac{N_0}{2}\sum_{n=1}^{N} c_{i,n}^2 \int_{(n-1)T_c}^{nT_c} (\cos(w_c t))^2\, dt \\ = & \quad \frac{N_0}{2}\sum_{n=1}^{N} c_{i,n}^2 \frac{T_c}{2} \\ = & \quad \frac{\mu_i T_b N_0}{4} \end{aligned} \tag{B-64}$$

Annex C

Annex C.1: Received signal components

From section 4.3.2 in Chapter 4, the decision variable of the 0^{th} data bit of user i is

$$Z_i = \quad Re\left\{\frac{1}{T_b}\int_0^{T_b} r(t)\sum_{n'=1}^{N} c_{i,n'}e^{-jw_{n'}t}\,dt\right\} \tag{C-1}$$

Where

$$r(t) = \quad s_i(t) + \sum_{\substack{k=1 \\ k\neq i}}^{K} s_k(t-\tau_k) + n(t) \tag{C-2}$$

By replacing Eq. C-2 in Eq. C-1, we obtain

$$Z_i = \quad \frac{1}{T_b}Re\left\{\int_0^{T_b}\left(s_i(t) + \sum_{\substack{k=1 \\ k\neq i}}^{K} s_k(t-\tau_k) + n(t)\right)\sum_{n'=1}^{N} c_{i,n'}e^{-jw_{n'}t}\,dt\right\} \tag{C-3}$$

1) Desired signal

It is assumed that the i^{th} receiver can acquire time and phase synchronization from the i^{th} transmitted signal. Therefore, time delays and phase angles are measured relative to τ_i and θ_i (we take $\tau_i = \theta_i = 0$). We can extract the desired signal $(n' = n)$ component

$$S_i = \quad \frac{1}{T_b}Re\left\{\int_0^{T_b} s_i(t)\sum_{n=1}^{N} c_{i,n}e^{-jw_n t}\,dt\right\} \tag{C-4}$$

Where

$$s_i(t) = \sqrt{\frac{2P}{N}} \sum_{n=1}^{N} d_i c_{i,n} e^{jw_n t} \quad \text{(C-5)}$$

By replacing Eq. C-5 in Eq. C-4, assuming $d_i = 1$ and taking the real part, we have

$$\begin{aligned} S_i &= \frac{1}{T_b} \sqrt{\frac{2P}{N}} \sum_{n=1}^{N} c_{i,n} c_{i,n} \int_0^{T_b} cos\big((w_n - w_n)t\big)\, dt \\ &= \frac{1}{T_b} \sqrt{\frac{2P}{N}} \sum_{n=1}^{N} c_{i,n}^2\, T_b \\ &= \sqrt{\frac{2P}{N}} N\mu_i \\ &= \sqrt{\frac{2P}{N}} D_i \end{aligned} \quad \text{(C-6)}$$

Where

$$D_i = N\mu_i \quad \text{(C-7)}$$

2) Interference

From Eq. C-3, the MUI_i signal component is

$$S_{k\neq i} = \frac{1}{T_b} Re\left\{ \int_0^{T_b} \sum_{\substack{k=1 \\ k\neq i}}^{K} s_k(t-\tau_k) \sum_{n'=1}^{N} c_{i,n'} e^{-jw_{n'}t}\, dt \right\} \quad \text{(C-8)}$$

Where

$$s_k(t-\tau_k) = \sqrt{\frac{2P}{N}} \sum_{n=1}^{N} d_k(t-\tau_k) c_{k,n} e^{j(w_n(t-\tau_k)+\theta_k)} \quad \text{(C-9)}$$

By replacing Eq. C-9 in Eq. C-8 and taking the real part, we have

$$S_{k\neq i} = \frac{1}{T_b}\sqrt{\frac{2P}{N}}\sum_{\substack{k=1\\k\neq i}}^{K}\sum_{n=1}^{N}\sum_{n'=1}^{N} c_{k,n}c_{i,n'}\int_0^{T_b} d_k(t-\tau_k)cos\big[(w_n - w_{n'})t + \vartheta_{k,n}\big]\,dt$$

$$= \sqrt{\frac{2P}{N}}MUI_i \qquad \text{(C-10)}$$

Where $\vartheta_{k,n} = \theta_k - w_n\tau_k$ and

$$MUI_i = \frac{1}{T_b}\sum_{\substack{k=1\\k\neq i}}^{K}\sum_{n=1}^{N}\sum_{n'=1}^{N} c_{k,n}c_{i,n'}\int_0^{T_b} d_k(t-\tau_k)cos\big[(w_n - w_{n'})t + \vartheta_{k,n}\big]\,dt \qquad \text{(C-11)}$$

By setting $n' = n$ in MUI_i, it becomes inter-symbol interference (ISI_i) as

$$ISI_i = \frac{1}{T_b}\sum_{\substack{k=1\\k\neq i}}^{K}\sum_{n=1}^{N} c_{k,n}c_{i,n}cos\big(\vartheta_{k,n}\big)\int_0^{T_b} d_k(t-\tau_k)\,dt \qquad \text{(C-12)}$$

Since $d_k(t)$ is of the following form given

$$d_k(t-\tau_k) = \begin{cases} d_{k,-1} & 0 \le t \le \tau_k \\ d_{k,0} & \tau_k \le t \le T_b \end{cases} \qquad \text{(C-13)}$$

It can be used to simplify the following term in ISI_i as

$$ISI_i = \frac{1}{T_b}\sum_{\substack{k=1\\k\neq i}}^{K}\sum_{n=1}^{N}\big[\tau_k d_{k,-1} + (T_b - \tau_k)d_{k,0}\big]c_{k,n}c_{i,n}cos\big(\vartheta_{k,n}\big) \qquad \text{(C-14)}$$

And by setting $n' \neq n$ in MUI_i, it becomes inter-channel interference (ICI_i) as

$$ICI_i = \frac{1}{T_b}\sum_{\substack{k=1\\k\neq i}}^{K}\sum_{n=1}^{N}\sum_{\substack{n'=1\\n'\neq n}}^{N} c_{k,n}c_{i,n'}\int_0^{T_b} d_k(t-\tau_k)cos\big[(w_n - w_{n'})t + \vartheta_{k,n}\big]\,dt \qquad \text{(C-15)}$$

Annex C.2 : Noise variance

The noise component at the receiver is

$$n_i = \frac{1}{T_b} Re\left\{\int_0^{T_b} n(t) \sum_{n'=1}^{N} c_{i,n'} e^{-jw_{n'}t}\, dt\right\} \tag{C-16}$$

Following the same notation of Annex C.1, the noise component at the receiver can be written as

$$n_i = \sqrt{\frac{2P}{N}}\left(\sqrt{\frac{N}{2P}}\frac{1}{T_b} Re\left\{\int_0^{T_b} n(t) \sum_{n'=1}^{N} c_{i,n'} e^{-jw_{n'}t}\, dt\right\}\right)$$

$$= \sqrt{\frac{2P}{N}} N_i \tag{C-17}$$

Where

$$N_i = \sqrt{\frac{N}{2P}}\frac{1}{T_b} Re\left\{\int_0^{T_b} n(t) \sum_{n'=1}^{N} c_{i,n'} e^{-jw_{n'}t}\, dt\right\} \tag{C-18}$$

The $n(t)$ is a band pass white noise with zero mean and PSD $S_N(f) = N_0/2$. The PSD is assumed to be zero outside of an interval of frequencies around $\pm w_{n'}$. It can be written as [58]

$$n(t) = Re\{z(t)e^{jw_{n'}t}\} \tag{C-19}$$

Where the low pass quantity $z(t)$ is called the complex envelop that has a zero mean and PSD $S_Z(f) = N_0$ [58] as

$$S_Z(f) = \begin{cases} N_0 & |f| \le B/2 \\ 0 & |f| > B/2 \end{cases} \tag{C-20}$$

The noise variance is obtained using mean as follows

$$Var\{N_i\} = E\{N_i^2\}$$

$$= \frac{N}{2P}\frac{1}{T_b^2}\sum_{n'=1}^{N} c_{i,n'}^2 \int_0^{T_b}\int_0^{T_b} E\{n(t)n(\alpha)\}\, cosw_{n'}t\ cosw_{n'}\alpha\ dtd\alpha \quad \text{(C-21)}$$

Knowing that $E_b = PT_b$ and $n(t)$ is assumed to be wide sense stationary (WSS) process with an ACF $E\{n(t)n(\alpha)\} = \theta_N(\alpha - t)$.

$$Var\{N_i\} = \frac{N}{2T_bE_b}\sum_{n'=1}^{N} c_{i,n'}^2 \int_0^{T_b}\int_0^{T_b} \theta_N(\alpha - t)\, cosw_{n'}t\ cosw_{n'}\alpha\ dtd\alpha \quad \text{(C-22)}$$

The relation between the AFC of $z(t)$ and $n(t)$ is (see [58] chapter 4 pp.159-162)

$$\theta_N(\alpha - t) = Re\left\{\theta_Z(\alpha - t)\mathrm{e}^{jw_{n'}(\alpha - t)}\right\} \quad \text{(C-23)}$$

Note that the ACF of the bandpass stochastic process $n(t)$ is uniquely determined from the ACF of its equivalent low-pass process $z(t)$ and the carrier frequency [58]. The limiting form ($B \to \infty$) of the ACF of the equivalent low-pass process $z(t)$ is (see [58] chapter 4 pp.159-162)

$$\theta_Z(\alpha - t) = N_0\delta(\alpha - t) \quad \text{(C-24)}$$

Then the ACF of $n(t)$ is

$$\theta_N(\alpha - t) = N_0\delta(\alpha - t)\cos w_{n'}(\alpha - t) \quad \text{(C-25)}$$

Then the noise variance of Eq. C.22 becomes

$$Var\{N_i\} = \frac{NN_0}{2T_bE_b}\sum_{n'=1}^{N} c_{i,n'}^2 \int_0^{T_b}\int_0^{T_b} \delta(\alpha - t)\cos w_{n'}(\alpha - t)\, cosw_{n'}t\, cosw_{n'}\alpha\, dtd\alpha \quad \text{(C-26)}$$

Using the following Dirac's delta function property

$$\int_0^{T_b} \cos w_{n'}(\alpha - t)\, cosw_{n'}\alpha\ \ \delta(\alpha - t)d\alpha = \cos w_{n'}(t - t)\, cosw_{n'}t = cosw_{n'}t \quad \text{(C-27)}$$

Eq. C-26 becomes

$$Var\{N_i\} = \frac{NN_0}{2T_bE_b}\sum_{n'=1}^{N} c_{i,n'}^2 \int_0^{T_b} cos^2\, w_{n'}t\, dt$$

$$= \frac{NN_0}{4E_b}\sum_{n=1}^{N} c_{i,n'}^2 \quad \text{(C-28)}$$

Knowing that $\mu_i = \sum_{n'=1}^{N} c_{i,n'}^2/N$, the above equation can also be written as

$$Var\{N_i\} = \frac{N^2N_0\mu_i}{4E_b} \quad \text{(C-29)}$$

Annex D

Annex D. 1: Periodic CCFs

The CCF at the receiver between $\boldsymbol{c_i}$ and $\boldsymbol{c_k}$ illustrated in Figure D-1.

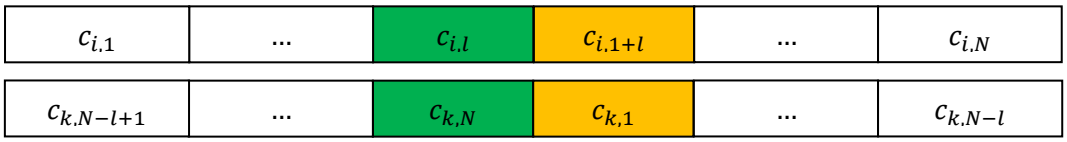

Figure D-1 Even periodic CCF.

From Figure D-1, the CCF can be written as

$$E_{c_k c_i}(l) = \sum_{n=1}^{N} c_{k,n} c_{i,(n+l) mod N} \tag{D-1}$$

Annex D.2: Current variance

The integral part of Eq. 5-6 is calculated bellow

$$\begin{aligned}
\int_0^{\infty} r_i(v)\, dv &= \int_0^{\infty} \frac{P_r}{\Delta_v} \sum_{k=1}^{K} d_k E_{c_i c_k}(\tau_k) \prod(v, n+\tau_k)\, dv \\
&= \frac{P_r}{\Delta_v} \sum_{k=1}^{K} d_k\, E_{c_i c_k}(\tau_k) \int_0^{\infty} \prod(v, n+\tau_k)\, dv \\
&= \frac{P_r}{\Delta_v} \sum_{k=1}^{K} d_k\, E_{c_i c_k}(\tau_k) \frac{\Delta_v}{N} \\
&= \frac{P_r}{N} \sum_{k=1}^{K} d_k\, E_{c_i c_k}(\tau_k)
\end{aligned} \tag{D-2}$$

References

[1] M. B. Pursley and D. V. Sarwate, "James L. Massey's Contributions in the Early Years of Spread-Spectrum Communication Theory Research," *IEEE Communication Surveys & Tutorials,* vol. 17, no. 03, pp. 1500-1510, 2015.

[2] D. V. Sarwate , "Bounds on Crosscorrelation and Autocorrelation of Sequences," *IEEE Transactions on Information Theory,* Vols. IT-25, no. 06, pp. 720-724, 1979.

[3] L. R. Welch, "Lower Bounds on the Maximum Cross Correlation of Signals," *IEEE Transactions on Information Theory,* vol. 20, no. 03, pp. 397-399, 1974.

[4] P. Fan and M. Darnell, "Sequence Design for Communications Applications," *Research Studies Press,* 1996.

[5] K. Takatsukasa, S. Matsufuji, Y. Watanabi, N. Kuroyanagi and N. Suehiro, "Ternary ZCZ Sequence Sets for Cellular CDMA Systems," *IEICE Transactions on Fundamentals of Electronics, Communications and Computer Sciences,* Vols. E85-A, no. 09, pp. 2135-2140, 2003.

[6] E. H. Dinan and B. Jabbari, "Spreading codes for direct sequence CDMA and wideband CDMA cellular networks," *IEEE Communications Magazine,* vol. 36, no. 09, pp. 48-54, 1998.

[7] I. A. Glover, Digital Communications, 3 ed., Harlaw, England: Pearson Education Limited, 2010.

[8] R. Gold, "Optimal binary sequences for spread spectrum multiplexing," *IEEE Transactions on Information Theory,* vol. 13, no. 04, pp. 619 - 621, 1967.

[9] K. Fazel and S. Kaiser, Multi-Carrier Spread-Spectrum, Germany: Springer-Science Business Media B.V., 2004.

[10] M. Golay, "Complementary Series," *IRE Transactions on Information Theory,* pp. 82-87, 1961.

[11] H. Ochiai and H. Imai, "OFDM-CDMA with Peak Power Reduction Based on the Spreading Sequences," *IEEE International Conference on Communication,* pp. 1299-1303, 1998.

[12] C. Tseng and C. Liu, "Complementary sets of sequences," *IEEE Transactions on Information Theory,* Vols. IT-18, pp. 644-652, 1972.

[13] P. Fan, N. Suehiro, N. Kuroyanagi and X. M. Deng, "Class of binary sequences with zero correlation zone," *Electronics Letters,* vol. 32, no. 10, pp. 777-779, 1999.

[14] X. H. Tang, P. Z. Fan and S. Matsufuji, "Lower bounds on correlation of spreading sequence set with low or zero correlation zone," *Electronics Letters,* vol. 36, no. 06, pp. 551 - 552, 2000.

[15] H. Torii, M. Nakamura and N. Suehiro, "A new class of zero-correlation zone sequences," *IEEE Transactions on Information Theory,* vol. 50, no. 03, pp. 559 - 565, 2004.

[16] T. Maeda, S. Kanemoto and T. Hayashi, "A Novel Class of Binary Zero-Correlation Zone Sequence Sets," *IEEE Region 10 Conference,* pp. 708-711, 2010.

[17] J. Cha, S. Kameda, M. Yokoyama, H. Nakase, K. Masu and K. Tsubouchi, "New binary sequences with zero-correlation duration for approximately synchronised CDMA," *Electronics Letters,* vol. 36, pp. 991-993, 2000.

[18] T. Hayashi, "A Class of Ternary Sequence Sets having a Zero-Correlation Zone for Even and Odd Correlation Functions," in *IEEE International Symposium on Information Theory*, Yokohama, Japan, 2003.

[19] L. Feng, J. Wang, R. Q. Hu et L. Liu, «New design of optical zero correlation zone codes in quasi-synchronous VLC CDMA systems,» *EURASIP Journal on Wireless Communications and Networking,* vol. 120, 2015.

[20] T. Matsumoto, H. Torii et S. Matsufuji, «Theoretical analysis of BER performance of optical ZCZ-CDMA system,» *International Journal of Computers and Communications* , vol. 01, pp. 18-25, 2013.

[21] A. Abudoukeremu, S. Matsufuji and T. Matsumoto, "On optical ZCZ codes with a good aperiodic autocorrelation property," in *15th International Conference on Advanced Communications Technology (ICACT),* PyeongChang, South Korea, 2013.

[22] T. H. Abd, S. A. Aljunid, H. A. Fadhil, R. A. Ahmad and N. M. Saad, "Development of a new code family based on SAC-OCDMA system with large cardinality for OCDMA network," *Optical Fiber Technology,* vol. 17, no. 04, pp. 273-280, 2011.

[23] M. Addad et A. Djebbari, «New code family for QS-CDMA visible light communication systems,» *Journal of Telecommunications and Information Technology*, vol. 03, pp. 5-8, 2018.

[24] J. H. Liang, X. Wang, F. H. Wang and Z. T. Huang, "Blind spreading sequence estimation algorithm for long-code DS-CDMA signals in asynchronous multi-user systems," *IET Signal Processing,* vol. 11, no. 06, pp. 704 - 710, 2017.

[25] F. Qu, X. Qin, L. Yang and T. C. Yang , "Spread-Spectrum Method Using Multiple Sequences for Underwater Acoustic Communications," *IEEE Journal of Oceanic Engineering,* vol. PP, no. 99, pp. 1-12, 2017.

[26] J. Khalife, K. Shamaei and Z. M. Kassas, "Navigation with Cellular CDMA Signals-Part I: Signal Modeling and Software-Defined Receiver Design," *IEEE Transactions on Signal Processing,* vol. PP, no. 99, pp. 1-13, 2018.

[27] F. T. Dagefu, G. Verma , P. Spasojevic and B. M. Sadler, "An Experimental study of quasi-synchronous multiuser communications in cluttered scenarios at low VHF," in *International Conference on Military Communications and Information Systems (ICMCIS)*, Oulu, Finland, 2017.

[28] A. Masmoudi , F. Bellili , S. Affes and A. Ghrayeb , "Maximum Likelihood Time Delay Estimation From Single- and Multi-Carrier DSSS Multipath MIMO Transmissions for Future 5G Networks," *IEEE Transactions on Wireless Communications,* vol. 16, no. 08, pp. 4851 - 4865, 2017.

[29] Q. Sun, S. Wang, S. Han and I. L. Chih, "Unified framework towards flexible multiple access schemes for 5G," *ZTE Communications,* vol. 14, no. 04, p. 26–34, 2016.

[30] R. M. Buehrer, Code Division Multiple Access (CDMA), Virginia, USA: Morgan & Claypool, 2006.

[31] H. H. Chen, The Next Generation CDMA Technologies, West Sussex, England: John Wiley and Sons Ltd, 2007.

[32] Tutorials Point, "Code Division Multiple Access," obtained from www.tutorialspoint.com consulted in September 2018.

[33] D. Divsalar and M. K. Simon, "CDMA With Interference Cancellation for Multiprobe Missions," TDA Progress Report 42-120, NASA, USA, 1995.

[34] J. P. Linnartz, Ed., Wireless communication, Vols. Wireless channels-Multipath fading, "http://www.wirelesscommunication.nl/reference/chaptr03/fading/delayspr.htm" consulted in August 2018.

[35] TELETOPIX Telecom Techniques Guide, "What is Rake Receiver and its Purpose in CDMA," http://www.teletopix.org/cdma/what-is-rake-receiver-and-its-purpose-in-cdma/ consulted in August 2018.

[36] D. Boudreau, G. Caire, G. E. Corazza, R. De Gaudenzi, G. Gallinaro, M. Luglio, R. Lyons, J. Romero-Garcia, A. Vernucci and H. Widmer, "Wide-band CDMA for the UMTS/IMT-2000 satellite component," *IEEE Transactions on Vehicular Technology*, vol. 51, no. 02, pp. 306 - 331, 2002.

[37] K. Fazel and S. Kaiser, Multi-Carrier and Spread Spectrum Systems, 2nd ed., West Sussex, UK: John Wiley & Sons, 2008.

[38] M. Chitre, S. Shahabudeen, L. Freitag and M. Stojanovic, "Underwater Acoustic Communications & Networking," in *OCEANS 2008*, Quebec City, QC, Canada, 2008.

[39] CCSDS, "Navigation Data-Definition and Conventions," Repport : Consultative Committee for Space Data Systems , Oxfordshire, UK, 2001.

[40] C. Vladeanu, "Optimum chaotic quantized sequences for asynchronous DS-CDMA system," in *13th European Signal Processing Conference*, Antalya, Turkey, 2005.

[41] G. L. Turin, Communication Through Random-Multipath Channels, Cambridge, Massachusets: PhD Thesis, Department of Electrical Engineering, Massachusets Institute of Technology (MIT), 1952.

[42] E. Geraniotis and M. Pursley, "Performance of Coherent Direct-Sequence Spread-Spectrum Communications over Specular Multipath Fading Channels," *IEEE Transactions on Communications*, vol. 33, no. 06, pp. 502 - 508, 1985.

[43] M. Pursley, "Performance Evaluation for Phase-Coded Spread-Spectrum Multiple-Access Communication- Part I: System Analysis," *IEEE Transactions on Communications,* vol. 25, no. 08, pp. 795-799, 1977.

[44] J. S. Lehnert and M. B. Pursley, "Multipath Diversity Reception of Spread-Spectrum Multiple-Access Communications," *IEEE Transactions on Communications* , Vols. COM-35, no. 11, pp. 1189-1198, 1987.

[45] M. K. Simon, J. K. Omura, R. A. Scholtz and B. K. Levitt, Spread Spectrum Communications Handbook, McGraw-Hill Companies, Inc, 2002.

[46] M. Addad, A. Djebbari and I. Dayoub, "Performance of ZCZ Codes in QS-DS-CDMA Communication Systems," *International Journal of Communication Systems,* p. recommended for publication with minor revision, 2018.

[47] E. Geraniotis, "Direct-Sequence Spread-Spectrum Multiple-Access Communications Over Nonselective and Frequency-Selective Rician Fading Channels," *IEEE Transactions on Communications,* vol. 34, no. 08, pp. 756 - 764, 1986.

[48] B. M. Popovic, "Spreading sequences for multicarrier CDMA systems," *IEEE Transactions on Communications,* vol. 47, no. 06, pp. 918 - 926, 1999.

[49] M. Addad and A. Djebbari , "Suitable Spreading Sequences for Asynchronous MC-CDMA Systems," *Journal of Telecommunications and Information Technology,* vol. 03, pp. 9-13, 2018.

[50] Q. Shi and M. Latva-aho, "Spreading sequences for asynchronous MC-CDMA revisited: accurate bit error rate analysis," *IEEE Transactions on Communications,* vol. 51, no. 01, pp. 8 - 11, 2003.

[51] H. Elgala , R. Mesleh and H. Haas, "Indoor Optical Wireless Communication: Potential and State-of-the-Art," *IEEE Communications Magazine* , vol. 49, no. 09, pp. 56-62, 2011.

[52] L. U. Khan, "Visible light communication: Applications, architecture, standardization and research challenges," *Digital Communications and Networks,* vol. 03, no. 02, pp. 78-88, 2017.

[53] V. T. B. Tram and M. Yoo, "Vehicle-to-Vehicle Distance Estimation Using a Low-Resolution Camera Based on Visible Light Communications," *IEEE Access,* vol. 06, pp. 4521 - 4527, 2018.

[54] A. Naz, H. M. Asif, T. Umer and B. S. Kim, "PDOA Based Indoor Positioning Using Visible Light Communication," *IEEE Access*, vol. 06, pp. 7557 - 7564, 2018.

[55] F. Miramirkhani and M. Uysal, "Visible Light Communication Channel Modeling for Underwater Environments With Blocking and Shadowing," *IEEE Access,* vol. 06, pp. 1082 - 1090, 2017.

[56] A. Garadi and A. Djebbari, "New technique for construction of a zero cross correlation code," *Optik - International Journal for Light and Electron Optics,* vol. 123, no. 15, pp. 1382-1384, 2012.

[57] E. Smith, R. Blaikie and D. Taylor, "Performance enhancement of spectral-amplitude-coding optical CDMA using pulse-position modulation," *IEEE Transactions on Communications* , vol. 46, no. 09, pp. 1176 - 1185, 1998.

[58] J. G. Proakis, Digital Communications, New York: McGraw-Hill, 1995.